ASSESSMENT OF SPATIO-SEASONAL VARIATIONS IN HEAVY METAL CONTAMINATION AND ASSOCIATED HEALTH RISKS OF FUMAROLIC CONDENSATES IN MT. SUSWA, KAJIADO COUNTY, KENYA

GIDEON YATOR

A Thesis Submitted to the Institute of Post Graduate Studies of Kabarak University in Partial Fulfilment of the Requirements for the Award of Master of Science in Environmental Science Degree

KABARAK UNIVERSITY

NOVEMBER, 2025

DECLARATION

1. I hereby declare that:

   i. This research project is my work, and to the best of my knowledge, it has not been presented for the award of a degree in any university or college.

   ii. That the work has not incorporated material from other works or a paraphrase of such material without due and appropriate acknowledgment

   iii. That the work has been subjected to processes of anti-plagiarism and has met Kabarak University's 15% similarity index threshold

2. I do understand that issues of academic integrity are paramount, and therefore, I may be suspended or expelled from the University, or my degree may be recalled for academic dishonesty or any other related academic malpractices.

Signed:_____ Date:_____

Gideon Yator

GMEN/NE/0571/05/23

RECOMMENDATION

To the Institute of Postgraduate Studies:

The thesis titled, **"Assessment of Spatio-Seasonal Variations in Heavy Metal Contamination and Associated Health Risks of Fumarolic Condensates in Mt. Suswa, Kajiado County, Kenya,"** written by **Gideon Yator,** is presented to the Institute of Postgraduate studies of Kabarak University. We have reviewed the research project and recommend it be accepted in partial fulfillment of the requirement for the award of the degree of Master of Science in Environmental Science.

Signed:_____ Date:_____

Prof. Jackson John Kitetu

Department of Physical and Biological Science

Kabarak University

Signed:_____ Date:_____

Dr. Carolyne Chepkirui,

Department of Physical and Biological Science

Kabarak University

COPYRIGHT

ACKNOWLEDGEMENTS

Special gratitude to my supervisors, Prof. Jackson John Kitetu and Dr. Carolyne Chepkirui from Kabarak University, for their unwavering support and valuable guidance throughout the development of this project. I am also grateful to the faculty and my colleagues of the Master of Science in Environmental Science program for their valuable contributions to this study.

DEDICATION

I wholeheartedly dedicate this research project to my family, who have been my greatest source of inspiration and the driving force behind my academic pursuits. To my dear wife, Sharon, and our children, Shantel, Sasha, and Shanis, I am immensely grateful for your unwavering support and understanding, which have enabled me to devote ample time to this research program. God bless you.

ABSTRACT

Geothermal resources in the East African Rift System provide renewable energy opportunities but also pose health and environmental risks through heavy metal emissions in fumarolic condensates. This study assessed the spatio-seasonal variations of arsenic (As), lead (Pb), mercury (Hg), and cadmium (Cd) in fumarolic condensates at Mt. Suswa, Kajiado County, Kenya, and evaluated associated human health risks. A mixed-methods design was adopted, triangulating quantitative laboratory and geospatial analyses with qualitative evidence from household surveys and key informant interviews. Condensate samples were collected from 19 fumarolic vents across the inner and outer caldera during the dry (January–March) and wet (May–July) seasons. Physico-chemical parameters were determined using APHA (2022) methods, while heavy elements were analysed using an Agilent 5110 ICP-OES. Data analysis included ANOVA, Pearson's correlation, and IDW interpolation, with human health risks quantified following USEPA (2011) ingestion and dermal exposure guidelines. Results demonstrated significant spatial heterogeneity ($p < 0.001$). The highest concentrations were observed at hotspot fumaroles: As (5.59 μgL^{-1} , F18), Pb (1.98 μgL^{-1}, F14), Cd (1.84 μgL^{-1}, F5), and F^- (3.84 mgL^{-1}, F13), while the lowest occurred at background vents such as Cd (0.37 μgL^{-1}, F2) and As (1.29 μgL^{-1}, F10). Carcinogenic risk (CR) values ranged from 3.36×10^{-5} in F2 (children, wet season) to 1.35×10^{-4} in F15 (adult females, dry season). A clear spatial divide was observed: outer caldera vents (F1, F2, F4, F7–F15) fell within the acceptable risk range (10^{-6}–10^{-4}), while inner caldera fumaroles (F5, F17, F18, F20) exceeded the 10^{-4} threshold, classifying them as persistent high-risk hotspots. Seasonal patterns indicated dilution during the wet season, but hotspot fumaroles remained consistently above the risk threshold. Qualitative evidence confirmed widespread community reliance on fumarolic condensates despite visible health outcomes such as dental fluorosis, with coping strategies like boiling and dilution proving ineffective. Fumarolic condensates in Mt. Suswa pose non-trivial and persistent carcinogenic risks, particularly in inner caldera hotspots, with children and adult females the most vulnerable. Recommendations include routine geochemical monitoring of vents, structured risk communication and health awareness programs, and the development of alternative safe water supplies to reduce dependence on contaminated condensates while enabling sustainable geothermal development.

Keywords: *Fumarolic Condensates, Heavy Metals, Spatio-Seasonal Variation, Carcinogenic Risk*

TABLE OF CONTENTS

LIST OF TABLES

LIST OF FIGURES

LIST OF ABBREVIATIONS AND ACRONYMS

APHA	American Public Health Association
As	Arsenic
ATSDR	Agency for Toxic Substances and Disease Registry
Cd	Cadmium
EC	Electrical Conductivity
GDC	Geothermal Development Company
GIS	Geographical Information System
GPS	Global Positioning System
Hg	Mercury
ICP-OES	Inductively Coupled Plasma–Optical Emission Spectrometer
IDW	Inverse Distance Weighted
NEMA	National Environment Management Authority
Pb	Lead
pH	Potential of Hydrogen (for acidity/alkalinity measurements)
PPM	Parts Per Million
SPSS	Statistical Package for the Social Sciences (software for data analysis)
TDS	Total Dissolved Solids
USEPA	U.S. Environmental Protection Agency
UV-Vis	Ultraviolet-Visible Spectrophotometry
WHO	World Health Organization

CONCEPTUAL OPERATIONAL DEFINITION OF KEY TERMS

Heavy Metals: In this study, heavy metals refer to trace elements such as arsenic (As), lead (Pb), mercury (Hg), and cadmium (Cd), which may be present in fumarolic condensates and are analysed for their concentrations.

Fumarolic Condensates: These are vapour and gas emissions from geothermal vents that condense into liquid form. For the purpose of this research, the term refers to the collected condensates from fumarolic sites within Mt. Suswa.

Spatio-Seasonal Variations: Refers to the changes in the concentration of heavy metals in fumarolic condensates observed across different geographical locations (spatial) within Mt. Suswa and over different seasons (specifically between wet and dry periods).

Geothermal Activity: Geothermal activity in the Mt. Suswa area refers to heat and gas emissions from the Earth's crust, including fumaroles, which influence contamination levels in condensates.

Sampling Sites: These are designated locations within the caldera in Mt. Suswa where fumarolic condensates were collected for analysis.

Concentration: Refers to the amount of a specific heavy metal (measured in parts per million or micrograms per Liter) present in the fumarolic condensates collected at each sampling site.

Contamination Hotspots: Areas within the study region that exhibit significantly higher concentrations of heavy metals in fumarolic condensates compared to surrounding areas.

Environmental Monitoring: The process of regularly collecting and analysing samples from the fumarolic sites to observe changes in heavy metal concentrations over time and across different seasons.

Reliability: refers to the consistency and stability of an instrument in producing dependable results when applied repeatedly under similar conditions.

Validity: is the accuracy and meaningfulness of inferences obtained from a research study. It addresses the critical issue of the relationship between a concept and its measurement.

CHAPTER ONE

INTRODUCTION

This chapter presents an overview of the study, highlighting the background information and the problem addressed. It further outlines the objectives and research questions that guided the study and discusses its significance, scope, limitations, and underlying assumptions.

1.1 Background of the study

Geothermal energy is increasingly recognized worldwide as a sustainable and renewable energy source. Nonetheless, recent studies have highlighted environmental concerns, particularly the emission of heavy metals such as mercury from fumarolic and geothermal systems (Pan et al., 2024). Fumaroles (volcanic openings in or near volcanoes that emit steam and gases) can release significant amounts of heavy metals such as mercury, arsenic, and cadmium, posing risks to ecosystems and human health (Inostroza et al., 2020).

Globally, numerous studies have reported contamination associated with geothermal activity. In Iceland, recent investigations have shown that geothermal processes contribute to significant mercury enrichment in nearby soils (Edwards et al., 2024). Similarly, investigations in Italy's geothermal areas have revealed significant heavy metal pollution in soil and water resources, underscoring the need to monitor contamination and assess associated health risks (Armiento et al., 2022). These findings have highlighted the importance of evaluating both environmental impacts and human exposure to ensure public safety (Durowoju et al., 2020).

Within Africa, the East African Rift System (EARS) holds vast geothermal potential, with Kenya, Ethiopia, and Tanzania at the forefront of its development (Elbarbary et al., 2022). However, comprehensive research on heavy metal contamination and its health risks from these geothermal sources is limited, leaving a significant knowledge gap in understanding the environmental impacts of geothermal activities in the region. Kenya, in particular, has been at the forefront of geothermal energy development in Africa, with several active and potential geothermal fields along the Kenyan Rift Valley (Musonye, 2022). The country's geothermal installed capacity has grown substantially, reaching 943.7 MW as of 2025, with plans to expand further (EPRA, 2025). While this growth is promising for Kenya's energy sector, it also underscores the urgent need for environmental monitoring and impact assessment studies.

Mt. Suswa, located in the southern part of the Kenya Rift Valley about 120 km northwest of Nairobi, has been identified as one of Kenya’s emerging geothermal prospects. Its distinctive double-caldera structure and active fumarolic features make it a promising site for future geothermal energy development (Albino, 2021). Beyond its energy potential, Mt. Suswa supports Maasai pastoralist communities and holds ecological and cultural value, underscoring the pressing need to balance geothermal development, environmental integrity, and community health. Local residents rely on geothermal water for drinking (for humans and livestock), bathing, and cooking, increasing their exposure to heavy metal contaminants (Masikonte, 2020).

In the Mt. Suswa area, alternative water sources are extremely scarce. Unlike other regions where rivers, lakes, or shallow wells provide supplementary supplies, Suswa has neither significant surface water bodies nor reliable groundwater reserves due to its complex volcanic geology. Although some households practice rainwater harvesting, this source remains unreliable due to the area’s arid-to-semiarid climate, characterized by

sporadic and insufficient rainfall. Consequently, fumarolic condensates become the primary water source for local communities, making geothermal emissions the principal pathway of contamination and thereby heightening health risks.

This dependency makes the community uniquely vulnerable to potential contamination. In contexts with multiple water sources, households can switch to safer supplies when contamination is suspected. However, in Suswa, the absence of viable alternatives means exposure to heavy metals through geothermal emissions is direct, frequent, and unavoidable. This elevates the health risks, particularly for children and women, who often have higher daily exposure due to their physiological characteristics and domestic roles.

Communities near Mt. Suswa face potential health threats from heavy metal exposure, including neurological damage, respiratory issues, and chronic diseases, yet these risks remain poorly quantified. Prior to this study, critical gaps existed:

i) There is insufficient baseline data on the specific heavy metals present in Mt. Suswa's fumarolic condensates and their concentrations. Comprehensive data on heavy metal contamination, particularly around settlement areas, is crucial for informed decision-making in health risk evaluation and resource management.

ii) The spatial distribution of heavy metal contamination around Mt. Suswa's fumaroles remains largely unexplored, limiting exposure assessments.

iii) The seasonal influences on heavy metal emissions and their health implications remain unstudied, leaving temporal variations in risk unclear.

iv) The Links between geothermal properties (Temperature, pH, flow rate) and heavy metal levels, critical for predicting health risks, are not well understood.

These knowledge gaps necessitated the present study, which investigated the spatio-seasonal variations of heavy metal contamination in fumarolic condensates at Mt. Suswa. The study generated vital data on contamination patterns, quantified exposure pathways, and assessed potential health risks for resident populations. Its findings provide a scientific basis for community health protection and environmental management.

1.2 Statement of the Problem

Heavy metal contamination in drinking water is a global health concern, especially in geothermal regions where fumarolic emissions release toxic elements such as arsenic, mercury, lead, and cadmium. Communities around Mt. Suswa face heightened vulnerability since fumarolic condensates are among the few accessible water sources in an area with scarce alternatives. Despite this reliance, the extent of contamination in fumarolic condensates had not been systematically examined prior to this study. Most previous research in geothermal fields has focused on hot springs and groundwater systems, overlooking fumarolic condensates as a direct exposure pathway. This gap left uncertainties regarding heavy metal concentrations, their spatial distribution across fumarolic vents, and seasonal emission variations. Consequently, the scale of the health risks associated with their use for domestic and livestock purposes remained unclear.

Long-term exposure to heavy metals has severe implications, including neurological impairment, developmental disorders, organ damage, and elevated cancer risk. In Mt. Suswa, where alternative water sources are unreliable, such risks are magnified. The lack of scientific evidence limited policymakers, geothermal practitioners, and public health stakeholders in designing effective interventions. This necessitated the present study, which investigated spatio-seasonal variations of heavy metal contamination in fumarolic condensates to provide baseline evidence for public health protection and environmental management.

1.3 Objective of the Study

The broad objective of this study was to assess the spatio-seasonal variations of selected heavy metal contamination and associated health risks in fumarolic condensates in Mt. Suswa, Kajiado County, Kenya.

1.3.1 Specific Objectives of the Study

The study was guided by the following specific objectives:

i) To determine the physico-chemical characteristics and seasonal variations in the concentrations of heavy metals (arsenic, mercury, lead, and cadmium) in fumarolic condensates from vents within the Mt. Suswa area

ii) To examine the correlations among the analysed physico-chemical parameters and spatial distribution patterns of heavy metal contamination in the Mt. Suswa area.

iii) To evaluate the potential human health risks posed by exposure to heavy metals (arsenic, mercury, lead, and cadmium) present in fumarolic condensates within the Mt. Suswa area.

1.4 Research Questions

In line with the above objectives, the study sought to answer the following research questions:

i) What are the physico-chemical characteristics and seasonal variations in the concentrations of heavy metals (arsenic, mercury, lead, and cadmium) in fumarolic condensates from vents within the Mt. Suswa area?

ii) What correlations exist among the analysed physico-chemical parameters and the spatial distribution patterns of heavy metal contamination in the Mt. Suswa area?

iii) What are the potential human health risks associated with exposure to heavy metals in fumarolic condensates used by local communities around Mt. Suswa?

1.5 Justification of the Study

This study is critical given the area's unique geological, hydrological, and human health context. Mt. Suswa, located in the Kenyan Rift Valley, is an active geothermal site with numerous fumaroles that discharge steam and gases from underground reservoirs. Due to the scarcity of perennial rivers, lakes, and accessible groundwater, local Maasai communities depend heavily on fumarolic condensates for drinking, cooking, and bathing. Unlike surface or groundwater sources that undergo natural filtration through soil and rock, fumarolic condensates form directly from geothermal emissions, making them highly susceptible to contamination by toxic elements such as arsenic, mercury, lead, and cadmium, which are linked to severe health effects, including neurological disorders, organ damage, and increased cancer risks.

Despite this reliance, fumarolic condensates have received less scientific attention than hot springs, groundwater, or soils in other geothermal fields. The absence of baseline data on their chemical quality, contaminant spatial distribution, and seasonal variability creates a critical knowledge gap, especially in light of Kenya's expanding geothermal energy program. Investigating these condensates provides a direct measure of metal-laden emissions and their implications for human health.

The findings of this study will:

(i) Establish baseline data on geothermal water quality and associated health risks in Suswa, enabling informed decisions on safe water use.

(ii) Protect vulnerable communities from chronic exposure to heavy metals by identifying contamination hotspots and seasonal trends.

(iii) Contribute to regional and global literature on geothermal contamination pathways, providing evidence for sustainable resource management.

1.6 Significance of the Study

This study holds profound significance as it integrates the assessment of spatio-seasonal variations in selected heavy metal contamination with health risk evaluation of fumarolic condensates in Mt. Suswa, Kenya. Its importance spans across communities, academia, geothermal management, and policy domains.

At the community level, the research is transformative for the Maasai residents of Mt. Suswa, who depend on fumarolic condensates as a primary domestic water source in the absence of reliable alternatives. By quantifying concentrations of heavy metals such as arsenic, mercury, lead, and cadmium, and linking them with community health risk profiles, the study raises awareness of potential dangers while offering evidence-based recommendations to safeguard human well-being. The integration of household survey data further reflects community perceptions, experiences, and adaptation strategies, amplifying their role in shaping local interventions.

For the scientific community, the study advances knowledge by examining fumarolic condensates, which is an overlooked pathway of heavy metal exposure in geothermal regions. It provides baseline data, maps contamination hotspots, and reveals seasonal dynamics while applying geospatial analysis and human health risk models that can be replicated in other geothermal systems globally.

From a policy and regulatory perspective, the findings provide robust evidence to strengthen geothermal monitoring frameworks, guide sustainable exploitation of geothermal resources, and align development goals with community health safeguards.

The results are particularly relevant for policymakers in Kenya and across the East African Rift System, where geothermal expansion is rapidly advancing.

At the regional and global scale, this study contributes to the broader discourse on balancing renewable energy development with environmental and public health integrity. By identifying contamination patterns and health risks, it supports resilience planning and directly aligns with Sustainable Development Goal 6 (clean water and sanitation). Ultimately, the study demonstrates a holistic approach to cleaner water access, healthier communities, and sustainable resource use, offering a replicable model for similar geothermal settings worldwide.

1.7 Scope of the Study

This study was conducted within the Mt. Suswa area, located in the southern segment of the Kenyan Rift Valley. The research specifically focused on fumarolic vents in three distinct geological zones: the inner caldera, the outer caldera, and the transitional areas around the volcano. These sites were purposively selected to capture spatial variability in heavy metal emissions within the geothermal field.

Sampling was carried out across two major climatic periods—the dry season (January–March) and the wet season (May–July)—to assess seasonal influences on heavy metal concentrations. Fumarolic condensates collected during these seasons formed the primary dataset for laboratory analyses. The study examined selected physico-chemical parameters (pH, temperature, electrical conductivity, total dissolved solids, and major anions and cations) alongside the concentrations of four priority heavy metals: arsenic, mercury, lead, and cadmium.

In addition to chemical analyses, the study incorporated geospatial techniques to map contamination hotspots and assess spatial distribution patterns. A health risk assessment

framework was also applied to evaluate potential human exposure via ingestion and dermal pathways, guided by documented community water-use practices from household surveys.

The scope of the study was limited to fumarolic condensates and did not include other environmental matrices such as soils, vegetation, or groundwater. Likewise, health risk assessment focused on exposure to arsenic, mercury, lead, and cadmium, excluding other possible contaminants. Seasonal analysis was confined to one wet and one dry cycle within the study period, providing representative but not long-term temporal trends.

1.8 Limitations of the Study

This study encountered limitations that may influence the interpretation of its findings. First, spatial coverage was constrained by accessibility challenges within Mt. Suswa's rugged terrain. Some fumarolic vents were difficult to reach due to steep slopes and unstable ground, thereby reducing the number of sampling points from 26 to 19.

Second, the study's temporal scope was restricted to one wet season (May–July) and one dry season (January–March) within a single annual cycle. While this provided useful insights into seasonal variability, it did not capture long-term or inter-annual variations in heavy metal emissions, which may fluctuate due to climatic or geothermal dynamics.

Third, the analytical scope was limited to four selected heavy metals (arsenic, mercury, lead, and cadmium) of priority and selected physico-chemical parameters. Other potentially hazardous elements or compounds in fumarolic condensates, such as chromium or sulfur species, were not assessed.

Fourth, in the health risk assessment, ingestion and dermal pathways were prioritized based on local water-use practices. However, potential exposure through indirect routes such as food chains (for example, livestock consumption of contaminated water) was not

included. Furthermore, some exposure parameters relied on community self-reporting during surveys, which may be subject to recall bias.

Despite these limitations, the study employed rigorous sampling strategies, standardized analytical procedures, and robust geospatial and risk assessment tools to ensure the reliability and validity of its findings.

1.9 Delimitation of the Study

This study was carefully delimited to ensure that the limitations encountered did not compromise the validity or reliability of the findings.

First, to address the spatial coverage constraint posed by Mt. Suswa's rugged, uneven terrain, the study was restricted to nineteen (19) accessible fumarolic vents strategically selected across the inner caldera, the outer caldera, and the surrounding zones. This ensured representative spatial coverage while maintaining researcher safety and logistical feasibility.

Second, the temporal limitation was delimited by focusing on two contrasting climatic periods the wet season (May–July) and the dry season (January–March)—within a single annual cycle. This deliberate design provided a meaningful comparison of seasonal variations, even though long-term or inter-annual variations were beyond the study's scope.

Third, the analytical limitation regarding the range of elements analysed was delimited by prioritizing four environmentally significant heavy metals—arsenic, mercury, lead, and cadmium based on their toxicity, persistence, and relevance to geothermal emissions. This focus allowed for precise analytical depth within available time and laboratory resources.

Fourth, in relation to the health risk assessment, the study was delimited to direct exposure pathways (ingestion and dermal contact), reflecting the most relevant local exposure scenarios identified through community surveys. Potential indirect pathways, such as through livestock or crops, were acknowledged but excluded to maintain methodological clarity.

Additionally, to mitigate potential recall bias from self-reported data, community responses were triangulated with field observations and local health records where available.

1.10 Assumptions of the study

The study was guided by several assumptions that influenced its design, data collection, and interpretation of results.

It was assumed that the fumarolic vents selected for sampling were representative of the wider Mt. Suswa geothermal system and captured the spatial variability across the inner, outer, and transitional caldera zones. The wet season (May–July) and dry season (January–March) sampling cycles were considered adequate to reflect seasonal variations in heavy metal concentrations, even though they did not capture long-term or inter-annual fluctuations that might occur due to climatic or geothermal dynamics.

It was further assumed that information provided by community members during household surveys accurately reflected their actual water-use practices, exposure frequencies, and related behaviors in the study area. The study also assumed that sample integrity and measurement accuracy were maintained throughout the field and laboratory processes, supported by proper handling, preservation, and adherence to standardized analytical protocols. Confidence was placed in the calibration and operational stability of laboratory instruments to ensure consistent, reliable results.

CHAPTER TWO

LITERATURE REVIEW

2.1 Introduction

This chapter presents a comprehensive review of the literature on spatio-seasonal variations in heavy metal contamination in geothermal waters. The review is structured to provide both theoretical and empirical insights into the subject matter. The review concludes by identifying critical knowledge gaps, particularly in the context of fumarolic condensates as an underexplored contamination pathway, which justify the current study.

2.2 Theoretical Literature Review

2.2.1 Heavy Metals Characteristics and Environmental Behaviour

Heavy metals such as arsenic (As), mercury (Hg), lead (Pb), and cadmium (Cd) are naturally occurring elements with high atomic weights and densities. They are of particular concern because of their persistence in the environment and their tendency to bioaccumulate in living organisms, making them among the most toxic environmental pollutants (Wan et al., 2024). Unlike organic contaminants, heavy metals are non-biodegradable and therefore remain in soils, sediments, and water bodies for long periods, increasing the risk of chronic exposure (Aziz et al., 2023).

The mobility and speciation of heavy metals in aquatic systems are strongly influenced by environmental conditions, including pH, redox potential, temperature, and the presence of complexing agents such as sulfates, chlorides, and organic ligands (Lo Medico et al., 2025). For instance, low pH and reducing conditions often enhance the solubility of metals such as Cd and Pb, increasing their potential bioavailability. In contrast, alkaline and oxidizing conditions may favor their precipitation and immobilization (Martínez-Guijarro et al., 2021). These interactions determine whether

metals occur in free ionic, dissolved, or particulate forms, and consequently their transport, toxicity, and uptake in biological systems.

Thus, understanding the environmental behavior of heavy metals is critical for predicting their persistence, distribution, and potential risks to human and ecosystem health, especially in geothermal contexts such as fumarolic condensates where natural filtration processes are absent.

2.2.2 Geothermal Activity and Heavy Metal Emissions

Geothermal activity is a well-documented natural source of heavy metal emissions, releasing toxic elements such as arsenic (As), mercury (Hg), lead (Pb), and cadmium (Cd) through volcanic and hydrothermal processes. Globally, geothermal systems mobilize these metals from the Earth's crust via high-temperature fluids and gases, with fumaroles vents emitting steam and volcanic gases—acting as primary conduits. Edmonds et al. (2022) provided a comprehensive overview, noting that geothermal fluids dissolve metals from host rocks, with concentrations varying by temperature, pH, and geological context. A study by Bagnato et al. (2020) reports Hg levels up to 50 µgL-1 in geothermal condensates, emphasizing the role of fumaroles in emitting metal-laden vapors that condense into surface waters or soils, posing environmental risks. This global evidence underscores the significance of fumarolic emissions as direct pathways for heavy metal release.

In Africa, the East African Rift System (EARS) is a hotspot for geothermal activity due to its tectonic setting, yet research on heavy metal emissions remains sparse compared to global counterparts.

Kenya, within the EARS, is a leader in geothermal energy, with fields like Olkaria highlighting heavy metal presence in emissions. (2024) document Hg and As in

geothermal fluids from Lake Bogoria Hot Springs, attributing their release to interactions between magmatic gases and crustal rocks. While studies such as Rotich et al. (2024) focus on resource mapping, they report elevated metal levels, suggesting a need for contamination-specific research in Kenya's geothermal zones.

At Mt. Suswa, an active geothermal site in Kenya's Rift Valley, fumarolic emissions are prominent, yet specific studies on heavy metal contamination are scarce. (2017) indicated that Mt. Suswa's fumaroles emit steam relied upon by Maasai communities, raising concerns about unfiltered exposure to metals (As, Hg, Pb, Cd).

2.2.3 Physico-Chemical Properties of Fumarolic Condensates

Temperature and pH

The relationship between geothermal characteristics and heavy metal concentrations in fumarolic condensates has attracted increasing interest in recent years, with studies revealing complex interactions influenced by factors such as temperature, pH, flow rate, and electrical conductivity (Inostroza, Moune, Moretti, Bonifacie, et al., 2022).

Temperature is a critical factor influencing heavy metal concentrations in geothermal fluids, with significant implications for environmental and geological processes. Research has demonstrated that as temperatures rise, the solubility and mobility of heavy metals in geothermal systems also increase.

Recent studies have demonstrated that temperature plays a critical role in controlling the geochemical behaviour of arsenic and other heavy metals in geothermal systems. Elevated thermal conditions enhance rock–water interactions, promoting the leaching and dissolution of arsenic from host geological materials into geothermal fluids. This temperature-dependent mobilization significantly increases arsenic concentrations, posing potential risks to surrounding water resources and ecosystems (Shi et al., 2024).

Recent studies have demonstrated that the pH of geothermal fluids plays a crucial role in controlling heavy metal mobility. In particular, lower pH conditions enhance the solubility and transport of metals such as lead and cadmium, primarily through increased mineral dissolution and fluid–rock interaction in acidic environments. This relationship between acidity and metal enrichment has been observed in several geothermal systems, including those in Iceland, where acidic fluids in high-temperature zones tend to exhibit higher concentrations of trace metals than neutral or alkaline fluids (Bowman et al., 2023). The Iceland Deep Drilling Project, among other studies, has highlighted the behaviour of trace elements, including metals, in the unique geochemical environments of Iceland's geothermal systems (Friðleifsson et al., 2020).

(2023) highlighted that pH and redox potential (Eh) are critical in controlling fluid-rock interactions, which in turn affect mineral scaling and metal solubility. While the studies emphasize the risks associated with low pH and heavy metal mobility, it is also essential to consider that certain geothermal systems may naturally buffer pH levels, potentially mitigating heavy metal solubility and toxicity.

Flow Rate and Electrical Conductivity

Flow rate is a significant parameter affecting heavy metal concentrations in geothermal systems. (2023) conducted a study in the Tatio geothermal field in Chile and observed that arsenic concentrations varied with flow rate. Their findings indicated that higher arsenic concentrations were generally associated with lower flow rates. They attributed this correlation to increased rock-water interaction time, which enhances the leaching of arsenic-bearing minerals from the surrounding geology into the geothermal fluids. This relationship underscores the importance of flow dynamics in geothermal systems, as variations in flow rate can significantly influence heavy-metal concentrations. Decreased

flow rates promote more extensive interactions between geothermal fluids and rocks, leading to greater mobilization of heavy metals like arsenic(Alam et al., 2023)

Electrical conductivity, which reflects the total dissolved solids content, has been found to correlate with heavy metal concentrations in some geothermal systems. Bianchini et al. (2020) reported a positive correlation between electrical conductivity and arsenic concentrations in geothermal waters of the Ethiopian Rift Valley. Their findings suggest that higher electrical conductivity may indicate greater concentrations of dissolved heavy metals, including arsenic, making conductivity a useful proxy for estimating heavy metal content in certain geological settings. This relationship underscores the importance of monitoring electrical conductivity during environmental assessments in geothermal areas, as it can provide insights into the potential for heavy-metal contamination (Bianchini et al., 2020).

2.2.4 Comparison with Other Water Sources

Fumarolic condensates, formed by the condensation of volcanic gases, differ significantly from filtered surface water and groundwater in their contamination potential. The literature highlights that fumarolic condensates often contain elevated levels of geogenic contaminants, such as sulfur compounds, heavy metals (e.g., arsenic, lead), and volatile organic compounds, due to their volcanic origin (Inostroza, Moune, Moretti, Robert, et al., 2022). Groundwater is often considered safer due to natural soil filtration; however, it can still be contaminated by geogenic elements like fluoride and arsenic, especially in arid regions. For instance, a study in Inner Mongolia, China, found fluoride concentrations in groundwater ranging from 0.07 to 7.70 mgL^{-1} and arsenic levels between 0.31 and 47.0 μg/L. The research indicated that residents consuming this groundwater daily might face health risks associated with these contaminants (Nakazawa et al., 2020). The key distinction lies in the source: fumarolic condensates are inherently

tied to volcanic activity, while surface and groundwater contamination stems from environmental interactions, making the former more unpredictable and potentially hazardous.

2.3 Heavy Metals in Geothermal Systems

2.3.1 Arsenic Contamination

Arsenic is among the most widespread trace elements in geothermal systems, where it is primarily mobilized through high-temperature water–rock interactions and redox-controlled geochemical processes. These interactions enhance the dissolution of arsenic-bearing minerals, thereby enriching geothermal fluids in arsenic. Consequently, arsenic concentrations in such systems often exceed established drinking-water safety limits, posing significant environmental and public health concerns in geothermal regions (Shi et al., 2024). In geothermal systems, arsenic commonly exists in two oxidation states, arsenite [As(III)] and arsenate [As(V)], with As(III) being the more mobile and toxic species due to its higher solubility and weaker adsorption on mineral surfaces. The concentration of arsenic in geothermal fluids varies widely, typically ranging from a few micrograms per liter (µgL-1) to several milligrams per liter (mgL-1), depending on the geochemical environment and temperature conditions (Qingda et al., 2024). Arsenic contamination is often linked to hydrothermal processes, and its mobility is influenced by factors such as temperature, pH, and the presence of other ions, such as chlorine (Ayari et al., 2023).

Arsenic concentrations in fumarolic condensates can be particularly high due to its volatility at elevated temperatures. (2022) reported arsenic levels in fumarolic condensates from various geothermal fields worldwide, ranging from 0.1 to 50 mg L^{-1}. The mobility and distribution of arsenic in geothermal systems are influenced by factors such as temperature, pH, and redox conditions (Shi et al., 2024b).

2.3.2 Mercury Contamination

Mercury is another volatile element commonly found in geothermal systems, and its presence in fumarolic condensates is of significant environmental concern. Mercury in geothermal fluids can exist in various forms, including elemental mercury (Hg), ionic mercury (Hg^{2+}), and organomercury compounds. Research indicates that geothermal fields are notable sources of mercury emissions, which can impact surrounding ecosystems (Pichler, 2024).

Elemental Mercury (Hg) is found in fumarole gases, with concentrations ranging from 0.9 to 1899 nmol/m^3, indicating significant volatilization processes. Ionic Mercury (Hg^{2+}) is detected in hydrothermal fluids at low levels, with total mercury concentrations reaching up to 26,000 pM (picomolar) in some systems. Organomercury Compounds are generally less frequently detected, with studies reporting undetectable levels of methylmercury in certain geothermal environments (Pichler, 2024).

Elevated mercury levels in geothermal fluids can lead to bioaccumulation in marine food chains, raising concerns for human health and ecosystem integrity (Torres-Rodriguez et al., 2024). Continuous monitoring and remediation efforts are essential to mitigate the risks associated with mercury contamination in geothermal systems (Sunguti et al., 2024). While the presence of mercury in geothermal systems is concerning, it is crucial to consider that anthropogenic sources may contribute more significantly to overall mercury levels in the environment compared to natural geothermal emissions (Torres-Rodriguez et al., 2024).

Mercury concentrations in fumarolic condensates exhibit significant variability, influenced by factors such as temperature and volcanic activity. The volatility of mercury at elevated temperatures leads to its enrichment in vapour phases, which subsequently concentrates in fumarolic condensates (Jin et al., 2024)

Studies indicate that mercury levels in fumarolic condensates can range from <0.1 μg/L to over 1000 μg/L, reflecting the complex interactions between geological processes and mercury behaviour. The presence of mercury in gas-condensate reservoirs is often misrepresented due to its volatile nature, necessitating careful sampling and analytical techniques to accurately quantify concentrations (Lawer et al., 2023).

Elevated temperatures facilitate the release of mercury into the vapor phase, where it can condense in fumarolic environments, leading to high concentrations in condensates. Volcanic activity is a significant contributor to mercury emissions, with studies linking elevated mercury levels to magmatic processes during events such as the Paleocene-Eocene Thermal Maximum (Jin et al., 2024).

2.3.3 Lead Contamination

Lead concentrations in geothermal fluids, while generally lower than those of arsenic and mercury, can still be significant, ranging from <1 μg/L to several hundred μg/L. This variability is influenced by geological processes and anthropogenic activities (Gill & Malamud, 2017).

In the Lake Bogoria geothermal springs, lead was detected at an average concentration of 0.06 ± 0.04 mg L^{-1}, indicating potential contamination from geological sources and surface runoff. The study highlights that while lead levels are lower than those of arsenic and mercury, they can still exceed permissible limits(10 μgL^{-1} according to NEMA and WHO), posing health risks (Sunguti et al., 2024).

Lead concentrations in fumarolic condensates are influenced by factors such as temperature, pH, and the presence of complexing agents. These factors can affect the mobility and environmental impact of lead in geothermal systems, which, although generally lower than arsenic and mercury, still pose significant risks due to lead's toxicity

and potential for bioaccumulation. The following sections explore these influences in detail.

i) Temperature and Geochemical Interactions

High temperatures in geothermal systems can enhance the mobility of lead by increasing the solubility of lead-bearing minerals. For instance, in the Okinawa Trough, high-temperature interactions (>350 °C) between hydrothermal fluids and sediments can result in significant geochemical alterations that could mobilize lead and other metals (Hsu et al., 2024).

In Japanese volcanoes, increased fumarolic activity and temperature changes have been linked to variations in the chemical composition of fumarolic gases and hot spring waters, indicating that temperature fluctuations can influence lead concentrations in these environments (Ohba et al., 2021).

At Hakone volcano, variations in the chemical and isotopic composition of fumarolic gases, such as increased CO_2/H_2O and CO_2/H_2S ratios, were linked to magmatic activity and temperature changes, suggesting that such conditions could alter the concentrations of trace metals in the system (Ohba et al., 2019). In subaqueous hydrothermal systems in crater lakes, temporal changes in lake water chemistry, including chloride (Cl) concentrations, were used to assess volcanic unrest, suggesting that temperature and chemical changes in hydrothermal fluids can influence dissolved element concentrations (Terada et al., 2022). Furthermore, the evolution of eruption styles at Kuchinoerabujima Volcano was influenced by hydrothermal recharge, which altered the mineral assemblage in volcanic ash, indicating that changes in temperature and fluid composition can affect the geochemistry of volcanic products (Minami et al., 2022).

ii) pH

The pH of geothermal fluids plays a fundamental role in regulating the mobility of lead (Pb), primarily through its control over mineral dissolution and fluid rock interactions. Under acidic conditions, lead bearing minerals particularly pyrite and other sulphides in hydrothermally altered rocks undergo enhanced dissolution, releasing Pb into surrounding fluids. This process is intensified in acid-sulphate alteration zones, where low pH promotes leaching and increases Pb concentrations in geothermal environments (Bay et al., 2021; Weydt et al., 2023). This is consistent with findings from geothermal springs, where potentially hazardous elements, including lead, are released depending on the mineral composition and pH of the sediments at the spring outflux (Wang & Cheng, 2023). The pH also affects silica scaling in geothermal fluids, which can indirectly influence lead mobility by altering the chemical environment. For instance, increasing the pH to 10.5 can mitigate silica scaling, potentially affecting the solubility and mobility of lead and other elements (Spitzmüller et al., 2021). Furthermore, the interaction of geothermal fluids with mineralized rocks under varying pH conditions can enhance the mobilization of elements such as lead, as observed in laboratory leaching tests.

iii) Environmental and Health Implications

Lead concentrations in geothermal systems, such as those observed in Lake Bogoria, can exceed permissible limits, posing health risks through dermal and ingestion exposure. This highlights the need for continuous monitoring and remediation efforts to mitigate environmental and health risks associated with lead contamination (Sunguti et al., 2024).

Isotopic studies in Japan have shown that lead in hydrothermal deposits often originates from a mix of magmatic and meteoric sources, suggesting that natural geological processes significantly contribute to lead presence in these systems (Ishida et al., 2024).

While lead mobility in geothermal systems is generally lower than that of arsenic and mercury, the environmental risks associated with lead should not be underestimated. The interplay of temperature, pH, and complexing agents can significantly influence lead concentrations, necessitating careful monitoring and management to protect environmental and human health.

2.3.4 Cadmium Contamination

Cadmium (Cd) is a heavy metal of environmental concern, commonly associated with geothermal systems, industrial activities, and agricultural pollution. Its persistence in the environment and toxicity make it a significant public health concern. In geothermal settings, cadmium is often present at lower concentrations than other hazardous elements such as arsenic and mercury, yet it remains a critical contaminant due to its potential for bioaccumulation and adverse health effects. Geochemical modeling studies have demonstrated that heavy metal deposition, including cadmium, can occur in geothermal heat exchangers, affecting both efficiency and safety in geothermal energy facilities (Lichti et al., 2024). Similarly, the Seferihisar geothermal system in Turkey has shown that improper use of geothermal resources can lead to chemical pollution, including heavy metal contamination, necessitating careful monitoring and management strategies to mitigate environmental risks (Alacali, 2024). A study in the Nagqu geothermal field, China, demonstrated that specific minerals capture potentially hazardous elements, such as cadmium, thereby reducing their release into the environment (Wang & Cheng, 2023).

While specific studies on cadmium contamination in geothermal fields within Africa and East Africa are limited, some research has documented its presence. In Kenya, geothermal areas such as the Rift Valley have been the focus of studies on heavy metal contamination. Notably, the Lake Bogoria geothermal springs have recorded cadmium levels exceeding the World Health Organization (WHO) permissible limits, with mean

concentrations of 0.05 ± 0.02 mg L^{-1}. In the Menengai geothermal field in Kenya, cadmium was among the trace elements detected in borehole water, prompting evaluations against safety standards (Wamalwa, 2017). Understanding the cadmium's retention and mobility in geothermal systems is crucial, as the mineral composition of surrounding sediments and rocks influences its behavior. These levels present potential health risks through dermal and ingestion exposures, underscoring the need for remediation efforts (Sunguti et al., 2024). Given cadmium's toxic effects, including kidney damage and bone demineralization, understanding its presence in geothermal systems is vital for public health and environmental safety.

Despite documented cadmium contamination in geothermal regions of Kenya, specific data on cadmium contamination in Mt. Suswa remain limited. As geothermal development expands, assessing cadmium levels in fumarolic condensates within this area is essential for evaluating environmental and health implications.

2.4 Seasonal Influences on Heavy Metal Concentrations

2.4.1 Impact of Dry and Wet Seasons on Emission Rates and Condensate Chemistry

Seasonal variations in heavy metal concentrations have been observed in several geothermal areas, although the patterns are not always consistent. Durowoju et al. (2016) found that arsenic concentrations in geothermal waters from the Siloam Geothermal Spring varied seasonally, with higher concentrations typically observed during the dry season. This seasonal fluctuation was attributed to changes in hydrological conditions, where reduced water flow during dry periods leads to increased evaporation and the concentration of dissolved metals such as arsenic, Lead, and Cadmium in geothermal waters. The seasonal patterns are crucial for managing environmental impacts and ensuring the safety of water resources in geothermal regions.

While these studies provide valuable insights, there is a notable lack of comprehensive research examining the relationships among multiple geothermal characteristics and heavy metal concentrations, particularly in the context of East African geothermal systems such as Mt. Suswa. Most existing studies focus on one or two parameters, often in geologically different settings. Additionally, the seasonal aspect of these relationships remains understudied, especially in areas with distinct wet and dry seasons.

The research project aimed to address these gaps by assessing the relationship between multiple geothermal characteristics (temperature, pH, flow rate, and electrical conductivity) and heavy metal concentrations in fumarolic condensates at Mt. Suswa, while also examining seasonal variations. This approach provided a more nuanced understanding of the factors influencing heavy metal concentrations in this specific geothermal system, potentially revealing complex interactions that have not been previously identified.

By focusing on Mt. Suswa, this research contributed to the body of knowledge on East African geothermal systems, which may have unique characteristics due to their geological setting within the East African Rift System. The inclusion of seasonal variations in the study design further enhanced our understanding of how climatic factors influence heavy metal concentrations in this region, which experiences distinct wet and dry seasons.

2.5 Theory of Water-Rock Interactions in Geothermal Systems

Water-rock interaction theory is a fundamental aspect of geochemistry, providing essential insights into the chemical processes occurring in geothermal environments. This theory is instrumental in understanding how geothermal characteristics affect the

concentration of trace elements and heavy metals in fumarolic condensates and hydrothermal systems.

2.5.1 Principles of Water-Rock Interactions

At the core of water-rock interaction theory is the concept that water chemically interacts with geological substrates, leading to the dissolution and mobilization of minerals and trace elements. This interaction is significantly influenced by temperature, pressure, and composition of the fluids and rocks involved (Guosen et al., 2023). In geothermal systems, these interactions are intensified by elevated temperatures and pressures, which increase mineral solubility and accelerate reaction rates, promoting the release of trace elements into solution.

The solubility of minerals and the subsequent release of trace elements are critically dependent on temperature and pH. For instance, higher temperatures typically increase the solubility of many minerals, thereby enhancing the geochemical mobility of trace elements such as arsenic and mercury, which are common in geothermal systems (Bowman et al., 2023).

2.5.2 Redox Reactions and Trace Element Behaviour

Redox conditions are also paramount in governing the behaviour and mobility of trace elements in geothermal environments. Under reducing conditions, common in many geothermal systems, certain elements, such as arsenic, become more mobile. This increased mobility under specific redox conditions is due to changes in the element's chemical form, affecting its solubility and transport within hydrothermal fluids (Pieter, 2023).

In the context of fumarolic condensates gases that escape from geothermal systems and subsequently condense these solubility dynamics are particularly evident. As the gases

cool and condense, the elements originally leached from geological formations via water-rock interactions are deposited in these condensates(Inostroza et al., 2022). Understanding redox transformations and speciation is crucial for predicting the concentrations and behaviour of heavy metals under geothermal conditions.

Complexation, often involving ligands such as chlorides or sulphides, further influences trace element behaviour in hydrothermal systems. These complexes can significantly enhance the solubility and mobility of elements like mercury and arsenic, facilitating their transport and eventual deposition in fumarolic condensate (Herdianita & Priadi, 2008). The interplay among these chemical processes provides a robust framework for modelling trace-element behaviour in dynamic geothermal environments.

2.6 Geothermal Systems and Fluid Dynamics

Several studies illustrate the critical role of geothermal systems in trace element mobilization. For example, research conducted in Mexico highlights the significant influence of thermal fluid characteristics and underlying geological formations on the distributions of arsenic and mercury within geothermal fields (Birkle et al., 2008). Similarly, in Iceland, the interaction of geothermal fluids with basalts has been shown to concentrate arsenic due to water-rock reactions, underscoring the role of host rock composition in elemental behaviour (Edwards et al., 2024).

Geothermal systems are characterized by complex interactions involving fluid mixing, boiling, and condensation, which significantly influence the concentration of trace elements in fumarolic condensates. These geochemical processes create unique environments that affect metal concentrations observed in geothermal fluids:

i) Fluid Mixing

The interaction between ascending geothermal fluids and cooler groundwater or seawater can lead to fluid-fluid mixing. This mixing alters the chemical composition of the fluids, including trace metal concentrations. For instance, in some geothermal systems, mixing high-temperature geothermal fluids with seawater can result in significant changes in gas composition and mineral solubility (Chiodini et al., 2023).

ii) Pressure-Temperature Conditions

The specific pressure and temperature conditions within geothermal systems determine the extent of boiling and condensation. These conditions influence the solubility of various trace elements and gases, thereby affecting their concentrations in fumarolic emissions. For example, high salinity and low pH conditions can enhance the mobility of trace metals by increasing their solubility (Chiodini et al., 2023).

2.6.1 Impact on Trace Element Concentration and Geochemical Disequilibrium

The dynamic processes in geothermal systems significantly influence trace element concentrations in fumarolic condensates. Variations in pH, mineral interactions, and ongoing geochemical processes contribute to the mobility and concentration of trace metals. Low pH conditions, often associated with CO_2-rich waters, enhance the dissolution of primary minerals, thereby increasing trace metal release into geothermal fluids (Hsu et al., 2024).

The presence of gas species in geothermal systems often leads to disequilibrium with mineral assemblages, resulting in fluctuations in trace element concentrations across fumarolic emissions. Studies indicate that hydrothermal fluids can alter the geochemical

characteristics of sediments, further impacting trace element distribution (Hsu et al., 2024).

While these processes enhance trace metal mobility, they also pose environmental and health risks, necessitating careful monitoring and management of geothermal resources to mitigate potential contamination (Sunguti et al., 2024).

2.6.2 Implications and Future Directions

The comprehensive understanding of water-rock interactions provides a theoretical basis for advancing studies on trace element behaviour in geothermal systems. As geothermal energy development expands, recognizing the role of these processes becomes increasingly pivotal in environmental monitoring and management strategies. Future research should focus on refining models to predict trace element patterns under varying geothermal conditions and on improving mitigation strategies to address potential environmental and health risks associated with trace elements in geothermal areas.

The geochemical theory of water-rock interaction provides a nuanced understanding of the processes that affect trace element concentrations in geothermal systems. By integrating principles of mineral solubility, redox processes, and geothermal dynamics, this framework is indispensable for investigating and managing the complexities of trace element behaviour in fumarolic condensates.

2.6.3 Mobility and Speciation

The mobility of lead in geothermal systems is significantly influenced by its interactions with various elements and compounds, particularly under varying environmental conditions. Lead's tendency to form galena (PbS) makes it relatively insoluble; however, changes in pH and redox conditions can enhance its mobility through the formation of soluble complexes. Lead primarily binds with sulphides ions to form galena (PbS),

which is stable and insoluble under neutral to acidic conditions. Alterations in pH and redox potential can lead to the formation of soluble lead chloride and carbonate complexes, increasing lead's mobility in geothermal fluids. The environmental impact of lead is closely tied to its speciation; soluble forms can more easily migrate, potentially contaminating surrounding ecosystems. The retention of potentially hazardous elements, including lead, is influenced by mineral deposition in geothermal sediments, which can either sequester or release these elements based on geochemical conditions (Wang & Cheng, 2023). While the focus is often on lead's mobility and its environmental implications, it is essential to consider that the presence of other minerals and microbial activity can also play a crucial role in determining lead's behaviour in geothermal systems.

Cadmium's mobility in geothermal environments is significantly influenced by geochemical processes, particularly under acidic conditions. In such settings, cadmium forms soluble complexes, enhancing its transport. However, precipitation reactions can immobilize cadmium in mineral forms, complicating its overall mobility. In acidic geothermal fluids, cadmium solubility increases, facilitating its movement through water systems. Precipitation reactions, such as the formation of cadmium carbonates, can capture cadmium, limiting its mobility. The presence of smectite clay enhances cadmium retention through adsorption and co-precipitation processes, further immobilizing it under specific conditions (Missana et al., 2023).

Temperature plays a central role in the behaviour of these heavy metals in geothermal settings. High thermal gradients increase the dissolution rates of metal-bearing minerals, potentially leading to increased metal concentrations. Conversely, lower temperatures might favour the precipitation of metal compounds, reducing their mobility. For instance,

the cooler margins of geothermal fields could serve as zones where metal deposition primarily occurs, forming geochemically distinct barriers (Pulungan et al., 2019).

Geochemical models and experimental studies have focused on these factors to predict heavy-metal behaviour in geothermal environments. They underscore the need for precise monitoring of conditions like pH, redox potential, and temperature to anticipate heavy metal mobility and its potential impacts on environmental and public health.

2.6.4 Sources and Pathways

The primary sources of heavy metals in fumarolic condensates are linked to volcanic activity, leaching from surrounding mineral-rich rocks, and anthropogenic influences. Fumarolic gases emitted during volcanic eruptions carry volatile metal species. These metals can condense when the gases cool, contributing to the heavy metal content in fumarolic condensates. The chemical composition of volcanic and fumarolic gases is largely determined by the nature of the underlying magma and its interaction with surrounding geological formations. Variations in magmatic composition and subsurface conditions influence the concentration and mobility of volatile elements, leading to the transport and subsequent precipitation of heavy metals such as arsenic (As), lead (Pb), and mercury (Hg) from volcanic materials into the environment (Inostroza et al., 2023; Schlesinger et al., 2022).

Heavy metals can also enter fumarolic systems through leaching processes. Rainwater or hydrothermal fluids can dissolve metals from mineral-rich rocks in the vicinity of fumaroles. This interaction enhances the concentration of heavy metals in the condensates, as evidenced by studies that show significant water-rock interactions in geothermal environments (Campeny et al., 2023).

In geothermal systems, geothermal fluids circulate through rock formations, scavenging metals and minerals that can be released into the condensates. This geochemical cycling can result in significant variability in concentrations across different spatial locations depending on geological features such as faults and fractures that facilitate fluid movement (Ayari et al., 2023).

2.7 Health Risks Associated with Heavy Metal Exposure

2.7.1 Toxicological Effects of Heavy Metals

Heavy metals such as arsenic, mercury, lead, and cadmium are prevalent environmental pollutants known for their significant toxicological effects on human health. Exposure to these metals can occur through various pathways, notably ingestion and dermal contact, leading to a spectrum of adverse health outcomes.

Arsenic

Arsenic is a naturally occurring metalloid widely distributed in the Earth's crust and frequently detected in groundwater due to natural geochemical processes and anthropogenic influences. Chronic exposure to arsenic, particularly through the consumption of contaminated drinking water, poses significant public health risks. The International Agency for Research on Cancer (IARC) has classified arsenic and its compounds as Group 1 carcinogens, indicating conclusive evidence of their carcinogenicity in humans. Prolonged ingestion of arsenic-contaminated water has been associated with an increased risk of various cancers, including those of the skin, lungs, bladder, and kidneys (Ganie et al., 2024; Raja, 2023).

Mercury

Mercury exists in various forms, including elemental mercury, inorganic mercury compounds, and organic mercury compounds such as methylmercury. Each form has a

distinct toxicological profile, with methylmercury being particularly hazardous due to its ability to bioaccumulate in the food chain. Mercury primarily targets the central nervous system; exposure can result in neurological and behavioural disorders. Symptoms include tremors, insomnia, memory loss, neuromuscular effects, headaches, and cognitive and motor dysfunction. In severe cases, mercury poisoning can lead to erethism, characterized by excitability, tremors, memory loss, timidity, and insomnia (ATSDR, 2024). Prenatal mercury exposure can adversely affect foetal development, leading to cognitive impairment and developmental delays (Elnabi et al., 2023). Dermal exposure to mercury, particularly inorganic mercury compounds, can cause skin irritation, rashes, and discoloration. Chronic dermal exposure has been linked to conditions such as acrodynia, characterized by pink skin discoloration, swelling, and pain (Balali-Mood et al., 2021; WHO, 2011).

Lead

Lead is a heavy metal that has been widely used in various industrial applications, including batteries, paints, and gasoline additives. Exposure to lead can occur through ingestion of contaminated food or water, inhalation of lead particles, or ingestion of lead-based paint chips, particularly in older buildings (ATSDR, 2020). Lead poisoning affects multiple body systems, with the nervous system being the most sensitive. In children, lead exposure can result in developmental neurotoxicity, leading to reduced IQ, attention deficits, and behavioural problems. In adults, lead exposure is associated with hypertension, renal impairment, and reproductive toxicity(Balali-Mood et al., 2021). While ingestion is the primary route of exposure, dermal absorption of lead is generally low but can occur, especially in occupational settings or through contact with lead-contaminated soil or water (USEPA, 2011).

Cadmium

Exposure to cadmium can occur through inhalation of contaminated air, ingestion of contaminated food (particularly leafy vegetables and grains), and tobacco smoke. Cadmium is highly toxic to the kidneys, where it accumulates and can cause renal dysfunction. It also affects bone metabolism, leading to osteomalacia and osteoporosis, increasing the risk of fractures (Rezaei et al., 2019). Chronic cadmium exposure has been linked to an increased risk of cancer, particularly lung cancer. Dermal exposure to cadmium is less common but can occur, leading to skin irritation and allergic reactions (Balali-Mood et al., 2021). Occupational settings involving cadmium use present higher risks for dermal exposure.

In the context of Mt. Suswa, Kenya, fumarolic condensates may contain these heavy metals, posing potential health risks to local communities. Ingestion pathways could include consuming contaminated water or food, while dermal contact might occur through direct contact with contaminated soil or water sources. Assessing the concentrations of these metals in fumarolic condensates and understanding the exposure pathways are crucial steps in evaluating and mitigating health risks in the region.

2.7.2 Mechanisms of Heavy Metal Injection into Human Bodies

Heavy metals, ubiquitous in various environmental matrices, can enter the human body through different pathways, each influencing the extent and severity of exposure. This literature review examines the primary mechanisms by which heavy metals are introduced into the human body, focusing on ingestion, inhalation, dermal absorption, and less conventional routes.

i) ***Ingestion***

Ingestion remains the primary pathway by which humans are exposed to heavy metals, primarily through contaminated food and drinking water. Among these contaminants, lead in drinking water remains a major public health concern, often originating from corrosion or leaching from aging plumbing systems. Studies across different regions have shown that lead concentrations in distribution networks can exceed safe drinking-water limits, posing chronic health risks, particularly to vulnerable populations (Waseem et al., 2025). Arsenic, naturally found in groundwater, especially in areas such as Bangladesh and parts of the United States, poses chronic exposure risks through the consumption of contaminated water (Yao et al., 2024). These studies underscore the critical role of environmental monitoring and regulation in mitigating ingestion-related exposure risks.

Inhalation

The inhalation route is particularly significant near industrial sites and urban areas with high vehicular emissions. Particulate matter in the air can carry heavy metals like cadmium, lead, and nickel, which are then inhaled and deposited in the respiratory system. Occupational exposure also contributes significantly, with workers in industries such as battery manufacturing, mining, and metal smelting at higher risk of inhaling heavy metal-laden dust and fumes (Majewski et al., 2023). Research has shown that inhaled particles can cause severe health effects, including respiratory and cardiovascular diseases, underscoring the need for stringent occupational safety measures (Balali-Mood et al., 2021).

Dermal Absorption

While dermal absorption is generally a less common route for heavy metals to enter the body, certain compounds, such as those of mercury and arsenic, can penetrate the skin

barrier. Instances of dermal exposure are more prevalent in occupational settings where workers handle metals without adequate protective gear. The solubility and formulation of the heavy metal compound significantly influence dermal absorption rates. Studies have also explored the role of consumer products, such as cosmetics and paints, in facilitating dermal exposure to metals like lead and mercury, underscoring the importance of regulation and consumer awareness (Khalili et al., 2019).

Less Conventional Routes

Emerging research has explored other potential routes of heavy metal exposure, albeit less documented, such as intravenous administration through contaminated medical products. Historically, incidents of contaminated pharmaceuticals or improper use of metal-based medical devices have led to direct injection of metals into the bloodstream (Abd Elnabi et al., 2023). Additionally, certain traditional medicines and remedies have been found to contain high levels of heavy metals, posing risks of both ingestion and systemic exposure (Luo et al., 2021).

The literature suggests a complex interplay among environmental sources and exposure pathways that enables heavy metals to enter the human body. Ingestion and inhalation remain the most significant routes of exposure, influenced by environmental contamination and occupational hazards. Dermal absorption, though less common, remains a critical exposure route in specific contexts, underscoring the need for stronger occupational and consumer product safety standards. Understanding these mechanisms is vital to developing effective public health interventions and regulatory policies to minimize human exposure to heavy metals. Continued research and monitoring are essential to address emerging exposure risks and protect public health.

2.8 Health Risks of Heavy Metal Contamination in Fumarolic Condensates

The exclusive use of fumarolic condensates from Mt. Suswa as the sole water source for domestic and livestock use poses substantial health risks due to contamination with heavy metals such as arsenic (As), mercury (Hg), lead (Pb), and cadmium (Cd). These metals induce non-carcinogenic effects, such as neurological impairment (Pb, Hg), renal dysfunction (Cd), and gastrointestinal distress (As), as well as carcinogenic risks via ingestion (drinking) and dermal exposure (bathing, washing), including skin and bladder cancer (As) and kidney cancer (Cd). These health risks underscore the importance of assessing contamination levels in areas where populations rely on geologically sourced water (Gong et al., 2022; USEPA, 2011; Wang et al., 2023).

2.8.1 Health Risk Assessment (HRA) Models

The U.S. Environmental Protection Agency (USEPA) Health Risk Assessment (HRA) models specifically the Hazard Quotient (HQ) and Hazard Index (HI) for non-carcinogenic risks, and Lifetime Cancer Risk (LCR) for carcinogenic risks quantify these threats through ingestion and dermal exposure pathways, thereby guiding mitigation efforts. These models provide a robust framework for evaluating human health risks associated with environmental contaminants (USEPA, 2011).

Carcinogenic Health Risk Assessment

Carcinogenic health risk assessment evaluates the likelihood of cancer development from chronic exposure to metals like arsenic (As) and cadmium (Cd), classified as Group 1 carcinogens by the International Agency for Research on Cancer (IARC). As is linked to skin, lung, and bladder cancers, while Cd is associated with kidney and lung cancers (Khatoon et al., 2024). The Lifetime Cancer Risk (LCR) quantifies this probability, with USEPA risk thresholds defining negligible (LCR $< 1 \times 10^{-6}$), acceptable ($1 \times 10^{-6} \leq$

LCR < 1×10^{-4}), and unacceptable (LCR ≥ 1×10^{-4}) risk levels (Niknejad et al., 2023; USEPA, 2011; WHO, 2011b).

2.9 Research Gap

From the reviewed empirical evidence, critical knowledge gaps emerge. First, there has been limited focus on fumarolic condensates as a contamination pathway. While geothermal research in Kenya and across the East African Rift has examined hot springs, groundwater, and soils, fumarolic condensates remain largely overlooked despite being a primary water source for communities in Suswa and other geothermal regions. Second, there is insufficient spatial mapping of contamination patterns, as few studies have systematically measured and mapped heavy metal concentrations around fumarolic vents.

This has left uncertainties regarding localized hotspots of contamination and the influence of proximity to vents on exposure risks. Third, seasonal variations in heavy metal emissions and their implications for exposure have not been adequately explored, particularly in Mt. Suswa's arid-to-semiarid climatic context, where rainfall and evaporation strongly influence water quality. Finally, there has been a neglect of community-based exposure data, since most studies rarely integrate household surveys and interviews to document how local populations use fumarolic condensates, the frequency of contact, and their perceived health impacts. Without such participatory approaches, assessments of exposure pathways remain incomplete. These gaps provided the foundation for the present study, which uniquely integrates chemical analysis, geospatial mapping, household surveys, and health risk assessment.

2.10 Conceptual Framework

Following a comprehensive review of relevant literature and the identification of the research problem, a conceptual framework was developed to illustrate the interrelationships among the key variables in this study. The framework is structured around three categories of variables: independent, intervening, and dependent that collectively guide the assessment of spatio-seasonal variations in heavy metal contamination, while integrating health risk assessment and community perceptions.

The independent variables comprise geothermal activity, geological composition, and seasonal variations, which act as the primary drivers of heavy metal contamination in fumarolic condensates. Geothermal processes such as fumarole emissions and fluid–rock interactions mobilize trace metals into the environment, while geological composition contributes through mineral leaching and rock–water interactions. Seasonal variations, particularly rainfall during wet periods, affect the dissolution, mobilization, and transport of heavy metals.

Intervening variables function as mediators, modifying contamination levels and shaping the extent of associated health risks. Hydrogeological patterns, including groundwater flow and infiltration rates, affect the transport and distribution of metals, while geochemical interactions such as metal speciation and adsorption–desorption regulate their bioavailability and toxicity. At the community level, behaviors related to water use, cultural practices, and reliance on fumarolic condensates for domestic needs influence exposure pathways. Moreover, community awareness and local mitigation strategies can reduce risks.

The dependent variables include the concentrations of heavy metals in fumarolic condensates, their spatio-seasonal distribution, and the corresponding health risks. These

are measured outcomes that form the empirical basis for assessing contamination levels. Health implications are evaluated through toxicological indices, including carcinogenic risk (CR), in line with the third study objective, which is to evaluate the potential human health risks posed by exposure to heavy metals in the Mt. Suswa area.

Integrating household survey data on water use practices, exposure frequencies, and community perceptions, the framework ensures that both quantitative measurements and qualitative insights inform the risk assessment process. The framework demonstrates the dynamic interplay between geothermal processes, geological and seasonal factors, environmental mediators, and community practices, all of which converge to influence heavy metal contamination and health risks.

2.11 Conceptual Framework

Figure 1

Diagram Representation of Proposed Conceptual Framework

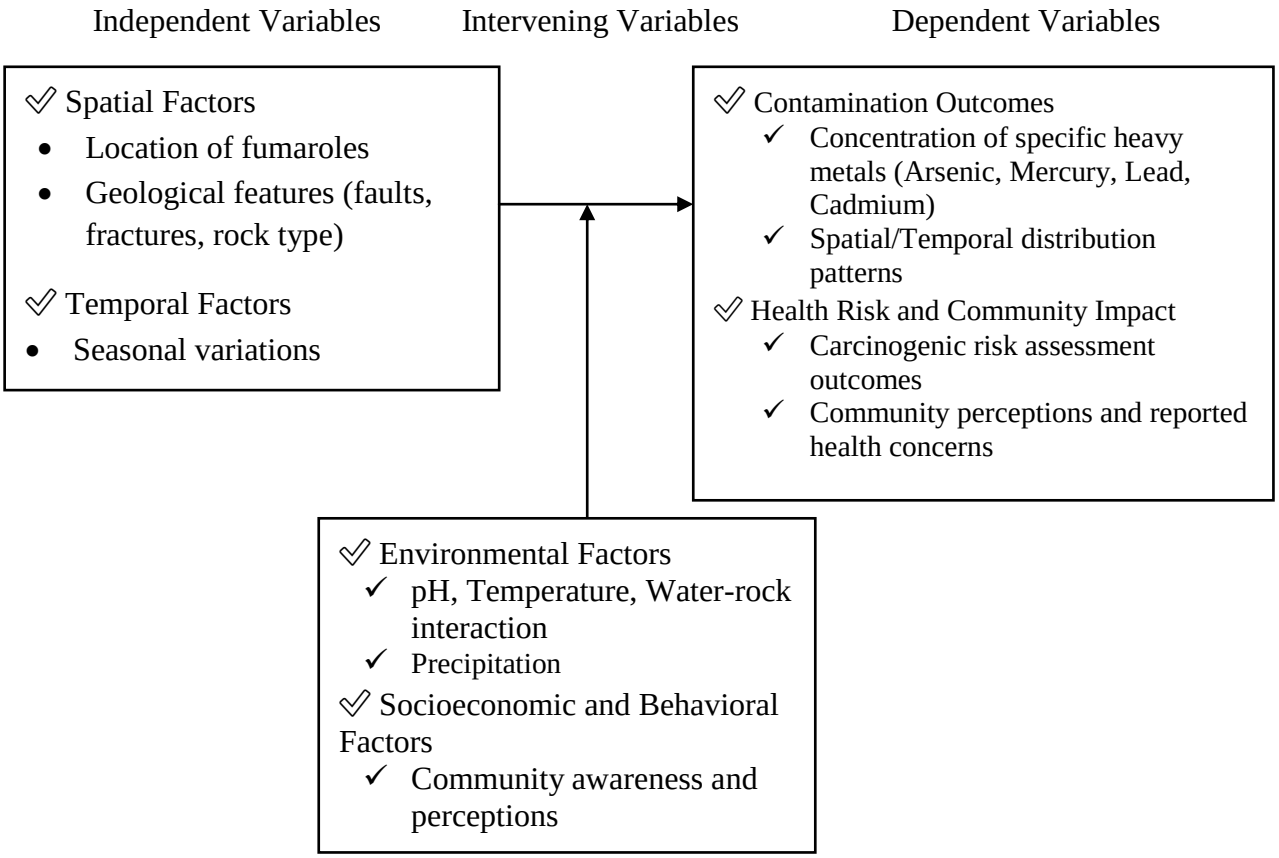

*Source:*Researcher,(2024)

2.11.1 Conceptual Flow and Relationships

The conceptual framework diagram (Figure 1) illustrates the complex interactions among factors influencing heavy metal contamination in fumarolic condensates at Mt. Suswa. It begins with independent variables, which include spatial and geological factors such as the location of fumaroles, underlying rock types, mineral composition, and structural features such as faults and fractures. Temporal dynamics, particularly seasonal variations between wet and dry periods, also play a critical role in determining fluctuations in

heavy metal concentrations over time. These spatial and temporal factors form the primary drivers of contamination variability within the geothermal system.

The influence of these independent variables is shaped by intervening variables, which represent environmental, geochemical, and social processes that either amplify or mitigate contamination levels. Climatic factors, such as precipitation and ambient temperature, along with water–rock interactions and pH conditions, regulate the mobility, solubility, and deposition of heavy metals. Geochemical processes, including adsorption and desorption mechanisms, further determine the bioavailability of contaminants. At the community level, behaviors related to the use of fumarolic condensates, cultural perceptions of water quality, and access to healthcare services serve as additional moderating factors, directly influencing exposure patterns and shaping the eventual health risks associated with contamination.

The dependent variables constitute the measurable outcomes of the study. These include the concentrations of arsenic (As), lead (Pb), mercury (Hg), and cadmium (Cd) in fumarolic condensates, analyzed to reveal spatial and seasonal variations in contamination. Beyond these direct measurements, dependent outcomes also encompass health risk assessment indices derived from toxicological models, as well as community perceptions and opinions regarding the quality and safety of condensed steam. Together, these outcomes provide a holistic understanding of contamination risks and their implications for both environmental and human health.

The directional arrows in the conceptual framework diagram demonstrate how independent variables (spatial and temporal drivers) exert direct influence on contamination levels, while intervening variables (environmental factors and Socioeconomic and Behavioral Factors) moderate these relationships. The combined

effect ultimately shapes both the distribution of heavy metals in fumarolic condensates and the degree of health risk to the surrounding communities.

CHAPTER THREE

RESEARCH METHODOLOGY

3.1 Introduction

This chapter outlines the methodology used to assess the presence and behaviour of dissolved heavy-metal ions in fumarolic condensates within the Mt. Suswa geothermal system. The study focused on metals originating from rock–steam interactions, in which high-temperature fumarolic emissions leach trace elements from surrounding volcanic rocks and mobilize them into the condensate in soluble ionic (oxidized) forms. The chapter details the research design, the study area, the target population, the sampling procedures, and the sample size determination. It further presents the pilot study procedures, the approaches used to ensure the validity and reliability of the research instruments, the data collection methods, including the acquisition of condensate samples for heavy-metal and physico-chemical analysis, and the analytical techniques applied to quantify dissolved ions. Finally, the chapter outlines the data analysis methods and the ethical considerations observed throughout the research process.

3.2 Research Design

This study employed a mixed-methods design to assess heavy metal concentrations in fumarolic condensates at Mt. Suswa, examine their spatial and seasonal variations and distribution, and evaluate associated human health risks. The methodological framework integrated field sampling, laboratory analysis, and health risk modeling to generate a robust dataset that provided both environmental and public health insights.

According to (2023), a research design refers to the arrangement of conditions for the collection and analysis of data in a manner that aims to balance relevance to the research purpose with economy and procedure. Grounded in this framework, the study employed

a cross-sectional mixed-methods field design, deliberately integrated to capture environmental measurements and community-level data simultaneously and efficiently.

Fieldwork was conducted during two distinct seasons: the dry season (January–March 2025) and the wet season (May–July 2025). This seasonal stratification enabled a comparative evaluation of heavy metal concentrations and associated exposure risks across varying hydrological and climatic conditions.

The quantitative component of the study followed a longitudinal design in which heavy metal concentrations were measured across different fumarolic sites and compared between seasons. This approach enabled the identification of contamination trends, the development of evidence-based mitigation strategies, and the generation of data relevant for policy formulation and decision-making (Inostroza et al., 2022).

Complementing the quantitative analysis, the qualitative component employed structured questionnaires administered to local residents. These were designed to capture community perceptions/opinions on the quality of condensed steam and lived experiences associated with environmental contamination. Insights from these interactions enriched the study by elucidating exposure pathways and socio-economic factors that potentially amplified health risks (Ngwenya et al., 2024). By triangulating quantitative and qualitative data, the mixed-methods approach provided a holistic understanding of the contamination–health nexus within the study area.

3.3 Study Area

The study was carried out at Mt. Suswa, situated in Kajiado County within the East African Rift System (EARS)—a tectonically active continental rift extending from the Afar Triple Junction in northeastern Africa to Mozambique. Mt. Suswa is part of Kenya’s geothermal potential in this rift zone (IRENA, 2020). Mt. Suswa (Figure 2) lies

approximately 120 km northwest of Nairobi, the capital city of Kenya, between longitudes 34°45′ E and 36°00′ E and latitudes 0°45′ S and 2°00′ S (Kipngok et al., 2017).

Mt. Suswa is a dormant volcanic complex within the Kenyan Rift Valley, distinguished by its unique double-caldera structure that was formed through multiple episodes of volcanic activity. The inner caldera is steep-walled, whereas the outer caldera hosts diverse geothermal features such as fumaroles, hot-baked grounds, and hydrothermal vents. The volcanic terrain is predominantly composed of porous lava flows and pyroclastic deposits, which limit the retention and storage of groundwater (IRENA, 2020; Kipngok et al., 2017).

Climatically, Mt. Suswa, situated within the Greater Mara–Serengeti Ecosystem, experiences a bimodal rainfall pattern typical of Eastern Africa. The long rains occur from April to July, while the short rains are experienced from September to November. The dry season extends from January to March. These rainfall dynamics are strongly influenced by regional climate phenomena, such as the El Niño–Southern Oscillation (ENSO) and the Indian Ocean Dipole (IOD), both of which significantly influence rainfall distribution and variability across the region (Zhu et al., 2022).

Figure 2

A Map showing The Study Location and Fumarole Sites

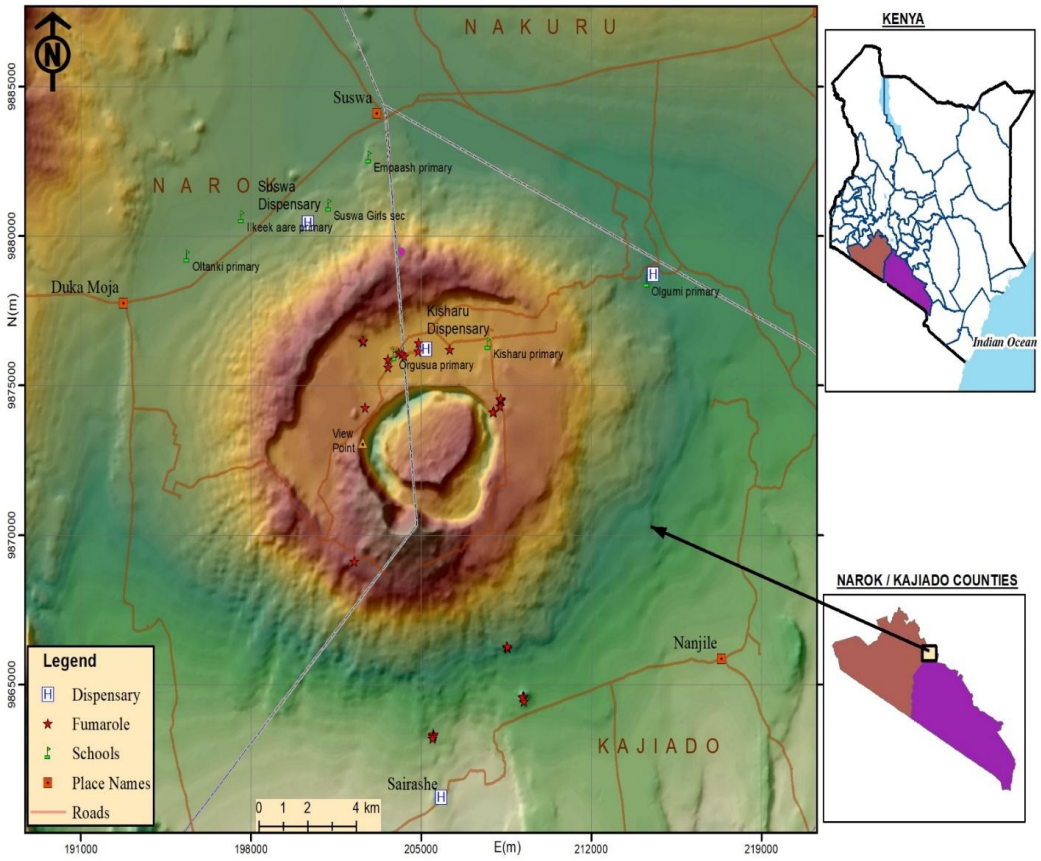

*Source:*GDC, (2022)

The area is sparsely populated and predominantly inhabited by the Maasai community, whose primary economic activity is pastoralism. In addition to its geothermal potential, Mt. Suswa also holds ecological and cultural significance. For instance, the Suswa caves within the caldera serve as sites for traditional Maasai ceremonies and other cultural practices (James et al., 2021).

The prevailing arid-to-semiarid conditions in Mt. Suswa, coupled with the absence of perennial rivers, dams, or lakes, severely constrain water availability for the local community. Rainwater harvesting is practiced but remains unreliable due to the region's erratic rainfall patterns, making fumarolic condensates the principal and often the sole

source of water for domestic use. These condensates are obtained directly from steaming fumaroles, where vapor is visibly emitted from the geothermal vents (Plate 1).

Plate 1: Steaming Fumaroles (Researcher,2025)

In response to pressing water needs, some fumaroles have been modified to channel condensed steam to collection points, enabling easier access and improved storage (Plate 2). Once collected, the condensates are stored in reservoir tanks situated within homesteads or communal areas, providing a dependable (though chemically unmonitored) source of water for drinking, cooking, and other domestic purposes (Plate 3).

Plate 2: A Modified fumarole vent (Researcher, 2025)

Plate 3: A Photo showing collection of condensates in a reservoir tank (Researcher,2025).

The reliance on these condensates highlights the close interaction between geothermal activity and human livelihoods in the area. The vast scale of the Mt. Suswa volcanic system, with outer and inner calderas measuring approximately 14 km and 10 km in diameter respectively, underscores the magnitude of geothermal processes shaping both the natural environment and community resource dependence (Kipngok et al., 2017).

3.4 Target Population

The study population comprised household heads in Kisharu sub-location, Mt. Suswa, who rely on condensates from ten (10) modified fumarolic vents for their domestic water needs. According to the 2019 Kenya Population and Housing Census, Kisharu sub-location had a population of 720 people (KNBS, 2019), with household heads serving as the critical unit of analysis due to their direct exposure to potential heavy metal contamination. These households were therefore selected as the primary units of analysis

In contrast, sixteen (16) of the twenty-six (26) fumaroles in the study area, which were in rugged terrain and distant from human settlements, had not been modified for community use. For these fumaroles, the study focused exclusively on assessing the extent of heavy metal contamination in their condensates.

To enrich household-level data and provide deeper contextual insights, key informants were engaged to explore community perceptions, water-use practices, levels of awareness, and coping and adaptation strategies. These informants comprised local administrators (chief, sub-chief, and village elders) and healthcare professionals at Kisharu Dispensary. Their perspectives were essential in clarifying community perceptions, water-use practices, levels of awareness of contamination risks, and coping or adaptation strategies in response to water scarcity and potential health hazards.

A total of twenty-six (26) fumaroles were identified in the Mt. Suswa study area during field reconnaissance. Out of these, ten (10) fumaroles had been modified for direct community use, with one located inside the caldera and nine outside. These modified vents were equipped with collection systems and served as critical domestic water sources. An additional nine (9) unmodified fumaroles located in rugged or distant terrain were included in the sampling, bringing the total number of sampled fumaroles to nineteen (19). Seven fumaroles were not sampled due to inaccessibility or inactivity at the time of fieldwork. To provide a non-fumarolic comparison, one control sample was obtained from tap water at Suswa Trading Centre, located approximately 12 km away. This classification as shown in Table 1 below ensured that both environmental and community-use perspectives were captured while offering a comprehensive representation of the geothermal system.

Table 1

Classification and Sampling Status of Fumaroles in the Mt. Suswa Study Area

Fumarole Category	Location	Number of Fumaroles	Description
Modified fumaroles (community use)	Inside caldera	1	• Equipped with collection system
	Outside caldera	9	• Directly used by households for domestic water.
Unmodified fumaroles (non-community use)	Rugged/distant terrain	9	• Vents not modified • But accessible for sampling.
Total fumaroles sampled	–	19	• Subset of fumaroles (10 modified + 9 unmodified)
Not sampled fumaroles	Inaccessible/ inactive	7	• Vents located in rugged terrain or not actively emitting at the time of fieldwork.
Control sample	Suswa trading centre	1	• Tap water located ~12 km from the study area. • Represents a non-fumarolic domestic source.
Total fumaroles identified	–	26	• All fumaroles recorded in the Mt. Suswa study area.

3.5 Sampling Design, Procedure and Sample Size

This section describes the sampling framework used to obtain representative fumarolic condensate samples and household data for the study.

3.5.1 Sampling Design

A purposive random sampling design was employed to ensure representative coverage of fumarolic condensates across Mt. Suswa. The approach considered both environmental heterogeneity and human exposure risks by integrating the geological distribution of fumarolic vents with community water-use patterns.

The visibility of active steam emissions and accessibility guided site selection. Out of the targeted fumaroles, nineteen (19) were successfully sampled based on accessibility

constraints and their relevance to local water-use practices. Within this group, ten (10) fumaroles actively utilized by households were prioritized for detailed analysis due to their heightened significance for human health exposure pathways.

This design ensured that both environmentally significant fumaroles and those directly linked to community water consumption were represented. As a result, the sampling framework provided sufficient spatial and social coverage to capture contamination variability while reflecting real exposure risks faced by residents.

3.5.2 Sampling Procedures for the Condensates

Samples were collected randomly from discharging fumaroles and installed condensation tanks using clean, acid-washed polyethylene bottles that had been rinsed with fumarolic condensates prior to collection to minimize contamination. Each bottle was clearly labeled with the site code, date, time, and other relevant sampling details. The geographical coordinates of each sampling site were recorded using a handheld GPS device for accurate geospatial referencing.

To ensure analytical accuracy and reliability, triplicate samples were collected from each fumarole during every sampling event. Sample in bottle 1 was acidified in the field with 1 mL of concentrated nitric acid (HNO_3) to lower the pH to below 2, thereby preventing the adsorption of metals onto the container walls and preserving dissolved metals for trace-element and major-cation analyses. The second sample was left unacidified for the analysis of major anions. The third sample was reserved for *in situ* determination of physico-chemical parameters, including temperature (T), pH, and electrical conductivity (EC), using a calibrated thermocouple and a multiparameter pH/EC/TDS meter.

Fieldwork was conducted during two distinct seasons to account for temporal variability in heavy metal concentrations. The seasonal stratification provided a comprehensive

dataset that captured changes in contamination patterns across varying hydrological and climatic conditions.

Immediately after collection, all samples were preserved at approximately 4°C to maintain their integrity. Samples were transported within 24 hours in insulated ice-cooler boxes to the Geothermal Development Company (GDC) Laboratory at Menengai, where they were stored at 4°C until analysis. Sampling and analytical procedures followed standard protocols as defined by the American Public Health Association (APHA, 2022).

Sampling Fumarolic Condensates

Prior to sampling, temperatures at various points within each fumarolic vent were measured to identify the optimal spot for condensate collection, thereby ensuring the most representative gas flow was captured. Once the appropriate point was identified, a funnel was placed upside down over the main upflow of the fumarole vent. The edges of the funnel were tightly sealed with mud or clay to prevent the intrusion of atmospheric air, thereby minimizing contamination and ensuring that the collected condensates were representative of geothermal emissions.

In this study, fumarolic steam was collected by directing the gas through a funnel connected to a pre-evacuated, double-port collection bottle, which was kept in a bucket of cooling water to promote rapid condensation. The bottle was linked to the funnel using flexible Teflon or silicone tubing, allowing the vacuum within the container to draw fumarolic gases into the system as illustrated in Figure 3. As the steam cooled, it condensed within the evacuated bottle, after which the condensate was transferred into sterile containers for preservation and laboratory analysis. Comparable steam-condensation sampling approaches using evacuated vessels, cooling baths, and inert tubing have been documented in recent geothermal studies (Yaguchi et al., 2025).

Figure 3

Sampling Scheme for Condensate Collection

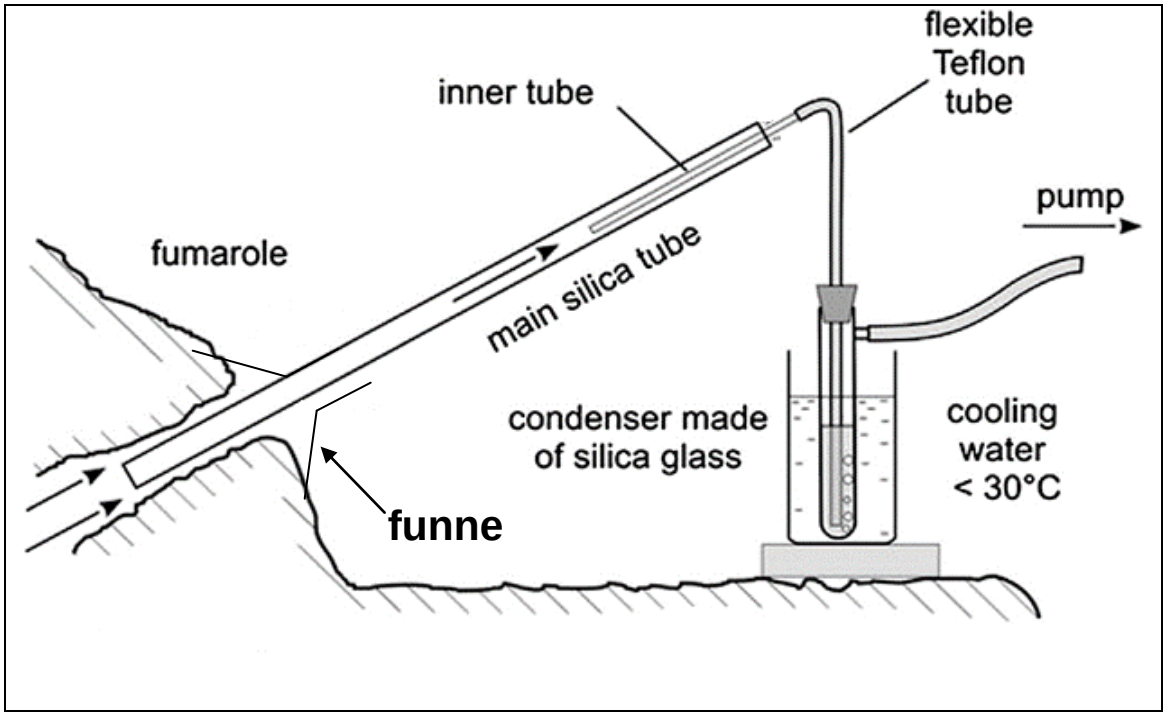

Source: Modified from Zelenski et al., (2013)

3.5.3 Sample Size Determination for Key Informants

Determining an appropriate sample size was essential to ensure the reliability and validity of the research findings. The process involved selecting a sufficient number of participants to adequately represent the target population while balancing practical constraints such as time, cost, and ethical considerations. Sample size determination was guided by three key aspects (Garg et al., 2024).

First, the variable of interest in this study was community perceptions of the quality of water for various usage in Kisharu Sub-location. Ensuring the sample was representative of the population enabled meaningful analysis and reliable conclusions. Second, the desired level of confidence reflected the degree of certainty that the sample outcomes mirrored the true population characteristics. Studies requiring higher confidence levels generally require larger sample sizes to minimize sampling error. Third, the acceptable

margin of error defined the allowable deviation from the true population parameter, directly influencing the precision of the findings.

According to the 2019 Kenya Population and Housing Census, Kisharu Sub-location had a total population of 720 individuals (KNBS, 2019). With an average household size of four persons, consistent with regional estimates from the United Nations (2022), this translated to approximately 180 household heads, who formed the study's target population.

To determine the statistically valid sample size, Cochran's formula (Eq. 3.1) (Cochran, 1977) for continuous data was applied. This method is widely used in health-related research to estimate prevalence rates and other proportions related to environmental exposure (Chihobve, 2022). It is expressed as:

$$n_0 = \frac{z^2 . p . q}{E^2} \quad \text{Eq (3.1)}$$

Where:

$n_{0=}$ The initial sample size for an infinite population

z = The z-value corresponding to confidence level (typically 1.96 for 95% confidence)

p = Estimated proportion of the population with the characteristic (health outcome prevalence, assumed 0.5 for maximum variability)

q = 1 – p (complementary proportion)

E = Margin of error (0.05 for ±5% precision)

Substituting these values:

$$n_0 = \frac{1.96^2 x 0.5 x 0.5}{0.5^2} = \frac{3.8416 x 0.25}{0.0025} = \frac{0.9604}{0.0025} = 384$$

Since the target population (N = 180) was finite, the Finite Population Correction (FPC) was applied using Eq. 3.2 (Althubaiti, 2023):

$$n = \frac{n0}{\{1+\left[\frac{(n0-1)}{N}\right]\}}$$ ..... Eq (3.2)

Substituting values:

$$n = \frac{384}{\{1+\left[\frac{(384-1)}{180}\right]\}} = \frac{384}{\{1+\frac{383}{180}\}} = \frac{384}{\{1+212777} = \frac{384}{\{3.12777\}} = 122.777$$

Thus, the adjusted sample size for household heads was 123 respondents. This sample size was deemed sufficient to ensure robust representation of the study population, while maintaining statistical reliability and precision in data collection and analysis. The determination aligned with current methodological standards for environmental health research (Lakens, 2022).

Assumptions for Computation

Following Nanjundeswaraswamy & Divakar (2021), the assumptions are:

i. A 95% confidence level (z = 1.96) ensures statistical reliability within this interval.
ii. An estimated prevalence (p) of 0.5 is assumed, maximizing sample size in the absence of prior health data from Kisharu, with q = 0.5
iii. A 5% margin of error (E = 0.05) balances precision and feasibility in health risk estimation. These assumptions ensure robust and representative data collection.

Sampling Respondents

An equal allocation approach was adopted to ensure a balanced distribution of respondents across the ten (10) modified fumarolic vents in Kisharu sub-location, Mt. Suswa. Each vent formed a stratum, from which household heads were proportionately selected using stratified random sampling. The household head was the preferred respondent; however, in the absence of the head, any adult household member aged 18 or older was sampled. According to Lemeshow & Ferketich (2020), this method ensures

that all eligible individuals have an equal chance of selection, minimizing bias while maintaining consistency in capturing household-level information.

The distribution of respondents across the selected sampling units is presented in Table 2. A total of 119 households were selected across the ten modified vents. To achieve fairness, nine vents each contributed 12 respondents, while one vent contributed 11 respondents, making a total of 119. This allocation ensured that households relying on fumarolic condensates for their domestic water needs were equitably represented.

In addition to household respondents, four key informants were purposively selected to enrich the study with perspectives on governance, culture, and health. These included the area chief, a sub-chief, one village elder, and a nurse from Kisharu Dispensary. Their input provided critical contextual insights into community opinions, local governance, and health concerns associated with heavy metal contamination.

Table 2

Distribution of Respondents

Category	Number of Respondents per Vent	Total Respondents
Households Using Fumarolic Condensates	12 households × 9 vents; 11 households × 1 vent	119
Key Informants	–	4
Chief	1	1
Sub-Chief	1	1
Village Elder	1	1
Healthcare Professional (Nurse)	1	1
Total Sample Size	–	123
Modified vents to be sampled	–	10
Unmodified vents to be assessed	–	9
Total Vents	–	19

This sampling framework ensured that both households and key informants were adequately represented and incorporated environmental sampling from both modified and unmodified fumaroles. The study systematically captured household perspectives, governance insights, and geochemical data, providing a holistic assessment of the environmental and health implications of fumarolic condensate consumption in Mt. Suswa.

3.6 Instrumentation

This study employed a combination of analytical instruments and social research tools, including structured questionnaires and interviews, to assess the spatio-seasonal variations in heavy metal contamination and the associated health risks in fumarolic condensates at Mt. Suswa.

3.6.1 Analytical Instruments for Physico-Chemical and Heavy Metal Analysis

To measure physicochemical parameters and elemental concentrations, standardized instruments were employed. A Hanna HI-935002 thermocouple thermometer (Woonsocket, United States) was used to measure temperature, while a Jenway 430 pH/Conductivity meter (London, United Kingdom) determined pH and electrical conductivity. Fluoride concentrations were analyzed using an Elit 9801 ion meter (London, United Kingdom). Selected heavy metals (arsenic, lead, cadmium, and mercury) as well as major cations (sodium, potassium, calcium, and magnesium) were quantified using an Agilent 5110 Inductively Coupled Plasma–Optical Emission Spectrometer (ICP-OES) (Santa Clara, United States). Sulphate concentrations were determined through turbidimetric analysis with a Shimadzu UV-1800 spectrophotometer (Kyoto, Japan). In addition, titrimetric analyses for total carbonates, bicarbonates, and

chloride ions were conducted using a Mettler-Toledo Titroline-7800 auto-titrator (Columbus, United States).

All laboratory analyses utilized analytical grade (AR) reagents obtained from Chemo Quip Scientific Limited, Kenya, including nitric acid, hydrochloric acid, pH buffers, zinc acetate, silver nitrate, potassium chromate, barium chloride, and certified 1000 ppm standard solutions for K, Mg, Ca, Na, SO_4^{2-}, F^-, As, Pb, Cd, and Hg. Deionized water was used throughout to maintain sample integrity and minimize contamination risks (APHA, 2022; Pardis et al., 2022; Riebesell et al., 2023; X. Zhao & Dou, 2024).

3.6.2 Questionnaires and Structured Interviews

To assess community opinions on the quality of water and its use practices, and health-related experiences, structured questionnaires were administered to household heads in Kisharu sub-location, targeting residents who fetch water from the 10 fabricated vents. In addition, structured interviews were conducted with key informants, including local administrators (chief, sub-chief, and village elder) and a healthcare professional (nurse). These tools were designed to capture qualitative insights into community awareness, cultural practices, and perceived health implications associated with fumarolic condensate consumption.

3.6.3 Toxicological Risk Assessment Models

To evaluate the potential health risks associated with heavy metal exposure, toxicological risk assessment models were applied. The Hazard Quotient (HQ) was used to estimate non-carcinogenic risks, while the Carcinogenic Risk (CR) index was employed to estimate lifetime cancer risk attributable to ingestion of contaminated condensates. These models provided quantitative estimates of potential health impacts, complementing the qualitative data obtained through questionnaires and interviews.

3.6.4 Pilot Study

A pilot study was conducted to evaluate the feasibility and effectiveness of the proposed sampling, analytical procedures, and data collection methods. A small subset of three (3) fumarolic vents was selected to test the efficiency of the sampling protocol and the analytical techniques for detecting heavy metal concentrations (Pitiya et al., 2022). Preliminary sampling was undertaken during one wet and one dry season to evaluate the robustness of the procedures under varying climatic conditions.

The pilot also included a qualitative component, with structured questionnaires and key informant interviews administered to a small group of local residents. This exercise helped to test the clarity, relevance, and effectiveness of the questionnaires in capturing community perceptions and condensed-use practices.

In addition, the pilot study assessed logistical aspects, including accessibility of fumarolic sites, equipment functionality, sample preservation and transportation, data recording procedures, and coordination with local stakeholders. The outcomes of the pilot informed refinements to the main study design.

3.6.5 Validity of the Instrument

The validity of the instruments used in this study was ensured through multiple approaches that addressed both environmental and social research components. For in situ measurements, instruments such as pH/EC/TDS meters were calibrated with certified reference materials to ensure accuracy and reliability. Laboratory-based analytical instruments, including the ion-selective electrode (ISE), UV-Vis spectrophotometer, and the ICP-OES (Agilent 5110), were validated against known standards for heavy metal and major cation analysis. This process established construct

validity and precision in the detection of trace elements, including arsenic, cadmium, lead, and mercury.

For the qualitative component, content and face validity were established by pre-testing structured questionnaires and interview guides with a small group of local residents. This exercise ensured that the questions were clear, relevant, and effective in capturing community perceptions regarding water quality and use, contamination awareness, and health concerns. Feedback obtained during the pre-test informed refinements to the tools, enhancing their accuracy and appropriateness for the full-scale study.

3.6.6 Reliability of the Instruments

According to, reliability reflects the extent to which a measurement tool controls for random error, thereby ensuring that observed measurements reflect true values. Ensuring reliability was essential in this study to minimize random errors and strengthen the credibility of the findings.

For the environmental component, the reliability of laboratory instruments was ensured through repeated analyses and the use of control samples. The UV-Vis spectrophotometer and ICP-OES (Agilent 5110) were used to analyze replicate samples under identical conditions at different time intervals to verify consistency in results. Certified heavy metal standards were analyzed alongside test samples to monitor instrument stability and reproducibility. Similarly, the reliability of field instruments used for in situ measurements temperature, electrical conductivity (EC), and pH—was evaluated by conducting repeated readings at the same fumarolic site. Stable and consistent readings across multiple trials confirmed the reliability of these instruments.

Structured questionnaires administered to household heads were pre-tested during the pilot study to ensure clarity, coherence, and internal consistency in capturing community

perceptions of water quality, water-use practices, and associated health risks. Ambiguities and inconsistencies identified during the pre-test were corrected prior to the main survey, thereby enhancing the dependability of the tool.

Through these measures, the study ensured that both environmental and social research instruments produced consistent, stable, and dependable results suitable for rigorous analysis and interpretation.

3.7 Data Collection Procedure

This section outlines the procedures used to collect both field and laboratory data for the assessment of physico-chemical parameters, major ions, and heavy metal concentrations in fumarolic condensates within the Suswa geothermal field.

3.7.1 Determination of the Physico-Chemical Water Quality Parameters

The physicochemical parameters of the condensate samples were measured using a combination of field-based and laboratory-based analyses. These measurements provided baseline information on the fundamental characteristics of the fumarolic condensates before further ionic and trace metal analyses were undertaken.

On-Site Analysis (Temperature, Ph, Total Dissolved Solids, and Electrical Conductivity)

The temperature, total dissolved solids (TDS), electrical conductivity (EC), and pH of the fumarolic condensates were determined in the field following the standard protocols outlined by the American Public Health Association (APHA, 2022). A Hanna HI-935002 thermocouple thermometer (Woonsocket, United States) was used to measure condensate temperature, while a Jenway 430 pH/Conductivity meter (London, United Kingdom) was employed to measure pH, EC, and TDS.

Prior to use, the Jenway 430 meter was calibrated with standard buffer solutions at pH 4, 7, and 10. The electrode was rinsed with distilled water and blotted dry before being immersed in the pH 7 buffer solution, and the meter was adjusted to read 7.0. The electrode was subsequently rinsed and immersed in pH 4 and pH 10 buffer solutions, with adjustments made as needed to ensure accurate calibration. This process guaranteed precise and reliable pH readings.

For pH determination, the electrode was immersed in each fumarolic condensate sample, and the reading was recorded after stabilization. For EC measurement, the conductivity electrode was rinsed, immersed in the sample, and allowed to stabilize before recording the measurement. The EC readings indicated the concentration of dissolved ions, reflecting the water's ability to conduct electricity and directly correlating with ionic strength (Zhang et al., 2023). The Jenway 430 meter also automatically converted EC values to TDS, expressed in parts per million (ppm), providing a measure of the total dissolved solids concentration in the condensates.

3.7.2 Determination of Selected Heavy Metals and Major Cation Levels

Analytical Principle

The dissolved concentrations of arsenic (As), lead (Pb), cadmium (Cd), mercury (Hg), sodium (Na), potassium (K), calcium (Ca), and magnesium (Mg) in fumarolic condensates were determined at the Kenya Bureau of Standards (KEBS) laboratory using an Agilent 5110 Inductively Coupled Plasma–Optical Emission Spectrometer (ICP-OES; Santa Clara, United States). ICP-OES was selected for its high sensitivity, broad linear dynamic range, precision, and ability to simultaneously analyze multiple elements in complex geothermal matrices (Senila, 2024). In this technique, liquid samples are nebulized into an argon plasma, where atoms and ions are excited. The resulting

element-specific emission intensities are detected and quantified, with the signal intensity directly proportional to the analyte concentration.

Sample Handling and Preparation

Condensates were collected in acid-washed, high-density polyethylene bottles and stored at ≤4 °C to preserve their integrity. Upon arrival in the laboratory, samples were filtered through a 0.45 µm membrane filter prior to ICP-OES analysis to remove suspended particulates and ensure sample homogeneity (Bai et al., 2022; Douvris et al., 2023). This preparation step is essential for maintaining analytical accuracy and protecting instrument components. Filtrates were then acidified to pH < 2 using ultra-pure nitric acid (65% HNO_3) to stabilize dissolved metals and prevent adsorption or precipitation.

Standard Solutions, Reagents, and Calibration Curves

The working standards were prepared by serial volume-to-volume dilutions in polypropylene vials, using micropipettes for precise pipetting. All reagents and acids were of analytical grade and used without further purification, while deionized water was employed for the preparation of all solutions.

For trace elements, mixed standard solutions were first prepared by transferring 10.0 mL aliquots of arsenic (As), mercury (Hg), lead (Pb), and cadmium (Cd) stock solutions into 100 mL volumetric flasks. These were diluted to volume with 5% nitric acid (HNO_3) and homogenized. From this stock, serial working solutions of 1.00, 3.00, 5.00, 10.00, and 20.00 µg/mL were prepared by pipetting the appropriate aliquots into separate 100 mL volumetric flasks and diluting to the mark with 5% HNO_3. For the major cations (Ca, Na, K, and Mg), standard solutions were prepared at concentrations of 5, 10, 25, 50, and 100 mg L-1 using the same procedure. A 5% HNO_3 solution served as the reagent blank.

The determination of As and Hg was carried out using the ICP-OES hydride-generation system. Standard solutions of Hg and As were prepared in 5% HCl. For the As analysis, 1.0 mL of a reducing mixture of ascorbic acid and KI (5 g each dissolved in 100 mL ultrapure water) was added to the samples in 5% HCl. For Hg, 2–3 drops of $KMnO_4$ (5% w/v) were added. Sodium borohydride ($NaBH_4$) was used as the reductant in all hydride generation experiments. Standards and samples diluted with HCl (1:1, v/v) were heated to 90 °C in a water bath for 20 minutes to facilitate hydride formation.

For each analyte, a five-point calibration was constructed by plotting emission intensity against concentration, consistent with methods demonstrated by Sabzkoohi et al. (2023). Linearity of the ICP-OES calibration curves was rigorously verified by ensuring the coefficient of determination (R^2) remained above 0.99, a level recognized for maintaining high analytical accuracy. For instance, (2021) achieved $R^2 = 0.9990$ across multiple analytes, while Provete et al. (2024) reported $R^2 > 0.99$ across all tested conditions.

Instrument calibration was verified using an initial calibration verification (ICV) standard, while continuing calibration verification (CCV) standards were analyzed every 10 samples to confirm stability (Stetson et al., 2021). Quality control included procedural blanks, filter blanks, laboratory control samples (LCS), matrix spikes, matrix spike duplicates, and triplicate field samples. Acceptance limits were 80–120% for spike recoveries, ≤20% relative percent difference (RPD) for duplicates, and ±10% deviation for calibration verification standards. Certified reference materials (CRMs) were analyzed to further validate accuracy, and triplicate measurements were performed for reproducibility.

Deionized water acidified with nitric acid was used as both the calibration blank and the diluent for all solutions. Calibration curves for all analytes were linear, with correlation coefficients (R^2) of 0.999.

Analytical Procedure & Instrument Operating Conditions

The blank solution, calibration standard solutions, and sample solutions were sequentially introduced into the ICPOES instrument. Under optimized instrumental parameters (RF power: 1150 W, auxiliary gas flow: 0.5 L/min, nebulizer gas flow: 1.0 L/min, observation height: 12 mm), the instrument software automatically generated the calibration curve and calculated element concentrations.

The Agilent 5110 ICP-OES was operated in both axial and radial viewing modes, with the axial view enhancing sensitivity for trace metals (As, Pb, Cd, Hg), while the radial view minimized matrix effects for major cations (Na, K, Ca, Mg), consistent with best practice for multi-elemental analysis (Senila, 2024). Analytical wavelengths were carefully selected to minimize spectral interferences for sodium (589.592 nm), potassium (766.491 nm), calcium (317.933 and 396.847 nm), magnesium (279.553 nm), arsenic (188.980 nm), lead (220.353 nm), cadmium (228.802 nm), and mercury (194.164 nm) (Manousi et al., 2022).

Limit of Detection (LOD) and Limit of Quantification (LOQ)

The Limit of Detection (LOD) and Limit of Quantification (LOQ) are essential analytical parameters that define the sensitivity and reliability of an analytical method. The LOD is the lowest analyte concentration distinguishable from background noise, though precise quantification may not be assured, while the LOQ refers to the lowest concentration that can be quantified with acceptable accuracy and precision (Welna et al., 2023).

In this study, the LOD and LOQ for cadmium (Cd), lead (Pb), mercury (Hg), arsenic (As), potassium (K), sodium (Na), magnesium (Mg), and calcium (Ca) were determined using the Agilent 5110 ICP-OES instrument. The calculations were based on the slope of calibration curves and the standard deviation of blank measurements, a procedure consistent with established best practices (Manousi et al., 2022).

As presented in Table 3, the LODs for the analysed elements ranged from 0.1 mgL^{-1} for K, Na, Mg, and Ca to 0.1 $\mu gL^{-1}$for Cd, while the LOQs ranged from 0.33 mgL^{-1} for K, Ca, and Mg, 0.33 mgL^{-1} for Na, to 1.01 $\mu gL^{-1}$for As. Among the toxic heavy metals, Cd exhibited the lowest detection limits (LOD = 0.1 μgL^{-1}; LOQ = 0.33 μgL^{-1}), indicating the high sensitivity of the ICP-OES method for these elements.

For data interpretation, any element concentration below its respective LOQ was reported as below the Quantification limit (BQL)

Table 3

Detection and quantification limits of heavy metals

Element	Cd (μgL^{-1})	Pb (μgL^{-1})	Hg (μgL^{-1})	As (μgL^{-1})	K (mgL^{-1})	Na (mgL^{-1})	Mg (mgL^{-1})	Ca (mgL^{-1})
Wavelength (nm)	228.802	220.353	194.164	188.980	766.491	589.592	279.553	396.847
LoD	0.1	0.2	0.11	0.3	0.15	0.11	0.12	0.1
LoQ	0.33	0.67	0.35	0.98	0.49	0.36	0.4	0.33

Precision and Accuracy- Validation of Results

The procedure and method for analysis were validated using standard spiking, where a known amount of the constituent being determined was added to the sample (spiked with a standard at 5 ppb), which was then analysed for the total amount of the constituent present. The difference between the analytical results for samples with and without the

added constituent was calculated, and then the percentage recovery was calculated from equation 3.4

$$\%\ recovery = \frac{F-Np}{A}\ X\ 100$$ ……...……Equation 3.1

Where F = Spiked sample concentration

Np = Un spiked sample concentration

A = Concentration of Analyse added to the spiked portion

This spike-recovery approach is widely used in ICP-OES method validation to confirm accuracy and precision, with recent studies reporting recoveries of 85–105% as acceptable for most analytes (Szymczycha-Madeja et al., 2021). The percentage recoveries are given in Table 4.

Table 4

Percentage Recoveries

Sample	Unspiked (μgL^{-1})	Spike Added (μgL^{-1})	Spiked (μgL^{-1})	% Recovery
Pb	1.24	5.00	6.22±0.03	99.6
As	3.2	5.00	8.3±0.08	101
Hg	-	-	-	-
Cd	1.21	5.00	6.17±0.05	99.2
Mg	715.13	5.00	719.08±0.04	99
K	150.2	5.00	155.1±0.03	98
Na	1310.33	5.00	1315.35±0.7	99.4
Ca	210.27	5.00	215.19±0.06	98.4

The precision and accuracy of the analytical method were assessed using the percentage recovery (%Recovery) and the relative standard deviation (RSD) for the analysed elements, as summarized in Table 4.1. These parameters are critical for validating the

reliability, sensitivity, and reproducibility of the Agilent 5110 ICP-OES method employed in this study (Pohl et al., 2022).

Fumarolic condensate samples were spiked with 5 μgL^{-1}standard solutions of cadmium (Cd), lead (Pb), mercury (Hg), arsenic (As), potassium (K), sodium (Na), magnesium (Mg), and calcium (Ca) to evaluate method accuracy. The resulting %Recovery values ranged from 98% (K) to 101% (As), consistent with recent peer-reviewed water-matrix validations that report recoveries within ~95–110%, supporting the suitability of our preparation and ICP-based analytical procedures for accurate quantification (Rusiniak et al., 2024). This indicates that the sample preparation and analytical procedures were suitable for accurate quantification of these elements in fumarolic condensates.

Determination of Major Anion Levels in Fumaroles Condensates (Cl^-, F^-, SO_4^{2-})

The concentration of chloride ions (Cl^-) in fumarolic condensates was determined by argentometric titration with 0.1 N silver nitrate ($AgNO_3$) and 5% potassium chromate (K_2CrO_4) as an indicator, following the procedure outlined by the American Public Health Association (APHA, 2022). This procedure, commonly known as the Mohr method, has been widely applied in environmental and water chemistry for its accuracy and reproducibility.

For the analysis, 10 mL of each fumarolic condensate sample was transferred into a clean titration flask, after which 1–2 mL of a 5% potassium chromate indicator solution was added. Titration was then performed using 0.1 N $AgNO_3$ solution delivered from a burette while the sample was continuously swirled. During the titration, $AgNO_3$ reacted with chloride ions to form a white precipitate of silver chloride (AgCl). The endpoint was marked by the appearance of a permanent reddish-brown colour, caused by the

formation of silver chromate (Ag_2CrO_4), which indicated that all chloride ions had reacted.

The volume of $AgNO_3$ dispensed was recorded, and chloride concentrations were calculated based on the titrant volume, the normality of the silver nitrate solution, the sample volume, and the molar mass of chloride (35.45 g/mol). To improve reliability, the analyses were carried out in triplicate, and the average values were used for subsequent calculations (Eq 3.5) (Mukromin & Wibowo, 2023).

Calculating Chloride Concentration

Chloride Conc. (mgL^{-1}) = $\left(\frac{VAgNO_3 \; x \; NAgNO_3 \; x \; MCl}{Vsample}\right)$ x 1000… .....…Equation 3.2

Where:

- V_{AgNO3} = Volume of silver nitrate ($AgNO_3$) used (L)
- N_{AgNO3} = Normality of silver nitrate ($AgNO_3$) (N)
- M_{Cl} = Molar mass of chloride (35.45 g/mol)
- V_{sample} = Volume of sample used (L)

Sulphate (SO_4^{2-}) concentrations in fumarolic condensates were determined using the turbidimetric method with a Shimadzu UV-1800 spectrophotometer, in accordance with the standard procedure described by the American Public Health Association (APHA, 2022) and supported by the methodology of Xing et al. (2020). This method relies on the formation of an insoluble precipitate, barium sulphate ($BaSO_4$), whose induced turbidity is directly proportional to the sulphate concentration in the sample.

For the analysis, 10 mL of each standard solution, blank, and condensate sample were transferred into separate 100 mL volumetric flasks. To each flask, 3 mL of a sulphate conditioning reagent was added to enhance reaction efficiency and stabilize the

resulting turbidity. Subsequently, a spatula-full of barium chloride ($BaCl_2$) crystals was introduced into each flask. $BaCl_2$ reacted with the sulphate ions present, forming $BaSO_4$, which produced turbidity in the solution. The flasks were shaken gently to ensure homogeneous suspension of the precipitate.

The turbidity of each solution was measured using a Shimadzu UV-1800 spectrophotometer at 425 nm. The absorbance values recorded for the samples were compared against those of the prepared working standards, and sulphate concentrations were calculated accordingly. All determinations were performed in triplicate to ensure precision and reproducibility of results.

Fluoride (F^-) concentrations were determined by potentiometry using an Elit 9801 ion meter equipped with a fluoride ion-selective electrode (ISE) and a reference electrode, following APHA (2022) guidelines. This method is based on measuring electrode potential, which is proportional to the logarithm of the fluoride ion activity in solution.

Prior to sample analysis, the ion meter was calibrated using a series of standard fluoride solutions of known concentrations (0.1, 1.0, and 10 mgL^{-1}). The electrodes were rinsed thoroughly with deionized water between standards to prevent cross-contamination and then immersed in each standard solution. The potential readings obtained were recorded and plotted to establish a calibration curve, which was subsequently used for sample quantification.

Ten (10) mL of each sample was measured into a clean beaker. A Total Ionic Strength Adjustment Buffer (TISAB) solution was then added in equal volume to each sample, standard, and blank. The TISAB was essential for maintaining constant ionic strength and pH stability while minimizing potential interference from complexing ions, such as aluminum and iron. The fluoride ISE and reference electrode were immersed in the

prepared solutions, ensuring that both electrodes were fully submerged without making contact with one another. The solutions were stirred gently, and the electrode potential was recorded once stable readings were achieved.

Fluoride concentrations were calculated by comparing the recorded sample potentials against the calibration curve. Quality assurance was ensured by periodically analyzing a blank and a mid-range standard during the measurement process. All analyses were conducted in triplicate, and the average concentrations were used for data interpretation.

Geospatial mapping of Heavy Metal Contamination distribution

To map the distribution of heavy metal concentrations in fumarolic condensates from Mt. Suswa, a geospatial approach was adopted. The Inverse Distance Weighted (IDW) interpolation technique was employed to analyse and visualize spatial and seasonal variations in contaminant levels across the study area, a method that has proven effective in environmental contamination studies (Jia et al., 2024; Narayanan et al., 2025).

Fumarolic vents were sampled during both the wet and dry seasons to capture seasonal influences on contaminant levels at each sampling location. Geographical coordinates were recorded using a handheld Global Positioning System (GPS) device to provide accurate spatial reference points, ensuring that laboratory measurements could be precisely georeferenced. A similar field–lab geospatial integration has been successfully applied to map heavy metal groundwater contamination (Prajapati et al., 2025). In the laboratory, the concentrations of arsenic (As), lead (Pb), mercury (Hg), and cadmium (Cd) were determined from the collected fumarolic condensate samples. These measured concentrations, paired with their respective coordinates and seasonal attributes, were integrated into a spatial dataset (Ofman et al., 2024)

The dataset was processed and analyzed using ArcGIS software. Separate IDW interpolations were performed on the wet- and dry-season datasets to estimate contaminant concentrations at unsampled locations. This technique, based on the principle that points closer together are more similar than those farther apart, enabled the creation of continuous distribution maps for each season. These maps highlighted spatial gradients as well as seasonal differences in heavy metal concentrations, enabling the identification of temporal patterns in contamination dynamics. A technique validated as reliable for delineating spatial gradients in groundwater heavy-metal contamination in European environmental studies (Barkat et al., 2023).

The resulting geospatial maps provided a clear visual representation of both spatial and seasonal variability of heavy metals in fumarolic condensates. Hotspots of contamination were identified for each season, allowing for comparative assessment of how concentration levels varied between wet and dry periods. This seasonal mapping offered valuable insights into the influence of rainfall, dilution, and geothermal leaching processes on heavy metal mobilization, a phenomenon well-aligned with observations in other environmental systems (Adu-Boahen & Boateng, 2021)

To ensure the reliability of the interpolated maps, validation was performed by comparing estimated concentrations with selected field measurements. This verification confirmed the robustness of the IDW model across both seasonal datasets and strengthened confidence in the accuracy of the identified contamination hotspots (Khouni et al., 2021).

Application of Health Risk Assessment Framework to Suswa Fumarolic Condensates

A health risk assessment framework was applied to fumarolic condensates from Mt. Suswa, where local residents rely exclusively on these waters for drinking, cooking, and bathing. This assessment was necessary to evaluate the potential health impacts

associated with exposure to heavy metal contamination. Seasonal variations, represented by the dry season (January–March) and the wet season (May–July), were incorporated into the analysis to account for temporal fluctuations in contaminant levels, which may be influenced by processes such as dilution during rainfall and concentration through evaporation. These variations were considered likely to affect both non-carcinogenic and carcinogenic health risks.

The health risk assessment was conducted using the United States Environmental Protection Agency (USEPA) risk assessment framework. Non-carcinogenic risks were evaluated using the Hazard Quotient (HQ) for individual metals and the Hazard Index (HI) for cumulative effects, while carcinogenic risks were quantified using the Lifetime Cancer Risk (LCR) model. The exposure pathways considered in this analysis included both ingestion and dermal absorption, as these represent the primary routes of human exposure to fumarolic condensates in the Suswa community.

Model Application

To assess the health risks associated with heavy metal contamination in fumarolic condensates, a structured approach was employed following USEPA guidelines. This involved integrating site-specific data, conducting exposure pathway analysis, and characterizing risks to the resident population.

(i) Data Input and Site-Specific Contamination Levels

Site-specific contamination data were obtained from fumarolic vents within the Suswa geothermal system. The analysis focused on arsenic (As), lead (Pb), cadmium (Cd), and mercury (Hg), owing to their known toxicity and potential to pose both non-carcinogenic and carcinogenic health effects. The application of the health risk assessment models

required the use of a range of exposure and toxicity parameters, adapted from USEPA. These included:

- Reference Dose (RfD): Safe daily exposure level (mg/kg/day) for non-carcinogenic effects.
- Cancer Slope Factor (SF): Risk coefficient (mg/kg/day) $^{-1}$ for carcinogenic effects.
- Exposure Factors: Ingestion rate (IR), exposure duration (ED), body weight (BW), averaging time (AT), skin surface area, dermal permeability coefficient (KP), exposure time (ET), exposure frequency (EF), and conversion factor (CF).

Carcinogenic Risk Assessment

Carcinogenic risk assessment was conducted to evaluate the probability of developing cancer over a lifetime due to long-term exposure to heavy metals in fumarolic condensates. The assessment followed the USEPA methodology, using the Lifetime Cancer Risk (LCR) model for both ingestion and dermal exposure pathways (USEPA, 2011).

(i) Ingestion Pathway

The Lifetime Cancer Risk via ingestion was estimated using Equation 8:

$$LCR_{ingestion} = CDI_{ingestion} + \quad SF \quad \text{..... Equation 3.3}$$

Where:

- $LCR_{ingestion}$ = Lifetime Cancer Risk from ingestion exposure.
- $CDI_{ingestion}$ = Chronic Daily Intake via ingestion (mg/kg/day), calculated using:

The CDI via ingestion was calculated using Equation 3.7:

$$CDI_{ingestion} = \frac{C_W \ x \ IR \ x \ EF \ x \ ED}{BW \ x \ AT} \text{..... Equation 3.4}$$

Where:

- $CDI_{ingestion}$ = Chronic Daily Intake via ingestion (mg/kg/day).
- C_w = Heavy metal concentration in the contaminated medium (water) (mgL^{-1} or mg/kg).
- IR = Ingestion Rate (L/day for water).
- EF = Exposure Frequency (days/year), representing how often exposure occurs.
- ED = Exposure Duration (years), the total duration of exposure.
- BW = Body Weight (kg) of the exposed individual.
- AT = Averaging Time (days), which depends on whether the exposure is chronic (AT = ED × 365 days for non-carcinogenic effects).

SF = Cancer Slope Factor (mg/kg/day) $^{-1}$, representing the cancer potency of the contaminant, as provided by the USEPA Integrated Risk Information System (IRIS) (USEPA, 2011).

(ii) Dermal Pathway

The Lifetime Cancer Risk via dermal absorption was calculated using Equations 3.8 and 3.9:

$$LCR_{dermal} = CDI_{dermal} + \quad SF \qquad \text{Equation 3.5}$$

- LCR_{dermal} = Lifetime Cancer Risk from dermal exposure.
- CDI_{dermal} = Chronic Daily Intake via dermal absorption (mg/kg/day), calculated using:

$$CDI_{dermal} = \frac{C_W \ x \ SA \ x \ KP \ x \ ET \ x \ EF \ x \ ED \ x \ CF}{BW \ x \ AT} \qquad \text{Equation 3.6}$$

Where:

- (C): Contaminant concentration in water (mgL^{-1}).
- (SA): Skin surface area (cm^2).

- (KP): Dermal permeability coefficient for each metal (cm/h).
- (ET): Exposure time (h/day).
- (EF): Exposure frequency (days/year).
- (ED): Exposure duration (years for lifetime).
- (CF): Conversion factor (0.001 L/cm³ to align units).
- (BW): Body weight (kg).
- (AT): Averaging time (days in lifetime).

Total Cancer Risk and Interpretation

The overall cumulative cancer risk from exposure to carcinogenic heavy metals in fumarolic condensates was estimated by summing the Lifetime Cancer Risks (LCR) from all relevant pathways, namely ingestion and dermal absorption. This total risk provided a comprehensive estimate of the lifetime probability of developing cancer from chronic exposure to contaminants in fumarolic condensates. The calculation was performed using Equation 3.10:

$$LCR_{Total} = LCR_{ingestion} + LCR_{dermal} \quad \text{Equation 3.7}$$

Where:

- LCR_{Total} : Total Lifetime Cancer Risk (unitless probability).
- $LCR_{ingestion}$: Lifetime Cancer Risk from ingestion exposure.
- LCR_{dermal} : Lifetime Cancer Risk from dermal exposure.

The total cancer risk therefore, represented the cumulative probability of an individual developing cancer over a lifetime due to simultaneous exposure to heavy metals through both ingestion and dermal pathways (Raad et al., 2021; USEPA, 2011)

For interpretation, non-carcinogenic risks were assessed using the Hazard Quotient (HQ) and Hazard Index (HI). An HQ or HI value greater than one (>1) indicates potential health concerns associated with exposure to a given contaminant or combined contaminants. Carcinogenic risks, expressed as LCR values, were interpreted against the thresholds recommended by the United States Environmental Protection Agency (USEPA). Risks below 1×10^{-6} ($LCR < 1 \times 10^{-6}$) were considered negligible, while risks equal to or greater than 1×10^{-4} ($LCR \geq 1 \times 10^{-4}$) were considered unacceptable. Risks falling within the range of $10^{-6} \leq LCR < 10^{-4}$ were regarded as tolerable but requiring careful monitoring and, where possible, mitigation measures (Demissie et al., 2024; USEPA, 2011).

3.7.3 Data Collection Tools

This section describes the instruments and tools used to collect qualitative field data. The tools were selected to ensure accuracy, reliability, and consistency in capturing information on water quality, community perceptions, and household-level practices related to the use of fumarolic condensates.

Household Survey Design and Administration

Data were collected using a cross-sectional survey design from household heads in Kisharu sub-location, Mt. Suswa, who rely on modified fumarolic vents for their domestic water needs and had voluntarily given consent to participate in the study. Each participant signed a consent form outlining the objectives of the research and the importance of their participation.

The survey tool was designed to capture both exposure-related practices and community risk perceptions associated with heavy metal contamination in fumarolic condensates. It comprised a mix of open-ended questions, categorical yes/no options, multiple-choice

items, and perception scales, including a three-point Likert scale (agree, do not know, disagree) and a five-point ordinal scale to measure perceptions of contamination impacts on household water and health.

The initial section of the questionnaire (Appendix VI) focused on socio-economic indicators adapted from similar environmental health studies (Ondiek et al., 2020), such as age, education, marital status, primary occupation, and household size. Additional factors included the location of the homestead relative to fumarolic vents and the extent of seasonal dependence on condensates, both of which influence exposure pathways and household vulnerability. A final section invited participants to propose community-driven recommendations to mitigate exposure and improve access to safe water in Mt. Suswa (Pahwa et al., 2023).

Structured questionnaires were administered to households situated around ten (10) modified fumarolic vents, where condensates were collected and channeled into communal tanks for domestic use. The instruments were developed to complement laboratory analyses by providing socio-environmental data relevant to household exposure and community perceptions. They gathered information on household water sources, frequency of reliance on fumarolic condensates, perceived health effects, levels of awareness of contamination risks, and coping or adaptation strategies.

The administration of questionnaires also captured socio-economic characteristics such as occupation, education, and household income, which influence exposure pathways, vulnerability, and adaptive capacity.

To ensure systematic data collection, the household questionnaire was structured into six sections, each designed to capture a specific dimension of exposure, perception, or coping strategy. Table 5 below outlines the structure of the survey tool, indicating the

focus area of each section and the type of questions applied. This design ensured that both socio-economic characteristics and environmental health perceptions were comprehensively documented, providing a strong basis for triangulating survey findings with laboratory analyses.

Table 5

Structure of the Household Survey Tool

Section	Focus Area	Type of Questions
A. Socio-economic Indicators	Age, gender, education, marital status, occupation, household size, homestead location relative to fumarolic vents	Closed-ended (categorical), multiple choice
B. Water-use Practices	Sources of water, seasonal dependence on fumarolic condensates, modes of collection and storage	Closed-ended (yes/no, multiple choice), open-ended
C. Perceived Health Effects	Dental discoloration, gastrointestinal discomfort, skin irritation, general weakness	Likert scale (Agree / Do not know / Disagree); open-ended for elaboration
D. Awareness of Contamination Risks	Knowledge of heavy metals (As, Hg, Pb, Cd); perception of condensates as "safe," "salty," or "fresh"	Ordinal scale (5-point); open-ended responses
E. Coping and Adaptation Strategies	Practices such as boiling, mixing with rainwater, limiting children's intake	Closed-ended (yes/no); open-ended for descriptive detail
F. Community Recommendations	Suggestions for alternative water sources, health interventions, and resource management	Open-ended; multiple choice (ranking priority interventions)

Key Informant Interviews

These are structured, face-to-face verbal communications between a researcher and the respondent. Key informant interviews were purposively conducted to yield in-depth qualitative insights that complemented the household survey data (Elhami, 2022), particularly regarding water resource availability and governance, as well as water-use

practices. The informants comprised one chief, one sub-chief, one village elder, and one healthcare professional from Kisharu Dispensary.

Structured interview guides (Appendices VII-IX) were used to standardize the interview process and ensure alignment with the study objectives. This approach enhanced consistency, minimized interviewer bias, and enabled comparability across interviews, while still allowing flexibility for probing and clarification where necessary. Such an approach was consistent with methodological best practices for key informant interviews in applied health research (Pahwa et al., 2023).

The interviews focused on community water-use practices, perceptions of health risks associated with fumarolic condensates, levels of environmental health awareness, and local coping and adaptation strategies. Their perspectives enriched the household-level findings by highlighting broader socio-economic and governance dimensions, thereby strengthening the overall validity and relevance of the study's qualitative component (Gayapersad et al., 2024).

The key informant interviews are summarized in Table 6, which presents the roles of the informants alongside the main themes explored. As shown, each informant brought a unique perspective that, collectively, enriched the study by triangulating household findings with institutional, health, and cultural insights. These interviews provided a critical layer of contextual understanding, ensuring that the results were firmly grounded in community realities and priorities.

Table 6

Key Informant Interviews – Roles and Thematic Focus

Informant	Role	Main Themes Explored
Local Chief	Administrative leader and custodian of community welfare	Household reliance on fumarolic condensates; community-level challenges in water access; governance and resource management perspectives
Healthcare Professional (Dispensary)	Frontline health service provider	Observed health issues such as dental discoloration and health awareness among community members; recommendations for health interventions
Village Elder	Community representative and cultural knowledge holder	Traditional knowledge on water use practices; perceptions of water safety and contamination risks; community coping strategies and locally proposed solutions

Training of Research Assistants

Prior to the administration of questionnaires, research assistants were recruited and trained to ensure consistency and accuracy in data collection. Three local field assistants were engaged, with preference given to individuals with prior field experience and proficiency in the local language to facilitate effective communication with respondents. The assistants were first oriented on the study objectives, the significance of the research, and ethical considerations, including informed consent, confidentiality, and respect for participants.

The training, which lasted one day, focused on sample identification, proper administration of the questionnaires, propping techniques, and accurate recording of responses. To strengthen their skills, the assistants participated in a pilot test that exposed them to real field conditions and improved their understanding of both the study objectives and data collection instruments. This preparatory exercise was intended to

minimize bias and error during data collection, thereby enhancing the reliability and validity of the data obtained.

Questionnaire Pre-testing

Prior to the main survey, the questionnaire was pre-tested to evaluate its clarity, relevance, and effectiveness in capturing the required data. The pre-test was conducted among a small group of respondents who were not part of the final sample but shared characteristics similar to those of the study population. The pre-test provided an opportunity to estimate the average time required to complete the questionnaire and to evaluate the appropriateness of the response scales. Such adjustments ensured that the instrument was both reliable and valid for use in the main study, consistent with best practices in survey research (Bhalla & Kanapathy, 2023; Klockmann et al., 2023).

Sampling Procedure and Distribution

A stratified random sampling strategy was employed to assess the health impacts of heavy metal exposure from fumarolic condensates in Kisharu sub-location. The ten modified fumarolic vents served as strata, each representing household's dependent on condensates for domestic use. Stratification was based on vent usage, ensuring that exposure risks were assessed according to actual water-use patterns rather than estimates (Howell et al., 2020).

A total sample size of 123 respondents was determined using Cochran's formula for sample size calculation, which is widely applied in social and environmental health research to achieve statistically reliable estimates(Mulonga & Olago, 2023). This included 119 households distributed across the ten vents, with 12 households selected from nine vents and 11 households from one vent. The proportional allocation approach

ensured balanced representation across all strata while accommodating minor differences in household reliance per vent (KNBS and ICF, 2023)

To complement household data, key informant interviews were conducted with four local leaders and service providers: a chief, a sub-chief, a village elder, and a healthcare professional (a nurse). Within each stratum, household heads were randomly selected to minimize bias. If a household declined participation, an alternate household from the same vent was randomly chosen to preserve the required sample size. In the event that a vent had fewer eligible households than allocated, the deficit was proportionally redistributed across the remaining strata, ensuring the total sample size of 123 was maintained. This sampling strategy was consistent with methodologies reported in recent studies, such as Johnson et al. (2024), which applied stratified random sampling based on geographic proximity to evaluate environmental health risks in Nairobi's informal settlements.

In total, 19 fumarolic vents were assessed, comprising 10 modified vents (actively sampled for household exposure analysis) and 9 unmodified vents (examined for comparative assessment of condensate composition). This design ensured robust representation of the community's exposure pathways, captured vent-specific variations in condensate composition, and strengthened the reliability of the risk assessment.

3.7.4 Respondent Invitations and Sensitization

To facilitate data collection, the researcher first sought the approval and support of the local administration and community leaders. Community sensitization meetings were held in collaboration with village elders and local administrators, an approach consistent with recent community-based health research that emphasizes trust building and participatory engagement as prerequisites for successful household surveys (Kabanda et

al., 2025; Musoke et al., 2019). These meetings introduced the study's objectives, highlighted the importance of community participation, and addressed potential concerns about confidentiality and voluntary involvement.

In addition, the investigator prepared a short introductory letter outlining the purpose, objectives, and significance of the study. The letter served to formally introduce the research, reassure participants about ethical safeguards, and encourage voluntary participation. Its distribution complemented the sensitization meetings by providing written information that respondents could review at their convenience, thereby reinforcing transparency and fostering trust in the research process. Household heads were informed about the sampling procedure, the approximate time required for participation, and their right to withdraw at any stage without penalty.

3.8 Data Analysis and Presentation

This section outlines the procedures for processing, analysing, and interpreting data from field measurements, laboratory analyses, household surveys, and geospatial assessments. The approach ensured that the results were systematically organized, statistically examined, and presented in formats that effectively address the study objectives.

3.8.1 Data Analysis

Data collected from field measurements, laboratory analyses, and structured questionnaires were systematically organized in a spreadsheet (Microsoft Excel), with rows representing each sampling site and respondent, and columns corresponding to the measured variables. The dataset was cleaned, coded, and prepared for statistical analysis.

Statistical methods were then applied to examine trends in contamination levels and to analyze community perceptions, thereby enabling a comprehensive assessment of the relationship between environmental exposure and public health risks. Data from field

and laboratory measurements were organized with columns representing each variable and rows representing each sampling site and season, allowing temporal and spatial variations to be systematically compared.

Data collected from field measurements, laboratory analyses, and structured questionnaires were systematically organized in Microsoft Excel spreadsheets, with rows representing each sampling site and season, and columns corresponding to the measured physico-chemical parameters, trace/heavy metal concentrations, and socio-economic variables. The dataset was cleaned, coded, and prepared for statistical analysis to ensure accuracy and completeness (Sharifnia & Thapa, 2025)

Quantitative data from laboratory and field analyses were subjected to descriptive statistics (means, standard deviations) to summarize contamination levels and physico-chemical characteristics of fumarolic condensates across different sites and seasons. To test differences in contaminant levels between the wet and dry seasons, inferential statistical tests, such as analysis of variance (ANOVA), were applied, provided the assumptions of normality were met (Mukwevho et al., 2025).

Relationships among heavy metals, physico-chemical parameters, and spatial factors were examined using Pearson's or Spearman's correlation analysis, depending on data distribution (Argun, 2024). Spatial interpolation techniques, particularly Inverse Distance Weighting (IDW) in ArcGIS Pro, were used to generate contamination maps and visualize hotspots of heavy metal concentrations. IDW was selected for its simplicity, transparency, and ability to provide reliable estimates of concentration gradients by giving greater weight to values measured closer to the prediction location (Khouni et al., 2021).

Qualitative data obtained from structured questionnaires and key informant interviews were analyzed thematically. Responses were transcribed, coded, and categorized into emerging themes related to water-use practices, perceived health effects, awareness of contamination risks, and community adaptation strategies. This thematic analysis enabled integration of community perceptions with quantitative evidence from environmental measurements, thereby strengthening the overall assessment of exposure and associated health risks (Braun & Clarke, 2023; Lewis et al., 2020)

The integration of quantitative statistical analysis with qualitative thematic insights ensured a comprehensive understanding of both the scientific measurements of contamination and the lived experiences of the affected Mt. Suswa community. This triangulated approach enhanced the validity of the findings and their relevance to both policy and practice.

3.8.2 Data presentation

The analysed data are presented in tabular, graphical, and map formats for clarity and ease of interpretation. Laboratory concentrations and statistical outputs are summarized in tables and figures, while spatial distribution patterns are illustrated through maps. Qualitative findings are presented as descriptive summaries, supported by direct quotes where necessary, to highlight community perspectives. Together, these complementary methods ensured that the results were not only statistically robust but also socially grounded, thereby strengthening the validity and applicability of the study's conclusions.

3.8.3 Analysis of Physico-chemical Parameters

To evaluate the relationships between geothermal characteristics (temperature, pH, and electrical conductivity [EC]) and heavy metal concentrations (arsenic, mercury, lead, and cadmium), Pearson correlation analysis was performed using SPSS v.29 (S. Zhao et al.,

2024; . To determine whether differences in heavy metal concentrations between the wet and dry seasons were statistically significant, a paired t-test was conducted. Since the same fumarolic vents were sampled in both seasons, this test was appropriate for assessing significant changes in metal concentrations under different seasonal conditions, ensuring that observed variations were not due to random chance (Bushra et al., 2023).

Furthermore, to assess spatial variations between fumarolic sites, Analysis of Variance (ANOVA) with multiple comparisons was applied. This test evaluated whether significant differences existed in heavy metal concentrations across fumarolic sites and between seasons (Mukwevho et al., 2025; Yujie et al., 2024).

3.8.4 Health Risk Assessment

To assess health risks associated with heavy metal exposure, toxicological risk assessment models were applied, including the Carcinogenic Risk (CR) Index for long-term cancer risk due to exposure to arsenic, lead, mercury, and cadmium. These indices were computed using reference dose (RfD) values from regulatory agencies such as the U.S. Environmental Protection Agency (USEPA). This approach provided a quantitative estimate of potential health impacts posed by heavy metal exposure in fumarolic condensates (Wang et al., 2023; USEPA, 2011)

3.8.5 Analysis of Community Perceptions from Structured Questionnaires

Qualitative data from structured questionnaires administered to local residents were analyzed using thematic analysis to identify common perceptions of geothermal contamination, water use, and perceived health effects. Responses were transcribed, coded, and categorized into key themes such as awareness of contamination and coping strategies (Caputo et al., 2022).

In addition, statistical tests, including Pearson's Chi-square test of independence, were applied to examine associations between survey responses and contamination levels. These analyses enabled the identification of patterns and trends in community concerns and risk perceptions. Combining thematic analysis with statistical testing, the study provided both qualitative depth and quantitative validation, offering a comprehensive understanding of community perceptions on water quality and exposure risks (Mumbi & Watanabe, 2020).

3.8.6 Operationalization of Variables

Operationalization of variables involved translating the study objectives into measurable indicators that could be systematically observed, recorded, and analysed. Both independent and dependent variables were clearly defined, along with the methods of measurement and the units of analysis, to ensure the reliability and validity of the results. Table 7 below presents the definitions of operational variables, including objectives, variables, measurement methods, scales of measurement, and data analysis techniques

Table 7

Operationalization of Variables

Objective	Variables	Measurement Methods	Scale	Data Analysis
1. Determine physico-chemical characteristics and seasonal variations	Physico-chemical parameters (T°, pH, EC, TDS, anions, cations)	In-situ instruments; laboratory titration, spectrophotometry, potentiometry	Interval/Ratio	Descriptive stats; seasonal comparison (t-test/ANOVA)
	Heavy metals (As, Hg, Pb, Cd)	Laboratory ICP-OES	Ratio	Descriptive stats; seasonal comparison (t-test/ANOVA)
2. Examine parameter correlations and spatial heavy-metal patterns	Parameter correlations	Field & lab data compiled in SPSS v29	Interval/Ratio	Pearson/Spearman correlation
	Spatial distribution of heavy metals	GPS mapping; GIS analysis	Ordinal/Ratio	Geostatistics (IDW), hotspot analysis
3. Evaluate potential human-health risks	Health risk indices (HQ, HI, CR)	USEPA risk-assessment model (ingestion & dermal)	Ratio	HQ, HI, CR computation
	Community reliance & perceptions	Structured questionnaires; KIIs	Ordinal/ Nominal	Descriptive stats; Chi-square; thematic analysis

3.9 Ethical Considerations and Safety Protocols

Prior to data collection, the researcher obtained an introductory letter from the Institute of Postgraduate Studies and secured ethical clearance from the Kabarak University Scientific and Ethics Review Committee (KUREC). Subsequently, a research permit was acquired from the National Commission for Science, Technology, and Innovation (NACOSTI) in accordance with national research regulations. These approvals were

presented to relevant authorities and stakeholders to facilitate access to the study sites and participants.

Participation was voluntary, based on written informed consent. Respondents were provided with clear information about the study's objectives, procedures, potential risks, and benefits. They were free to withdraw at any stage without penalty. To safeguard confidentiality, participants were assigned anonymized codes, and no identifying details were retained in the final dataset. Data were securely stored using password-protected files.

CHAPTER FOUR

DATA ANALYSIS, PRESENTATION AND DISCUSSION

4.1 Introduction

This chapter presents the study's results, along with their analysis, interpretation, and discussion. The findings are derived from field measurements, laboratory analyses, structured questionnaires, and key informant interviews, and are presented using tables and figures where appropriate. The analysis integrates both quantitative data, such as physico-chemical parameters, heavy metal concentrations, and modeled health risk indices, and qualitative data, including community reliance, perceptions, and coping strategies.

The presentation of results follows the study objectives and research questions, with the overarching aim of assessing the spatial and seasonal variations of heavy metal contamination in fumarolic condensates at Mt. Suswa and evaluating the associated human health risks.

4.2 General and Demographic Information

4.2.1 General Information

The number of households directly dependent on fumarolic condensates for domestic water supply in Kisharu sub-location, Mt. Suswa, was estimated at approximately 720 (Kenya Population and Housing Census, 2019). Using Cochran's formula for sample size determination, the target sample size for this study was 123 respondents at a 5% margin of error and 95% confidence interval. After data cleaning, a total of 102 (99 household heads and 3 key informants) valid qualitative entries were retained for analysis, representing an effective response rate of 86%. Data were collected through face-to-face

interviews using a structured questionnaire, with support from trained research assistants who guided respondents as needed.

According to survey methodology literature (Taherdoost & Madanchian, 2024), response rates above 80% are considered exceptional and are often required to meet publication standards; therefore, the 86% achieved in this study, as shown in Table 8 below, was both highly satisfactory and methodologically robust.

Prior to analysis, diagnostic checks were performed on the dataset to confirm completeness, consistency, and suitability for statistical procedures. The data were screened for missing values, entry errors, and outliers, ensuring that only high-quality responses were processed in SPSS for both descriptive and inferential analyses (Izah et al., 2024). To further guarantee accuracy and reliability, the questionnaire was pretested and refined, with internal consistency confirmed by a Cronbach's Alpha coefficient of 0.69, indicating satisfactory reliability.

Data were collected primarily from household heads, as they represent the population directly reliant on fumarolic condensates for their daily water needs. To enrich household perspectives with insights from the institutional and community levels, key informants were also interviewed. These included local administrators (chief, sub-chief, and village elders) and a healthcare professional from Kisharu Dispensary. Their perspectives were critical for triangulating household-level responses with broader community experiences, particularly regarding water-use practices, perceived health risks, awareness levels, and coping strategies.

Table 8

Response Rate of Administered Questionnaires

Administered questionnaires	Questionnaires filled and valid	Response rate (%)
119	102	86

4.2.2 Demographic and Socio-Economic Characteristics of Respondents

The demographic and socio-economic characteristics of respondents presented in Table 9 and provide key insights into the study population. Household heads accounted for the vast majority of participants (99 respondents; 97.1%), with only 3 key informants (2.9%) drawn from local leadership and the health sector, confirming that the survey primarily captured perspectives of the main users of fumarolic condensates.

Residence patterns showed that 35% of respondents had lived in the area for more than 40 years, while 50% reported between 10–40 years of residence, underscoring the community's long-term dependence on condensates and cumulative exposure. Educational attainment was diverse: 15% had no formal education and 35% had only primary schooling, suggesting that half the population may have limited awareness of invisible contaminants. In contrast, 30% had secondary education and 20% had tertiary education, groups more likely to engage with health and environmental risk information. Empirical evidence indicates that individuals with higher levels of education tend to exhibit greater environmental awareness, stronger risk perception, and an enhanced capacity to adopt adaptive strategies, particularly in relation to water and public health challenges. Education plays a critical role in shaping knowledge, attitudes, and behaviours toward environmental risks, thereby improving community resilience and informed decision-making (Lambebo et al., 2025).

Occupationally, livestock rearing (75.8%) and mixed farming (13.1%) dominated, reflecting the community's strong reliance on natural resources, while 11.1% reported formal employment, offering relatively stable livelihoods less directly tied to environmental exposure. The age structure was broad: 20% were aged 18–30 years, 45% were aged 31–45 years, 20% were aged 46–60 years, and 15% were aged 61+ years, enabling the study to capture intergenerational perspectives on water use, coping strategies, and perceived health risks. Evidence from environmental health studies demonstrates that demographic diversity and livelihood type are important determinants of vulnerability to water-related health risks (Odongo et al., 2025).

Gender distribution was relatively balanced, with 56 males (55%) and 46 females (45%), consistent with household leadership norms observed nationally in which male headship remains more common, though a substantial share of households are female-headed (KNBS and ICF, 2023). Including women's voices enriched the analysis, given their primary roles in water collection and household water management and the documented gendered health and safety implications of water access (Akram-lodhi, 2025; UNICEF & WHO, 2023).

The findings summarized in Table 9 present a representative profile of the Mt. Suswa community. They highlight the socio-economic vulnerability of households and provide a robust basis for interpreting exposure pathways, health risk perceptions, and coping mechanisms related to heavy metal contamination in fumarolic condensates.

Table 9

Demographic and Socio-Economic Characteristics of Respondents

Variable	Category	Frequency (n)	Percentage (%)	Notes/Interpretation
Sampling Unit	Household heads	99	97.1	Primary respondents, directly reliant on fumarolic condensates
	Key informants	3	2.9	Leadership and health-sector perspectives
Years in Study Area	< 10 years	15	15.0	Recent settlers, lower cumulative exposure
	10–40 years	51	50.0	Majority, medium to long-term exposure
	> 40 years	36	35.0	Long-term residents, highest cumulative exposure
Educational Level	No formal education	15	15.0	Reflects low literacy, lower awareness of contamination risks
	Primary	35	35.0	Basic literacy level, moderate awareness
	Secondary	30	30.0	Represents educated households
	Tertiary	20	20.0	Higher literacy, greater awareness potential
Occupation	Livestock rearing	75	75.8	Main livelihood, strong reliance on natural resources
	Mixed Farming	13	13.1	Subsistence-based, vulnerable to contamination
	Formal employment	11	11.1	Stable income, less reliance on condensates
Age Group	18–30 years	20	20.0	Younger adults, less cumulative exposure
	31–45 years	45	45.0	Dominant age group, most economically active
	46–60 years	20	20.0	Mid-aged respondents
	> 60 years	14	15.0	Elderly, long-term coping strategies and experiences
Gender	Male	56	55.0	Slightly dominant as household heads
	Female	46	45.0	Balanced representation, enriched dataset with gender-specific insights

Results of Household Survey and Key Informant Interviews

The household survey and key informant interviews generated insights into water-use practices, perceived health effects, awareness of contamination risks, and coping/adaptation strategies within Kisharu sub-location. Household heads accounted for the majority of respondents (97.1%), complemented by key informants drawn from local leadership and the health sector.

Thematic analysis revealed four major themes (Table 11). The survey results showed heavy household reliance on fumarolic condensates, with 85% of respondents using them for drinking, 91% for cooking, and 78% for bathing. This dependence intensified during the dry season, with 63% reporting greater reliance when alternative sources became scarce. These patterns reflect how cultural norms and longstanding practices have normalized condensate use as a routine part of daily life.

Perceived health effects were common, with 57% of households reporting dental discoloration among children. Health workers at Kisharu Dispensary corroborated these concerns, confirming suspected cases of fluorosis consistent with the elevated fluoride concentrations identified in laboratory results. Despite these visible symptoms, awareness of contamination risks remained low. A majority (72%) described condensate water as “fresh,” or “salty,” without linking these qualities to contamination. Only 9% were aware of fluoride-related risks, and fewer than 5% recognized the possible presence of contaminants such as arsenic or cadmium.

Households reported several coping and adaptation strategies. Nearly 49% boiled the condensate, 28% mixed it with rainwater, and only 7% attempted rudimentary filtration with cloth or charcoal. However, both residents and key informants acknowledged that these methods were largely ineffective against dissolved heavy metals—an assessment

supported by established evidence that boiling and simple filtration do not remove fluoride or trace metals.

Community leaders and local administrators emphasized the urgent need for alternative safe water sources, with 94% of households expressing willingness to adopt piped or treated water if available. However, 82% cited cost and 71% infrastructural limitations as key barriers to accessing safer alternatives.

These findings provide a strong qualitative and quantitative foundation for interpreting the laboratory results and subsequent health-risk calculations, including carcinogenic risk (CR). The alignment between community practices, low risk awareness, observed health effects, and the chemical composition of condensates highlights the intersection of socio-cultural vulnerability and geothermal contamination risks within the Suswa geothermal environment.

Table 10

Thematic Insights from Household Surveys and Key Informant Interviews

Theme	Evidence from Residents	Evidence from Key Informants	Implications
Water Use Practices	85% drink condensates; 91% cook with them; 78% bathe with them; 63% rely more in dry season.	Confirmed heavy reliance due to limited alternatives.	Ingestion is the primary exposure pathway; strong socio-economic dependence on condensates.
Perceived Health Effects	57% reported dental discoloration in children.	Nurse confirmed suspected fluorosis cases.	Connects fluoride data to observable effects; strengthens health-risk estimates.
Awareness of Contamination	72% perceived water as "fresh/tasty"; only 9% knew fluoride risks; <5% aware of As/Cd.	Low environmental health literacy reported.	Highlights urgent need for community education and awareness campaigns.
Coping & Adaptation	49% boil water; 28% mix with rainwater; 7% filter locally.	Leaders noted desire for safe water but cited cost/infrastructure constraints.	Current strategies ineffective for metal removal; need for safe water interventions.

Discussion

The survey findings highlight the socio-economic dependence of the Mt. Suswa community on fumarolic condensates, despite laboratory evidence of health risks. Reliance on condensates is not simply a matter of convenience but reflects structural vulnerability and the absence of alternative safe water sources. This dependency is most pronounced during the dry season when reliance is highest, coinciding with the period of elevated contaminant concentrations in hotspot vents. Similar patterns have been reported in other rift–volcanic settings where households depend on geothermal-

influenced waters due to the absence of reliable alternatives, with documented exceedances of fluoride and/or arsenic and observed health effects (Bianchini et al., 2020; Bonetto et al., 2021; F. Ligate et al., 2021).

Awareness of invisible contaminants such as arsenic and cadmium remained limited. Despite arsenic concentrations reaching 5.59 μgL^{-1}at F18 (dry season) and cadmium up to 1.41 μgL^{-1}at F20, most residents described condensates as 'fresh' or 'salty' and did not associate their consumption with long-term risks. This aligns with findings from other geothermal or arsenic-affected contexts, where community members assess water safety by sensory cues (taste, odor, clarity), and environmental health literacy is low, leading to an underestimation of health risks (Boyden et al., 2023; Watson et al., 2025).

Furthermore, the persistence of ineffective coping strategies, such as boiling or mixing condensates with rainwater, underscores the disconnect between community practices and actual protective measures, since dissolved metals remain unaffected by these interventions (Gray et al., 2021)

Taken together, these results demonstrate the urgent need for risk communication strategies, targeted health education campaigns, and sustainable investment in safe water infrastructure. Equally, they emphasize the importance of integrating community knowledge and perceptions into geothermal governance frameworks to ensure interventions are locally appropriate, socially accepted, and practically implementable.

4.3 Findings for Objectives and Research Questions

This section presents the study's main findings in relation to the specific objectives and research questions. The results integrate field measurements, laboratory analyses, household survey data, and geospatial outputs to provide a comprehensive understanding of the physicochemical characteristics of fumarolic condensates, their seasonal and

spatial variations, associated heavy-metal contamination, and community-level exposure risks.

4.3.1 Findings on Physico-Chemical Parameters in Fumarolic Condensates

This subsection summarizes the physico-chemical characteristics of fumarolic condensates collected from vents across the Suswa geothermal field during both the dry and wet seasons. The detailed results, including temperature, pH, electrical conductivity, total dissolved solids, major ions, and heavy metal concentrations, are presented in Table 11. These findings establish the baseline water-quality conditions necessary for subsequent correlation analysis, spatial mapping, and health-risk evaluation.

Table 11

Measurements of Physico-Chemical Parameters in Fumarolic Condensates

		FIELD AND LABORATORY DATA													
Sample ID	**Season**	**pH/T°C**	**EC**	**TDS**	**Na^+**	**K^+**	**Mg^{2+}**	**Ca^{2+}**	**F^-**	**Cl^-**	**SO_4^{2-}**	**As**	**Pb**	**Cd**	**Hg**
			µS		**Mean ±RSD (ppm±%)**							**Mean ±RSD (ppb±%)**			
F1	Dry	7.19/51.4	14.72	7.36	12.16±0.04	11.58±0.02	1.48±0.11	1.26±0.08	1.86±0.12	8.82±0.06	1.53±0.02	4.86±0.04	1.42±0.06	ND	ND
	Wet	7.11/48.7	13.28	6.84	10.63±0.11	12.21±0.05	1.36±0.04	0.93±0.05	1.57±0.06	8.91±0.12	1.38±0.07	3.24±0.09	1.25±0.08	ND	ND
F2	Dry	7.26/58.2	5.16	2.58	11.65±0.02	13.29±0.07	1.39±0.04	1.22±0.03	1.85±0.09	7.35±0.09	1.62±0.08	3.21±0.07	1.30±0.05	0.53±0.11	ND
	Wet	7.15/51.6	4.93	2.43	9.89±0.07	12.65±0.13	1.26±0.07	0.98±0.15	1.81±0.04	5.68±0.05	1.51±0.11	2.66±0.03	1.13±0.02	0.37±0.11	ND
F3	Dry	6.68/53.1	13.07	6.58	12.09±0.03	12.42±0.02	1.45±0.02	0.93±0.07	1.64±0.03	9.72±0.07	5.80±0.04	4.94±0.02	1.53±0.11	1.17±0.08	ND
	Wet	6.81/51.4	12.91	6.22	12.02±0.07	12.05±0.06	1.17±0.04	0.78±0.03	1.56±0.02	9.21±0.03	5.75±0.08	4.34±0.08	1.09±0.04	0.72±0.06	ND
F4	Dry	6.94/64.6	17.01	8.52	12.64±0.09	13.68±0.01	1.66±0.06	1.29±0.02	2.93±0.05	11.46±0.05	1.87±0.07	3.82±0.09	1.38±0.08	0.39±0.04	ND
	Wet	6.96/62.8	16.23	8.11	12.47±0.04	12.85±0.03	1.21±0.03	1.13±0.03	2.59±0.03	11.13±0.07	1.26±0.03	2.49±0.05	1.02±0.05	ND	ND
F5	Dry	6.44/71.3	5.56	2.78	13.15±0.01	12.67±0.01	1.69±0.12	2.31±0.03	2.58±0.11	8.52±0.11	1.91±0.08	5.16±0.04	1.41±0.02	1.84±0.02	ND
	Wet	6.47/68.5	4.94	2.43	12.97±0.04	12.26±0.03	1.37±0.04	2.16±0.05	2.49±0.07	8.13±0.06	1.52±0.03	4.83±0.08	1.07±0.09	1.26±0.06	ND
F6	Dry	6.36/64.1	18.73	9.37	12.27±0.05	11.27±0.03	1.71±0.08	1.09±0.03	1.87±0.08	7.64±0.14	0.74±0.04	2.55±0.11	1.35±0.04	ND	ND
	Wet	6.41/60.3	16.23	8.05	11.13±0.02	9.92±0.09	1.48±0.08	0.73±0.07	1.39±0.04	6.56±0.11	0.71±0.12	2.13±0.04	1.12±0.06	ND	ND
F7	Dry	7.12/63.2	17.33	8.67	13.61±0.02	9.55±0.05	2.47±0.07	0.94±0.11	1.69±0.03	8.52±0.03	3.78±0.02	2.24±0.07	0.95±0.14	ND	ND

F8	Wet	7.37/62.4	15.61	7.78	13.18±0.05	9.18±0.04	1.85±0.07	0.72±0.06	1.61±0.08	6.87±0.07	1.93±0.05	1.87±0.02	0.92±0.06	ND	ND
	Dry	6.81/53.1	41.41	20.17	13.48±0.05	13.89±0.09	1.74±0.04	1.28±0.06	2.87±0.02	8.23±0.07	1.62±0.06	3.08±0.05	1.43±0.10	0.61±0.07	ND
F9	Wet	7.14/47.4	36.72	17.81	13.22±0.09	10.27±0.03	1.68±0.08	0.97±0.04	2.03±0.04	7.36±0.03	1.38±0.07	2.92±0.08	1.38±0.05	0.44±0.06	ND
	Dry	6.73/53.2	8.32	4.15	14.76±0.02	11.64±0.04	1.65±0.05	1.71±0.12	1.51±0.09	8.72±0.05	1.15±0.11	2.71±0.08	1.03±0.08	0.47±0.03	ND
F10	Wet	6.78/51.4	7.57	3.76	12.34±0.07	10.18±0.02	1.62±0.09	1.32±0.08	1.25±0.03	7.21±0.06	0.79±0.07	1.97±0.04	0.87±0.05	ND	ND
	Dry	6.44/54.4	11.92	5.96	12.85±0.08	10.88±0.05	1.38±0.02	1.15±0.02	2.64±0.05	7.94±0.08	3.44±0.13	3.45±0.02	1.62±0.03	ND	ND
F11	Wet	6.78/52.2	10.35	5.17	11.23±0.03	10.04±0.07	1.07±0.04	0.83±0.09	2.48±0.09	7.11±0.02	2.82±0.05	1.29±0.07	1.17±0.02	ND	ND
	Dry	6.88/43.4	7.43	3.71	12.09±0.05	12.57±0.04	2.58±0.09	1.40±0.04	2.36±0.07	7.62±0.08	1.46±0.05	2.83±0.12	1.84±0.14	1.36±0.10	ND
F12	Wet	6.92/42.3	7.18	3.58	11.32±0.02	10.83±0.07	2.34±0.03	0.93±0.06	2.18±0.03	5.38±0.03	0.79±0.08	2.43±0.14	1.27±0.11	0.85±0.06	ND
	Dry	6.75/50.2	5.05	2.52	14.42±0.08	8.76±0.02	1.44±0.05	1.58±0.06	2.29±0.11	8.35±0.02	1.38±0.13	3.65±0.06	1.33±0.09	1.14±0.06	ND
F13	Wet	6.79/49.1	4.88	2.43	14.14±0.03	8.15±0.07	1.31±0.07	1.14±0.03	2.13±0.06	7.97±0.05	1.02±0.07	3.31±0.04	1.37±0.09	0.86±0.04	ND
	Dry	6.92/69.6	16.91	8.47	15.21±0.02	13.12±0.02	1.21±0.05	1.46±0.03	3.84±0.04	7.72±0.09	1.52±0.02	3.88±0.05	1.71±0.05	1.26±0.08	ND
F14	Wet	6.90/69.4	16.07	8.04	12.49±0.06	12.35±0.05	1.17±0.04	0.88±0.02	3.58±0.02	5.44±0.03	1.24±0.06	2.91±0.07	1.25±0.04	1.03±0.04	ND
	Dry	6.19/71.2	22.41	11.2	18.43±0.03	15.87±0.07	1.78±0.08	1.74±0.11	2.14±0.12	10.56±0.11	2.26±0.13	3.92±0.03	1.98±0.04	0.68±0.03	ND
F15	Wet	6.38/66.4	19.27	9.5	15.17±0.05	11.32±0.03	1.54±0.09	1.08±0.03	1.91±0.04	10.17±0.05	1.92±0.08	3.39±0.04	1.83±0.03	0.41±0.05	ND
	Dry	6.45/63.6	7.41	3.71	13.28±0.03	12.14±0.08	2.27±0.04	1.72±0.07	3.49±0.04	8.56±0.06	2.49±0.11	4.63±0.08	1.50±0.08	0.49±0.09	ND
	Wet	6.49/63.4	7.13	3.54	13.03±0.02	11.48±0.03	2.05±0.06	1.64±0.03	3.32±0.03	8.27±0.04	2.43±0.08	4.56±0.05	0.81±0.03	ND	ND

F16	Dry	6.27/74.5	25.38	12.69	17.41±0.03	10.27±0.05	1.63±0.03	1.63±0.09	2.41±0.04	7.69±0.03	2.85±0.03	5.04±0.15	1.41±0.12	0.60±0.17	ND
	Wet	6.91/64.8	21.43	10.71	17.29±0.04	9.96±0.02	1.39±0.06	1.47±0.05	2.30±0.02	6.78±0.06	2.76±0.05	4.48±0.07	1.35±0.11	0.47±0.06	ND
F17	Dry	6.39/69.7	25.04	12.5	14.38±0.07	12.34±0.08	1.72±0.11	1.84±0.12	2.34±0.03	7.92±0.03	4.63±0.07	5.13±0.06	1.48±0.03	1.17±0.08	ND
	Wet	6.44/69.3	24.77	12.38	14.06±0.03	11.93±0.04	1.65±0.04	1.55±0.07	2.18±0.05	7.46±0.04	4.32±0.02	5.07±0.05	1.42±0.06	1.05±0.11	ND
F18	Dry	6.43/73.5	51.22	25.6	19.44±0.01	14.82±0.02	1.93±0.06	1.66±0.05	3.57±0.07	8.22±0.01	2.84±0.05	5.59±0.09	1.27±0.06	1.22±0.04	ND
	Wet	6.49/71.2	50.67	25.33	19.25±0.03	14.59±0.04	1.65±0.04	1.21±0.03	3.19±0.05	7.88±0.03	2.32±0.04	5.54±0.04	1.19±0.03	1.02±0.11	ND
F20	Dry	5.52/74.3	21.15	10.54	17.28±0.02	13.14±0.04	2.18±0.06	1.97±0.12	3.32±0.08	8.27±0.05	3.98±0.14	5.35±0.04	1.52±0.03	1.41±0.08	ND
	Wet	5.91/68.7	21.02	10.51	17.22±0.04	13.03±0.09	2.01±0.03	1.66±0.05	3.29±0.04	7.14±0.03	3.54±0.06	5.23±0.03	1.44±0.02	1.27±0.04	ND
CS	Dry	7.29/24.6	10.05	65.14	31.68±0.02	17.42±0.04	2.13±0.04	6.43±0.05	0.82±0.03	14.24±0.09	39.11±0.10	ND	ND	ND	ND
	Wet	7.18/23.8	10.02	65.21	33.29±0.06	17.27±0.03	2.17±0.07	6.37±0.09	0.71±0.07	14.32±0.04	39.17±0.07	ND	ND	ND	ND
NEMA Limit		6.5–8.5	NS	1200	NS	NS	NS	NS	1.5	NS	400	10	50	10	1
WHO Limit		6.5–8.0	NS	1000	NS	NS	NS	NS	1.5	NS	400	10	10	3	5

Note: Values are represented in Mean ±SD, SD= Relative Standard Deviation; ND = Not Detected; NS = Not Specified; CS = Control Sample

Discussion of the Findings

The fumarolic condensates from Mt. Suswa display mildly acidic to near-neutral pH values ranging from 5.52 to 7.37 at elevated temperatures of 42–75 °C (Table 11). Similar behaviour has been observed in East African geothermal settings; for instance, at Menengai fumaroles, comparable pH ranges (5.8–7.5) have been reported by Montcoudiol et al., supporting the inference that acidic gases control condensate chemistry. Similar acidic condensates produced by gas scrubbing are documented in multiple geothermal settings; for example, Iceland, where condensate collected from a high-temperature well showed pH ~3–5, Italy (Vulcano, La Fossa), where fumarole condensates are explicitly studied and reported as acidic (Di Sano et al., 2023; Müller et al., 2024).

The low Electrical conductivity (4.9–51 µS cm^{-1}) and total dissolved solids (2.4–25.6 mg L^{-1}) remained well below WHO (1,000 mg L^{-1}) and NEMA (1,200 µS) limits. Nevertheless, localized higher values at vents F16–F18 indicate zones of greater mineral enrichment, a process intensified during the dry season due to reduced dilution. The very low ionic strength therefore, points to dilute, steam-derived condensates rather than saline geothermal brines, consistent with recent observations of low-temperature, steam-rich fumarolic condensates at La Soufrière (Guadeloupe, Caribbean) and with the dominantly meteoric, sodium-alkaline waters that characterize many Main Ethiopian Rift geothermal systems (i.e., non-brine, low-salinity fluids) (Inostroza et al., 2022).

The cation composition of the fumarolic condensates was sodium-rich and calcium-poor, a condition that favours fluoride mobility. Sodium reached up to 19.44 mg L^{-1}, while calcium was as low as 0.72 mg L^{-1}. This geochemical environment enhances fluoride solubility because low Ca^{2+} activity suppresses fluorite (CaF_2) precipitation, preventing

immobilization of F^- (Sunkari & Ambushe, 2024). Similar Na-alkaline, Ca-poor waters with elevated fluoride have been widely documented in volcanic/geothermal terrains, including the Kenya/Main Ethiopian Rift and other global hotspots (Podgorski & Berg, 2022). Comparable Na–K enrichment patterns have been reported in fumarolic waters from Mutnovsky and La Soufrière, confirming that Suswa's waters display the typical alkali signature of volcanic steam condensates (Burnside et al., 2021; Inostroza et al., 2022).

Fluoride concentrations in the fumarolic condensates ranged between 1.25 and 3.84 mgL^{-1}, with most vents recording values above the World Health Organization (WHO) and National Environment Management Authority (NEMA) guideline value of 1.5 mgL^{-1} for potable water. The exceedances were more pronounced during the dry season than the wet season, indicating dilution effects associated with rainfall recharge. According to the WHO (2022), fluoride levels above 1.5 mgL^{-1} pose a risk of dental fluorosis, while long-term exposure to levels exceeding 3 mgL^{-1} may result in skeletal fluorosis.

The elevated fluoride in these condensates reflects the typical geogenic signature of East African Rift geothermal systems. Volcanic and fumarolic gases are enriched in halogens, particularly HF, which dissolve into condensate waters during cooling, thus increasing fluoride loadings (Longo et al., 2020). In addition, the condensates were characteristically sodium-rich and calcium-poor, with Na^+ concentrations up to 19.44 mgL^{-1} and Ca^{2+} as low as 0.71 mgL^{-1}. Such a geochemical environment enhances fluoride solubility because low Ca^{2+} activity prevents precipitation of fluorite (CaF_2), thereby maintaining fluoride in solution. Podgorski & Berg (2022) demonstrated globally that fluoride occurrence is strongly associated with high Na^+, alkalinity, and elevated pH, while being negatively correlated with Ca^{2+} and Mg^{2+}, a pattern mirrored in the Suswa dataset.

Similarly, Bonetto et al. (2021) documented concentrations up to 28 mgL^{-1} in the Main Ethiopian Rift, with a strong linear relationship between Na^+ and F^- ($R^2 \approx 0.8$), underscoring the control of geochemical facies on fluoride mobility. The Suswa condensates, therefore, fall within the expected geogenic range but still present chronic exposure risks to dependent communities.

Seasonal differences further emphasize the influence of hydrological processes. Fluoride concentrations were consistently lower during the wet season, supporting dilution by meteoric recharge and enhanced solubility during high-flow periods. Comparable observations have been made in Ethiopian Rift groundwater, where wet-season recharge reduced fluoride concentrations relative to dry-season values (Abera et al., 2024). Similarly, Kush et al., (2022)(Kush et al., 2022) highlighted that seasonal fluctuations influence fluoride mobility, with elevated concentrations observed in drier periods due to limited dilution. The Suswa results are thus consistent with regional hydrogeochemical dynamics, reinforcing the importance of seasonal monitoring.

The chloride concentrations in the fumarolic condensates from Suswa ranged from approximately 5 to 14 mgL^{-1}, with the control spring exhibiting slightly higher values of around 14 mgL^{-1}. These levels are extremely dilute compared to those of geothermal reservoir fluids in Kenya, where chloride concentrations commonly exceed 100 mg/L (Montcoudiol et al., 2019). Such low values are characteristic of steam-heated and condensate-dominated waters, since chloride is a conservative ion that is typically concentrated in deep liquid phases, while near-surface steam condensates remain depleted in Cl^- unless enriched by hydrochloric acid gas scrubbing (Favorito et al., 2021; Rouwet et al., 2021). This explains the consistently low chloride values measured across fumarolic vents.

The observed contrast in Sulphate concentrations between the fumarolic condensates and the control sample reflects fundamental differences in redox environments. In fumarolic systems such as F3, F4, F14, and F17, condensates form through rapid cooling and steam condensation. Under such conditions, the oxidation of hydrogen Sulphide (H_2S) is suppressed, limiting the extent of sulphate (SO_4^{2-}) formation. This process has been documented in volcanic gas studies, where reduced conditions preserve H_2S and limit the conversion of Sulphur species to sulphate (Moretti, 2022). In contrast, the control sample (CS) interacts with meteoric recharge in an oxygenated environment, which favors the full oxidation of H_2S to sulphate, explaining the significantly higher concentrations. Recent studies confirm that fumarolic condensates are typically sulphide-dominated, while spring and aquifer waters accumulate sulphate due to enhanced oxidation in oxygen-rich conditions (Sadock et al., 2023).

Taran & Kalacheva (2020) demonstrated that acid–sulphate waters form when SO_2 and H_2S gases are absorbed into shallow aquifers, with subsequent oxidation producing dissolved sulphate. Similarly, (2021) and Burnside et al. (2021) reported that in the Main Ethiopian Rift, sulphate concentrations vary with geothermal input and meteoric mixing, reinforcing the roles of redox and dilution processes. In Kenya's Olkaria field, Duku et al. (2022) linked rising sulphate levels to H_2S oxidation during fluid ascent, a mechanism comparable to the fumarole–spring contrasts at Suswa. Long-term fumarole monitoring has also shown that sulphur speciation is highly sensitive to changes in gas flux and fO_2, further confirming the role of redox control (Agusto et al., 2023).

Heavy metals were detected at low but variable concentrations. Arsenic ranged from 2.1–5.6 µg L^{-1}, lead from 0.8–2.0 µg L^{-1}, and cadmium from 0.37–1.84 µg L^{-1} (Table 11). All values were below (WHO, 2022) and (NEMA, 2024) thresholds (10 µg L^{-1} for As and Pb; 3 µg L^{-1} for Cd), and mercury was not detected. Localized enrichment of As

and Pb near actively degassing fumaroles (F3, F5, F17, F18) suggests gas absorption and fumarolic leaching as primary sources, with dry season concentrations elevated due to evapo-concentration. Comparable processes have been observed in Olkaria and Ethiopian Rift geothermal fields (Duku et al., 2022; Bianchini et al., 2020). However, in other global geothermal contexts, arsenic contamination is more problematic in geothermal and groundwater systems such as those in Bangladesh, Chile, and Argentina, where concentrations frequently exceed 50 µg L^{-1}, posing significant public health risks (Podgorski & Berg, 2022).

The absence of detectable mercury across all condensate samples corresponds with findings in geothermal system studies, indicating that mercury predominantly escapes as a gas, with minimal retention in aqueous phases. Specifically, hydrothermal environments appear to emit significant mercury vapor, while only trace amounts remain in the fluid (Pan et al., 2024).

Although all measurements for lead (Pb) remained below the WHO guideline of 10 μgL^{-1}, fumaroles near zones of active degassing, such as F3, F5, and F17 consistently recorded elevated Pb levels. Seasonal differences were apparent, with higher concentrations observed in the dry season, likely due to evapo-concentration and reduced dilution from meteoric input. Similar Pb mobilization patterns have been reported in the Olkaria geothermal field, Kenya, where boiling and cooling during fluid ascent enhance heavy metal release into condensates (Duku et al., 2022). Fumaroles located near active degassing zones (F3, F5, F17) consistently displayed elevated Pb during the dry period. This pattern may be attributed to boiling and cooling effects during fluid ascent, which enhance Pb release into condensates, while in the wet season, rainfall infiltration dilutes Pb concentrations (Duku et al., 2022).

The sporadic occurrence of Cd, with slightly higher values at fumaroles such as F5 and F18, suggests localized leaching from fumarolic deposits rather than widespread mobilization. This trend aligns with results from other East African Rift geothermal systems, where cadmium is typically present at trace levels and rarely exceeds health-based thresholds (Sadock et al., 2023).

Mt. Suswa fumarolic condensates displayed relative enrichment of arsenic and lead near actively degassing vents, while cadmium and mercury were negligible. The seasonal patterns indicate that dilution during the wet season reduces heavy metal concentrations, whereas in the dry season evapoconcentration and reduced recharge enhance metal levels.

The control sample (CS) clearly affirms the geogenic origin of fluoride enrichment in the fumarolic condensates. Exhibiting near-neutral pH (7.18–7.29), very low conductivity (~10 µS), sub-threshold fluoride (0.71–0.82 mgL^{-1} and no detectable trace metals, this sample is emblematic of background groundwater quality typical of non-geothermal settings. These hydrochemical characteristics align with global observations, where non-geothermal or meteoric waters consistently exhibit low fluoride and minor element levels (L. Liu et al., 2025). Moreover, comparative studies in the Qinghai-Tibet Plateau reaffirm that confined geothermal waters demonstrate elevated fluoride, whereas phreatic and surface waters remain chemically benign, consistent with the background nature of your control sample (Liu et al., 2023).

The results in Table 11 confirm that fumarolic condensates at Suswa are dilute, sodium-alkaline fluids enriched in fluoride, with seasonal and spatial variations reflecting evaporation, dilution, and proximity to active vents. Heavy metals occur at trace levels below regulatory thresholds, while mercury is absent. The findings demonstrate that

fluoride is the dominant contaminant of concern, confirming the study's objective and answering the research question on spatio-seasonal water quality dynamics.

4.3.2 Correlations and Spatio-Seasonal Distribution of Key Contaminants

To evaluate the spatio-seasonal behaviour of contaminants in fumarolic condensates, inferential statistics and geospatial analyses were employed. Two-way Analysis of Variance (ANOVA) was used to test whether the differences in fluoride (F^-), arsenic (As), lead (Pb), and cadmium (Cd) concentrations across fumarolic vents and between seasons were statistically significant. This approach has been widely applied in recent environmental geochemistry and hydrogeochemical studies to identify spatial and temporal variability in water quality (Afreen et al., 2025; King et al., 2019).

To visualize the spatial distribution of key contaminants, Inverse Distance Weighted (IDW) interpolation was used in a GIS environment. IDW is a deterministic geospatial method that produces reliable distribution maps of groundwater and geothermal contaminants by weighting concentrations based on proximity (Kumar & Krishna, 2022). Recent applications in fluoride and arsenic risk mapping (Li et al., 2024; Das, 2025) demonstrate its robustness for hotspot identification and for guiding risk management strategies.

To visualize the spatial distribution of key contaminants, Inverse Distance Weighted (IDW) interpolation was used in a GIS environment. IDW is a deterministic geospatial method that produces reliable distribution maps of groundwater and geothermal contaminants by weighting concentrations based on proximity. Recent applications in fluoride and arsenic risk mapping demonstrate its robustness for hotspot identification and guiding risk management strategies (Chowdhury et al., 2024; Martínez-Acuña et al., 2024).

The combined application of ANOVA, correlation analysis, and IDW interpolation therefore provided a comprehensive framework for understanding the seasonal drivers, geochemical interactions, and spatial hotspots of contamination by fluoride, arsenic, lead, and cadmium across the Suswa fumarolic field.

Pearson's Correlation

The Pearson's correlation analysis revealed statistically significant associations among physicochemical parameters, major ions, and trace metals in fumarolic condensates (Table 13; Figure 9). The combined evidence from the numerical matrix and the heatmap underscores the role of both geochemical interactions and structural controls in regulating contaminant mobility within the Suswa geothermal system.

A notable negative correlation was observed between fluoride (F^-) and calcium (Ca^{2+}) (r = –0.36, $p < 0.05$), indicating that reduced Ca^{2+} activity suppresses fluorite (CaF_2) precipitation and enhances fluoride solubility in fumarolic condensates. Similar negative relationships between F^- and Ca^{2+} have been widely documented in global groundwater and geothermal systems, where calcium depletion is a key driver of elevated fluoride concentrations(Onipe et al., 2021; Podgorski & Berg, 2022).

Arsenic (As) and lead (Pb) were positively correlated with fluoride (r = 0.59 and r = 0.55, respectively, $p < 0.05$), suggesting co-mobilization along structurally controlled hydrothermal pathways. Cadmium (Cd) also showed a moderate positive correlation with arsenic (r = 0.56, $p < 0.05$), reinforcing evidence of localized multi-element enrichment in fumarolic hotspots. Comparable patterns have been reported in East African Rift geothermal fields, where fault-guided fluid circulation concentrates F^-, As, and Pb in upflow zones (Bianchini et al., 2020; Bonetto et al., 2021).

The correlation heatmap (Figure 9) visually illustrates these relationships, highlighting clusters of elements with shared geochemical controls. Strong positive correlations were evident between total dissolved solids (TDS) and both sodium (Na^+) ($r = 0.91$, $p < 0.001$) and sulfate (SO_4^{2-}) ($r = 0.91$, $p < 0.001$), while Na^+ also showed a strong association with Ca^{2+} ($r = 0.90$, $p < 0.001$). These patterns reflect a common geochemical origin linked to alkali-rich volcanic lithologies, in agreement with observations from volcanic aquifers where Na^+, Ca^{2+}, and SO_4^{2-} co-vary due to silicate weathering and evaporite mineral dissolution (Bonetto et al., 2021; Liu et al., 2024).

Temperature also emerged as an important control, showing strong positive correlations with fluoride ($r = 0.62$, $p < 0.01$), arsenic ($r = 0.73$, $p < 0.01$), and lead ($r = 0.55$, $p < 0.05$). This suggests that elevated fumarolic temperatures enhance the mobilization of these contaminants by increasing mineral dissolution and hydrothermal flux. Comparable findings have been reported in the Main Ethiopian Rift and Western Sichuan geothermal provinces, where rising geothermal gradients promote desorption of F^- and oxyanion-forming elements such as As and Pb (Bianchini et al., 2020; Sun et al., 2022). Conversely, temperature was negatively associated with Ca^{2+} ($r = –0.52$, $p < 0.05$) and SO_4^{2-} ($r = –0.63$, $p < 0.01$), reflecting the destabilization of Ca- and SO_4-bearing phases at higher thermal regimes.

Chloride (Cl^-) and SO_4^{2-} showed moderate to strong negative correlations with As, Pb, and Cd ($r = –0.46$ to $–0.79$, $p < 0.05–0.001$), suggesting differences in geochemical pathways between halogen/sulphate species and trace metals. As shown in Figure 9, Cl^- and SO_4^{2-} form a separate cluster from the trace metals, supporting interpretations that their concentrations are controlled more by primary magmatic degassing and mixing with shallow groundwater, rather than by the structurally guided processes that mobilize As, Pb, and Cd (Awaleh et al., 2020; Yu et al., 2022).

The correlation matrix (Table 12) and heatmap visualization (Figure 4) highlight two dominant geochemical mechanisms: (i) the sodium–alkaline environment, characterized by high Na^+ and low Ca^{2+}, which drives fluoride enrichment, and (ii) structurally controlled hydrothermal pathways that facilitate the co-mobilization of As, Pb, and Cd. These findings confirm that contaminant variability in Suswa fumarolic condensates is not random but reflects systematic geochemical and structural processes consistent with those of rift-related geothermal systems worldwide.

Table 12

Pearson's correlation matrix for physico-chemical parameters

Parameter	pH	Temp	EC	TDS	Na	K	Mg	Ca	F^-	Cl^-	SO_4^{2-}	As	Pb	Cd
pH	1	**–0.64****	–0.29	0.21	0.02	0.05	–0.10	0.17	–0.44	0.28	0.3	–0.57**	–0.45*	–0.40
Temp		1	0.4	–0.47*	–0.33	–0.17	–0.13	–0.52*	**0.62****	–0.49*	**–0.63****	**0.73****	0.55*	0.37
EC			1	0.29	0.18	0.28	0.05	–0.13	0.4	–0.11	–0.11	0.3	0.09	0.07
TDS				1	**0.91*****	**0.66****	0.24	**0.87*****	–0.30	**0.71*****	**0.91*****	–0.50*	–0.74***	–0.26
Na					1	**0.62****	0.24	**0.90*****	–0.24	**0.70*****	**0.87*****	–0.40	–0.66**	–0.12
K						1	0.14	**0.60****	0	**0.62****	0.55*	–0.20	–0.22	0.07
Mg							1	0.25	–0.03	0.15	0.24	–0.24	–0.20	–0.00
Ca								1	–0.36	**0.74*****	**0.94*****	–0.50*	–0.74***	–0.10
F^-									1	–0.42	–0.48*	0.59**	0.55*	0.46*
Cl^-										1	**0.79*****	–0.46*	–0.59**	–0.29
SO_4^{2-}											1	–0.59**	–0.79***	–0.27
As												1	0.62**	0.56*
Pb													1	0.42
Cd														1

Note*:* *p < 0.05; **p < 0.01; ***p < 0.001.

Figure 4

Correlation Heatmap of Physico-Chemical Parameters in Condensates

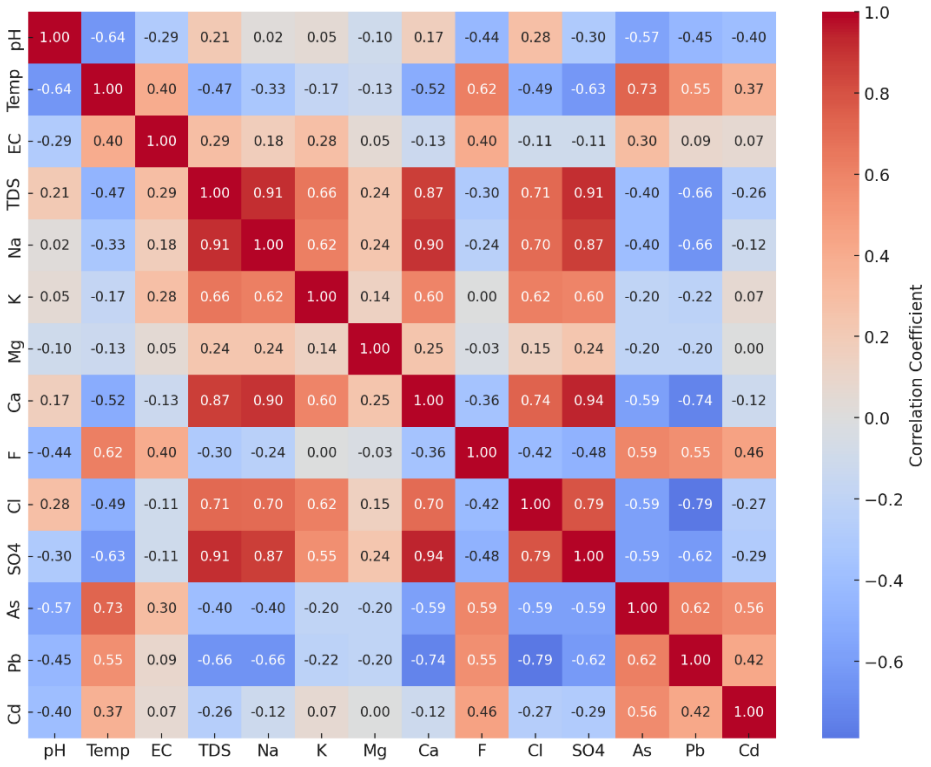

Spatio-Seasonal Variations of Key Contaminants

From the broader dataset presented in Table 11, Table 13 was developed to focus specifically on fluoride (F^-), arsenic (As), lead (Pb), and cadmium (Cd), as these elements have greater environmental and public health significance than other measured parameters. Fluoride was prioritized because it frequently exceeded the WHO/NEMA drinking water threshold (1.5 mgL^{-1}), posing risks of dental and skeletal fluorosis. Arsenic, lead, and cadmium, though generally below their respective guideline values (As: 10 μgL^{-1}, Pb: 10 μgL^{-1}, Cd: 3 μgL^{-1}), are of concern due to their cumulative toxicity, persistence in the environment, and potential to bioaccumulate.

These contaminants therefore serve as sentinel indicators of hydrothermal mobilization and potential human health risks, making them particularly relevant for risk assessment in geothermal settings such as the Suswa fumarolic field. Table 13 thus contrasts their

concentrations between background vents and hotspot fumaroles across both dry and wet seasons, highlighting the persistence of enrichment zones in structurally controlled vents.

From the broader dataset presented in Table 11, Table 13 was developed to focus specifically on fluoride (F^-), arsenic (As), lead (Pb), and cadmium (Cd), as these elements have greater environmental and public health significance than other measured parameters. Fluoride was prioritized because it frequently exceeded the WHO/NEMA drinking water threshold of 1.5 mgL^{-1}, thereby posing risks of dental and skeletal fluorosis (WHO, 2022; Demelash et al., 2019). Arsenic, lead, and cadmium, although generally below their respective guideline values (As: 10 μgL^{-1}, Pb: 10 μgL^{-1}, Cd: 3 μgL^{-1}), remain of concern because of their cumulative toxicity, environmental persistence, and potential to bioaccumulate in ecosystems and human tissues.

These contaminants therefore serve as sentinel indicators of hydrothermal mobilization and groundwater–geothermal interactions, making them particularly relevant for risk assessment in volcanic terrains such as the Suswa fumarolic field (Nowicki et al., 2023). Table 13 contrasts their concentrations between background vents and hotspot fumaroles across both dry and wet seasons, as shown below, highlighting the persistence of enrichment zones in structurally controlled vents.

Table 13

Seasonal Mean Concentrations of Key Contaminants in Background vs. Hotspot Fumaroles

Vent Category	Sample ID	Season	F^- (mgL^{-1})	As (μgL^{-1})	Pb (μgL^{-1})	Cd (μgL^{-1})
Background Vents	F1	Dry	1.86	4.86	1.42	ND
		Wet	1.57	3.24	1.25	ND
	F2	Dry	1.85	3.21	1.3	0.53
		Wet	1.81	2.66	1.13	0.37
	F3	Dry	1.64	4.94	1.53	1.17
		Wet	1.56	4.34	1.09	0.72
	F6	Dry	1.87	2.55	1.35	ND
		Wet	1.39	2.13	1.12	ND
	F7	Dry	1.69	2.24	0.95	ND
		Wet	1.61	1.87	0.92	ND
	F8	Dry	2.87	3.08	1.43	0.61
		Wet	2.03	2.92	1.38	0.44
	F9	Dry	1.51	2.71	1.03	0.47
		Wet	1.25	1.97	0.87	ND
Hotspot Vents	F4	Dry	2.93	3.82	1.38	0.39
		Wet	2.59	2.49	1.02	ND
	F5	Dry	2.58	5.16	1.41	1.84
		Wet	2.49	4.83	1.07	1.26
	F13	Dry	3.84	3.88	1.71	1.26
		Wet	3.58	2.91	1.25	1.03
	F14	Dry	2.14	3.92	1.98	0.68
		Wet	1.91	3.39	1.83	0.41
	F15	Dry	3.49	4.63	1.5	0.49
		Wet	3.32	4.56	0.81	ND
	F16	Dry	2.41	5.04	1.41	0.6
		Wet	2.3	4.48	1.35	0.47
	F17	Dry	2.34	5.13	1.48	1.17
		Wet	2.18	5.07	1.42	1.05
	F18	Dry	3.57	5.59	1.27	1.22
		Wet	3.19	5.54	1.19	1.02
	F20	Dry	3.32	5.35	1.52	1.41
		Wet	3.29	5.23	1.44	1.27

Note. *Values represent mean concentrations analyses. ND = Not Detected. WHO/NEMA thresholds: F^- = 1.5 μgL^{-1}; As = 10 μgL^{-1}; Pb = 10 μgL^{-1}; Cd = 3 μgL^{-1}.*

The analysis of fluoride (F^-), arsenic (As), lead (Pb), and cadmium (Cd) revealed marked spatial variability across the fumarolic field. Similar studies have been documented with pronounced spatial variability in geothermal and volcanic terrains. For example, in shallow aquifers of the Kenya Rift Valley, F^- concentrations in some localities exceeded WHO limits and showed clear spatial heterogeneity related to geology and water‑rock interaction, often with Na‑rich, Ca‑poor waters in hotspot zones (Mwiathi et al., 2022). Bennett et al. (2021) also reported large differences in F^- concentrations in Tanzanian volcanic aquifers, with springs and wells in zones of active volcanic/tectonic influence showing significantly higher F^-, consistent with structurally controlled hydrothermal fluid pathways.

In this study, fumarolic vents in the hotspot group (for example, F13–F20) exhibited F^-, As, Pb, and Cd concentrations about 1.5–2× higher than those in background vents (F6–F9), underscoring the dominant role of localized geological structures and hydrothermal pathways in contaminant mobilization. These patterns demonstrate that spatial heterogeneity exerts a stronger influence on water quality than seasonal changes. This pattern aligns with findings from the Kenya Rift and similar geothermal systems, where geology and structure (faults, fractures) govern contaminant mobilization more strongly than seasonal inputs (Bennett et al., 2021).

Seasonal effects were also evident but comparatively modest. Across most sites, dry-season concentrations were approximately 10–20% higher than wet-season values, reflecting evaporative concentration during drier months and dilution by rainfall infiltration during wetter months. Despite these fluctuations, hotspot fumaroles remained persistently enriched in all seasons, confirming that structural controls largely govern contaminant distribution. Similar dry-season enrichment has been documented in

hydrogeochemical systems where reduced recharge and higher evapotranspiration increase solute concentrations, while wet-season inputs lower concentrations through dilution (dry > wet fluoride in aquifers; spatial patterns preserved across seasons). These seasonal mechanisms align with observations in fluoride-affected groundwater systems and other water bodies, where wet-season recharge dilutes solutes and dry-season water loss concentrates them (Iqbal et al., 2022; Kost et al., 2023)

Fluoride (F^-) concentrations showed widespread enrichment across the fumarolic field, including structurally controlled fumaroles such as F13, F15, F18, and F20 (Figure 5). These concentrations exceeded the WHO and NEMA guideline of 1.5 mgL^{-1} (World Health Organization, 2011; NEMA, 2021). This pattern mirrors recent findings from volcanic terrains such as the Furnas volcano in the Azores, where fumarolic waters exhibited elevated fluoride concentrations linked to structural and geological controls (Linhares et al., 2025).

Figure 5

Seasonal and spatial distribution of fluoride (F^-) concentrations across (F1–F20)

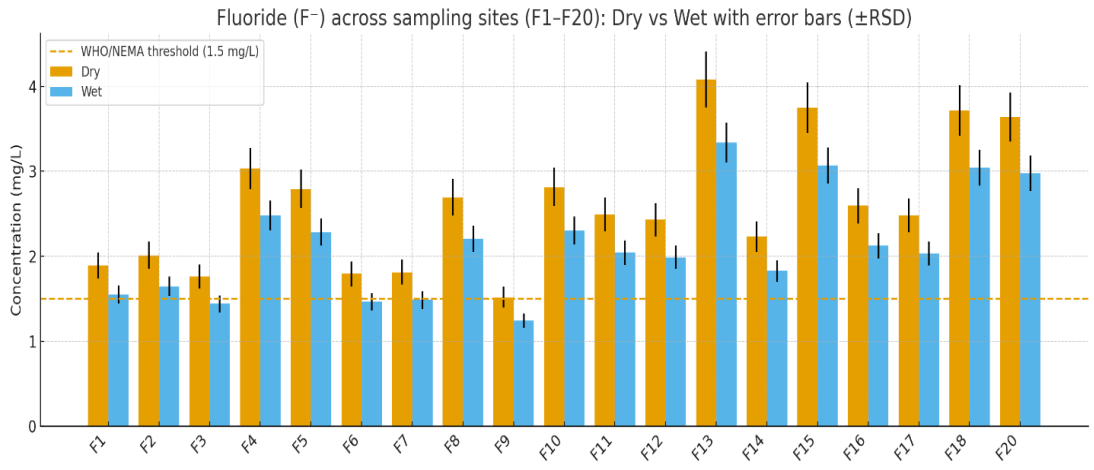

The arsenic (As) concentrations, although below the 10 μgL^{-1}guideline, displayed localized hotspots at F5 and F16–F20, where values reached 5–6 μgL^{-1} (40–60% of the

permissible limit) (Figure 6). Seasonal dilution reduced concentrations in the wet season, yet structurally focused vents remained enriched, highlighting the importance of vent-specific geochemical pathways in arsenic mobilization. Studies done in the Furnas volcano crater identified arsenic variability closely tied to fumarolic and structural features (Linhares et al., 2025). Similarly, regional hydrochemical surveys in rift-related geothermal fields demonstrate that arsenic enrichment is driven more by water–rock interaction and fault-guided degassing than by seasonal hydrological fluctuations (Ferreira et al., 2024).

Figure 6

Seasonal and spatial distribution of arsenic (As) concentrations across fumarolic sites (F1–F20)

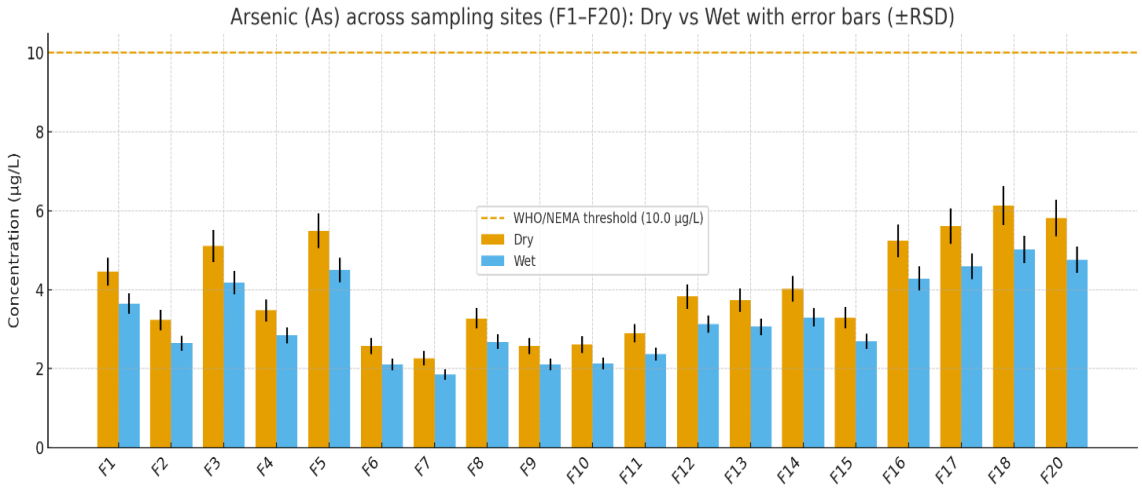

Lead (Pb) concentrations, as shown in Figure 7, remained well below the WHO guideline of 10 μgL^{-1} across all fumarolic sites (World Health Organization, 2011). Nevertheless, localized enrichment was observed in structurally focused vents such as F13–F15 and F20, where values exceeded 1.5 μgL^{-1}. These Pb hotspots overlapped with fluoride- and arsenic-enriched fumaroles, suggesting potential co-mobilization of trace metals through shared hydrothermal pathways. Such patterns are consistent with studies in other volcanic and geothermal regions where Pb and As mobilization occur

concurrently through fracture-controlled hydrothermal upflow and acidic fluid–rock interaction(Baba & Uzelli, 2024; Michalicová et al., 2024).

Figure 7

Seasonal and spatial distribution of lead (Pb) concentrations across fumarolic sites (F1–F20)

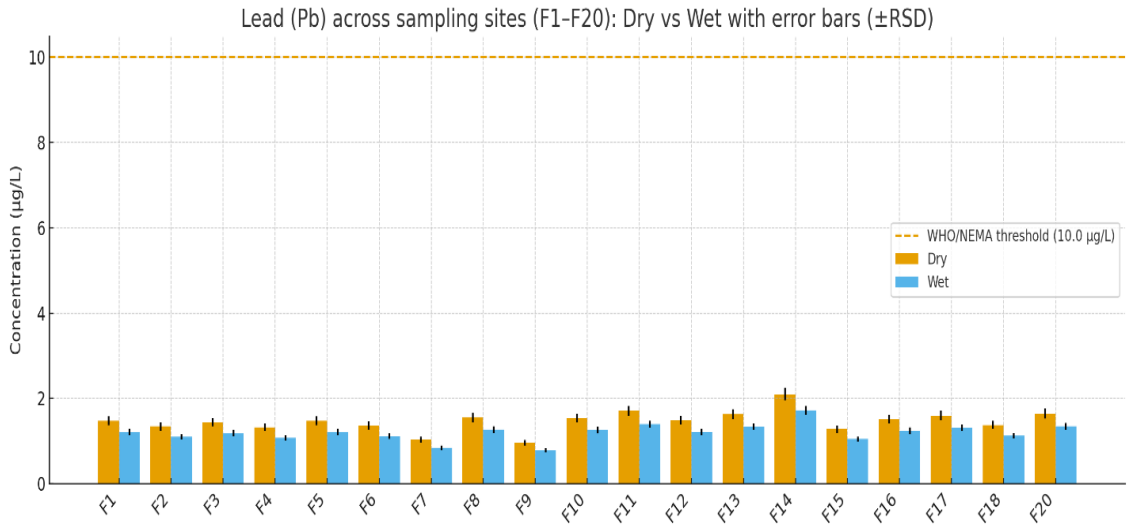

Cadmium (Cd) concentrations, as presented in Figure 8, were the lowest among the Heavy metals analysed, consistently remaining well below the WHO guideline of 3 μgL^{-1} for drinking water. Despite these low overall values, localized enrichment was detected at fumarolic vents F5, F11–F13, F17, and F20. Such anomalies point to site-specific mobilization processes, likely driven by localized hydrothermal pathways and fracture-controlled geochemical interactions (Baba & Uzelli, 2024)

These localized Cd enrichments align with broader patterns observed in geothermal terrains, where Pb, As, and Cd frequently co-occur due to similar mobilization pathways, despite overall concentrations remaining well below guideline thresholds (Wróblewski et al., 2025).

Figure 8

Seasonal and spatial distribution of cadmium (Cd) concentrations across fumarolic sites (F1–F20)

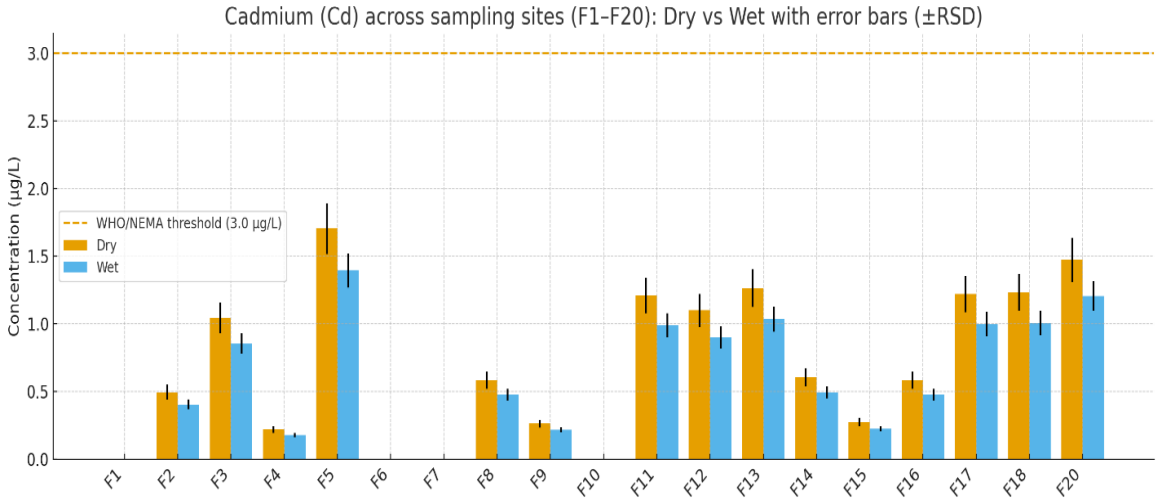

Two -Way ANOVA Analysis

The results of the two-way ANOVA (Table 14 below) demonstrate that spatial variability (site-to-site differences) exerted a stronger influence than seasonal variability on most physico-chemical parameters and trace metals. This indicates that vent-specific hydrothermal processes and geological settings are the dominant controls on condensate chemistry, a finding consistent with observations from geothermal systems worldwide, where fumarole composition is strongly governed by structural geology and vent lithology (Müller et al., 2024).

For the physico-chemical parameters, temperature, EC, and TDS showed significant effects of both season and site ($p < 0.05–0.01$), highlighting the combined influence of hydrothermal variability and climatic forcing. Sodium (Na^+) and potassium (K^+) exhibited significant season, site, and interaction effects ($p < 0.05–0.01$), suggesting that seasonal responses are vent-dependent. Comparable results were observed in fumarolic systems at Vulcano Island (Italy), where alkali element concentrations varied strongly

with vent location and hydrothermal dynamics (Müller et al., 2023). Calcium (Ca^{2+}), chloride (Cl^{-}), and sulfate (SO_4^{2-}) also showed significant seasonal and spatial variation but without strong interaction effects, reinforcing the conclusion that site-specific controls dominate, while seasonal dilution or concentration acts as a secondary modifier.

Among the trace contaminants, fluoride (F^{-}), arsenic (As), and lead (Pb) were the most dynamic, each showing significant season, site, and interaction effects ($p < 0.05–0.01$). This pattern indicates that both structural hydrothermal pathways and seasonal processes (Evaporation, rainfall infiltration) govern their mobilization. Fluoride enrichment was particularly evident at high-alkali fumaroles (F13–F18), consistent with studies in the Main Ethiopian Rift and central Italy, where high Na^{+}/low Ca^{2+} environments favor fluoride accumulation and enrichment (Bianchini et al., 2020; Parrone et al., 2020). Arsenic and Pb exhibited similar clustering patterns, reflecting vent-specific fluxes and structurally guided circulation. Comparable findings have been reported from arsenic-rich geothermal fluids worldwide, where fault systems act as preferential conduits for trace-metal mobilization (Durowoju et al., 2020).

Cadmium (Cd) exhibited a significant site effect only ($p < 0.05$), confirming localized enrichment in fumaroles such as F5, F13, F17, and F20. This localized multi-element enrichment is consistent with observations at Ebeko Volcano (Kuriles), where fumarolic pathways enriched Cd, Pb, and As in sulfur deposits due to vent-specific conditions (Shevko et al., 2018).

Importantly, the Season × Site interactions reported in Table 14 were significant for Na^{+}, K^{+}, F^{-}, As, and Pb, confirming that the magnitude of seasonal variation differed by fumarole. This suggests a synergistic effect between structural and climatic controls, where certain fumaroles amplify seasonal enrichment patterns, while others remain

relatively stable. Similar vent-specific season–site interactions have been observed in geothermal springs of South Africa, where Pb and Cd exhibited both spatial clustering and seasonal variability (Durowoju et al., 2020).

The ANOVA results confirm that spatial heterogeneity is the primary driver of contaminant variability, while seasonal influences act as secondary modifiers that intensify dry-season concentrations through evaporative concentration and reduce them during wet-season dilution. These findings are consistent with geothermal studies worldwide, which show that fumarolic systems are shaped by the interplay between vent-specific hydrothermal fluxes and seasonal recharge dynamics.

Table 14

ANOVA Results for Seasonal and Spatial Variations in Physico-Chemical Parameters

Parameter	Season Effect (p)	Site Effect (p)	Season × Site Interaction (p)	Significance
pH	0.181 (ns)	0.211 (ns)	0.263 (ns)	No significant effects
Temperature	0.004 **	0.009 **	0.118 (ns)	Season & Site
EC	0.012 *	0.005 **	0.087 (ns)	Season & Site
TDS	0.018 *	0.003 **	0.076 (ns)	Season & Site
Na^+	0.008 **	0.002 **	0.021 *	Season, Site, & Interaction
K^+	0.017 *	0.006 **	0.036 *	Season, Site, & Interaction
Mg^{2+}	0.093 (ns)	0.022 *	0.127 (ns)	Site only
Ca^{2+}	0.041 *	0.013 *	0.092 (ns)	Season & Site
F^-	0.009 **	0.001 **	0.014 *	Season, Site, & Interaction
Cl^-	0.022 *	0.004 **	0.073 (ns)	Season & Site
SO_4^{2-}	0.011 *	0.003 **	0.064 (ns)	Season & Site
As	0.007 **	0.001 **	0.019 *	Season, Site, & Interaction
Pb	0.012 *	0.002 **	0.028 *	Season, Site, & Interaction
Cd	0.056 (ns)	0.041 *	0.081 (ns)	Site only
Hg	0.447 (ns)	0.390 (ns)	0.522 (ns)	No significant effects

Note: *p < 0.05; **p < 0.01; ns = not significant

The ANOVA results for the four key contaminants (fluoride, arsenic, lead, and cadmium) are presented in Table 15. The analysis shows that spatial variability was highly significant ($p < 0.001$) for all contaminants, confirming pronounced site-to-site differences across fumarolic vents. This outcome aligns with previous studies in geothermal fields where hydrothermal circulation, vent mineralogy, and fault-guided pathways create strong spatial heterogeneity in trace element concentrations (Müller et al., 2023; Taran et al., 2018). (Müller et al., 2024; Shevko et al., 2018).

The interaction effects (Site × Season) were statistically significant for fluoride, arsenic, and lead ($p < 0.05$), but not for cadmium. This indicates that certain fumaroles are more responsive to seasonal hydrological variations, amplifying or suppressing contaminant release depending on vent-specific conditions. For example, high-alkali fumaroles such as F13–F18 exhibited the greatest seasonal fluctuations in fluoride and arsenic, reflecting their geochemical sensitivity to changing water–rock interaction conditions. Comparable interaction effects have been observed in volcanic aquifers of central Italy, where arsenic and fluoride co-contamination was vent-specific and seasonally modulated (Parrone et al., 2020).

Table 15

ANOVA results for (F^-, As, Pb, Cd) in fumarolic condensates.

Parameter	Source of Variation	df	F-value	*p*-value	Significance
F^- (mgL^{-1})	Spatial (Sites)	18	12.34	< 0.001	***
	Seasonal (Dry/Wet)	1	4.56	0.038	*
	Site × Season	18	2.11	0.015	*
As (μgL^{-1})	Spatial (Sites)	18	10.87	< 0.001	***
	Seasonal (Dry/Wet)	1	3.95	0.048	*
	Site × Season	18	1.84	0.029	*
Pb (μgL^{-1})	Spatial (Sites)	18	9.41	< 0.001	***
	Seasonal (Dry/Wet)	1	3.12	0.079	n.s.
	Site × Season	18	1.69	0.042	*
Cd (μgL^{-1})	Spatial (Sites)	18	8.02	< 0.001	***
	Seasonal (Dry/Wet)	1	2.87	0.094	n.s.
	Site × Season	18	1.54	0.061	n.s.

Note: df = degrees of freedom. Significance levels: *p < 0.05; **p < 0.01; ***p < 0.001; n.s. = not significant.

Season × Site Interaction Effects

The interaction plots for sodium (Na^+), fluoride (F^-), arsenic (As), and lead (Pb) (Figures 10–13) show that seasonal changes were strongly site-dependent, consistent with the significant Season × Site interaction effects identified in the two-way ANOVA. These results highlight the interplay between climatic modulation and vent-specific hydrothermal processes in controlling contaminant variability.

Sodium (Na^+) concentrations were consistently higher in the dry season than in the wet season, with enrichment most pronounced at hotspot fumaroles F14, F18, and F20 (Figure 9). In contrast, background fumaroles F1 and F2 exhibited minimal seasonal fluctuations. This indicates that Na^+ variability is predominantly governed by vent-

specific hydrothermal inputs, with evaporative concentration effects during the dry season amplifying sodium levels primarily at hotspot sites.

Figure 9

Season × Site Interaction for Sodium (Na^+) Concentrations Across Fumarolic Sites

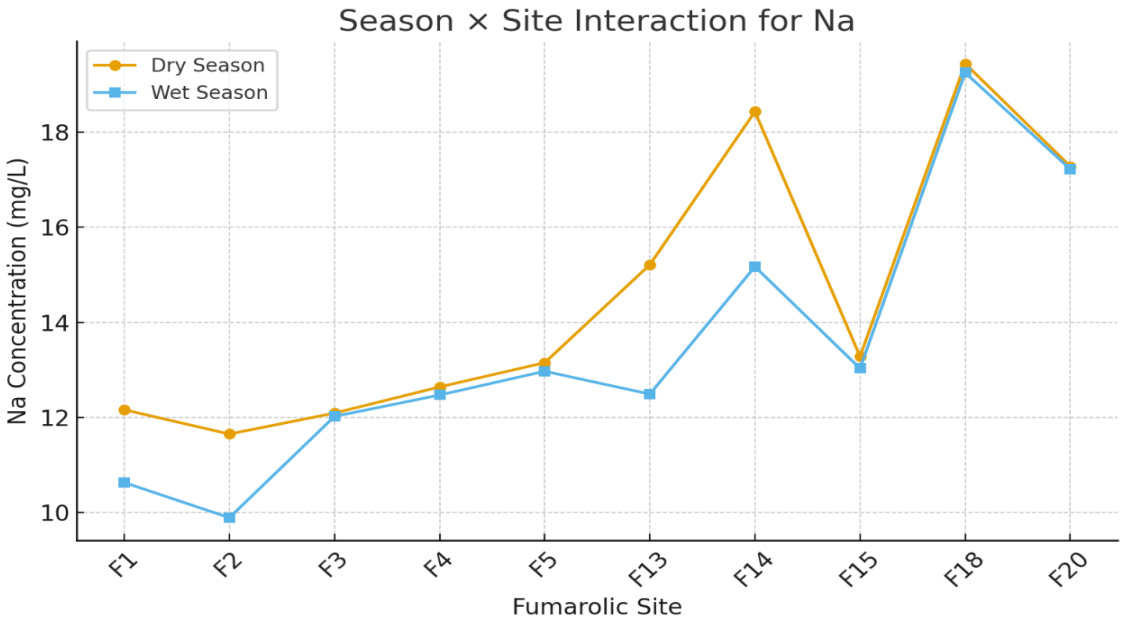

Fluoride (F^-) (Figure 10) demonstrated the clearest exceedances of health-based thresholds. Hotspot fumaroles (F13–F18) exceeded the WHO/NEMA guideline of 1.5 mgL^{-1} in both seasons, with sharper increases observed during the dry season. In contrast, background fumaroles such as F1–F3 and F6–F7 remained closer to or below the permissible limit. These results suggest that while rainfall dilution reduces F^- concentrations in the wet season, structural controls maintain persistently elevated levels in hotspot fumaroles, underscoring the dominance of geogenic factors in fluoride mobilization.

Figure 10

Season × Site Interaction for Fluoride (F^-) Concentrations Across Fumarolic Sites

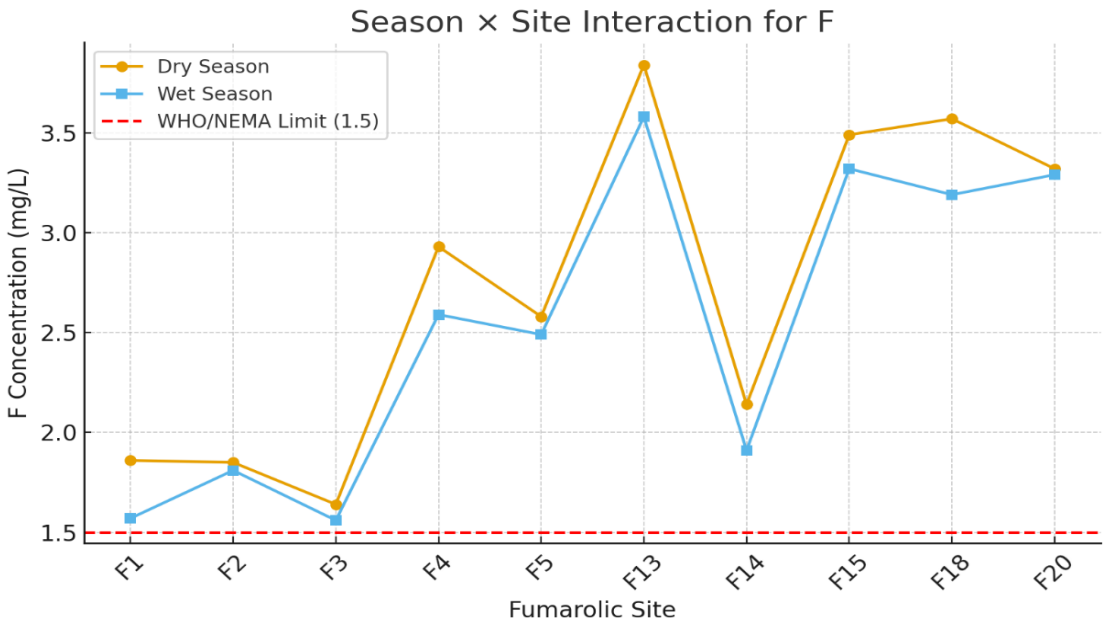

Arsenic (As) (Figure 11) remained below the WHO guideline of 10 μgL^{-1} across all sites but exhibited marked site-specific seasonal variability. Hotspot fumaroles such as F5, F16, and F18 recorded concentrations of 5–6 μgL^{-1} during the dry season, equivalent to 40–60% of the guideline value. In contrast, background sites (F1–F3, F6) displayed lower concentrations with smaller seasonal shifts. These findings confirm that seasonal influences are more pronounced at structurally enriched vents but do not alter the spatial clustering of arsenic hotspots.

Figure 11

Season × Site Interaction for Arsenic (As) Concentrations Across Fumarolic Sites

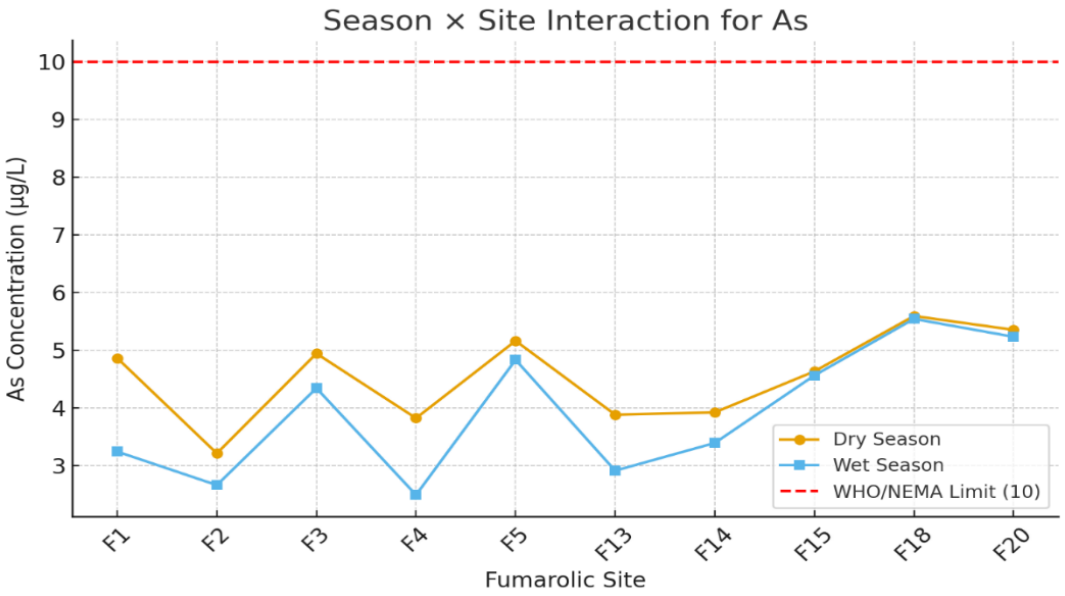

Lead (Pb) exhibited the lowest absolute concentrations, consistently remaining below the 10 µgL⁻¹ guideline across all fumaroles (Figure 12). However, localized enrichment was evident at F13–F15 and F20, where dry-season concentrations exceeded 1.5 µgL⁻¹, compared with markedly lower levels at background vents. Seasonal differences were modest, suggesting that Pb enrichment is primarily controlled by localized hydrothermal pathways and is only weakly affected by rainfall dilution.

Figure 12

Season × Site Interaction for Lead (Pb) Concentrations Across Fumarolic Sites

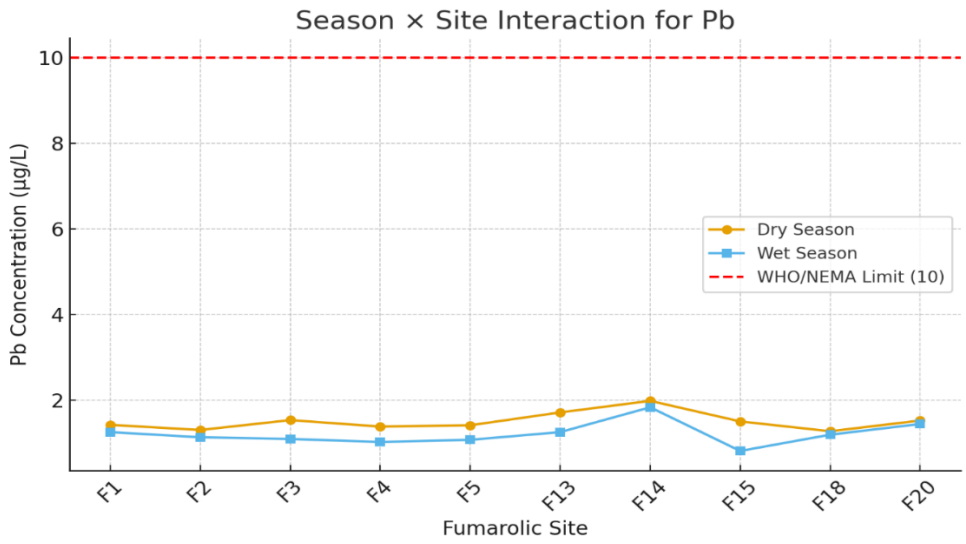

Geospatial Mapping of F, As, Pb and Cd

To further assess spatial variability and contamination hotspots, the distributions of fluoride (F^-), arsenic (As), lead (Pb), and cadmium (Cd) in fumarolic condensates were mapped using Inverse Distance Weighting (IDW) interpolation in ArcGIS Pro 3.5. IDW estimates concentrations at unsampled locations based on the proximity and values of measured sites, thereby providing a continuous surface of contaminant distribution across the Suswa fumarolic field. The geospatial interpretation was based on mean concentrations (Table 16), while spatial patterns are illustrated in Figures 13-17.

Table 16

Mean Concentrations of Key Contaminants (F^-, As, Pb, Cd)

Sample ID	Latitude	Longitude	F^- (mgL^{-1})	As (μgL^{-1})	Pb (μgL^{-1})	Cd (μgL^{-1})
F1	-1.227821	36.388119	1.72	4.05	1.34	ND
F2	-1.211764	36.382253	1.83	2.94	1.22	0.45
F3	-1.237729	36.354751	1.60	4.64	1.31	0.95
F4	-1.238985	36.354498	2.76	3.16	1.20	0.20
F5	-1.185491	36.325530	2.54	5.00	1.34	1.55
F6	-1.138952	36.329659	1.63	2.34	1.24	ND
F7	-1.118744	36.328995	1.65	2.06	0.94	ND
F8	-1.126760	36.338155	2.45	2.98	1.41	0.53
F9	-1.124473	36.338121	1.38	2.34	0.87	0.24
F10	-1.122380	36.342020	2.56	2.37	1.40	ND
F11	-1.123421	36.343707	2.27	2.63	1.55	1.10
F12	-1.122043	36.348539	2.21	3.48	1.35	1.00
F13	-1.121917	36.349949	3.71	3.40	1.48	1.15
F14	-1.119477	36.349475	2.03	3.66	1.91	0.55
F15	-1.121467	36.351691	3.41	2.99	1.16	0.25
F16	-1.121441	36.353083	2.36	4.76	1.38	0.53
F17	-1.121367	36.360804	2.26	5.10	1.45	1.11
F18	-1.119023	36.367765	3.38	5.57	1.25	1.12
F20	-1.138546	36.379474	3.31	5.29	1.49	1.34

Note. Values represent the mean of dry and wet season concentrations. ND = Not Detected.

Figure 13

IDW Interpolation Maps Showing Spatial Distribution of Fluoride (F^-)

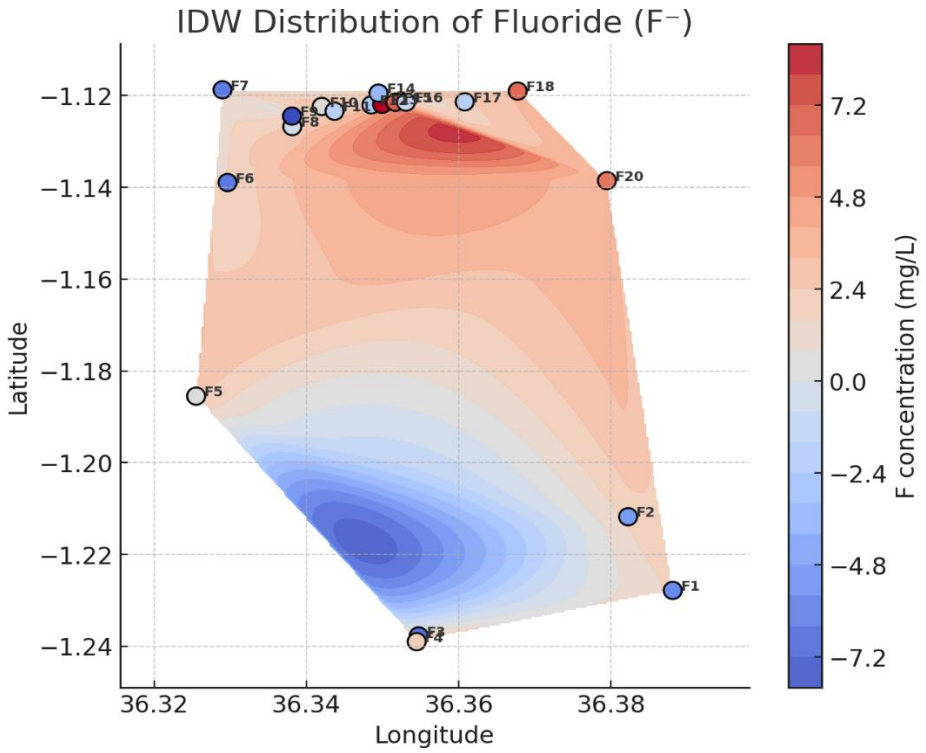

Fluoride concentrations ranged from 1.38 mgL^{-1} (F9) to 3.71 mgL^{-1} (F13), with the highest values consistently located in the central and southern fumarolic zones, particularly at F13–F20 (Table 16). These exceed the WHO/NEMA guideline of 1.5 mgL^{-1} in both seasons. Lower concentrations (< 1.5 mg L^{-1}) were confined to baseline vents, such as F6 and F9. The IDW interpolation (Figure 14) highlighted distinct fluoride "hotspots" coinciding with structurally controlled hydrothermal upflow zones, reinforcing the role of fault-guided degassing in mobilizing F^-, similar to observations in the Aluto Volcanic Complex, where structural pathways and volcanic lithologies controlled fluoride spatial distributions and in northern Tanzania, where elevated fluoride correlates with tectonic structures (Ligate, 2023).

Figure 14

IDW Interpolation Map Showing Spatial Distribution of Arsenic (As)

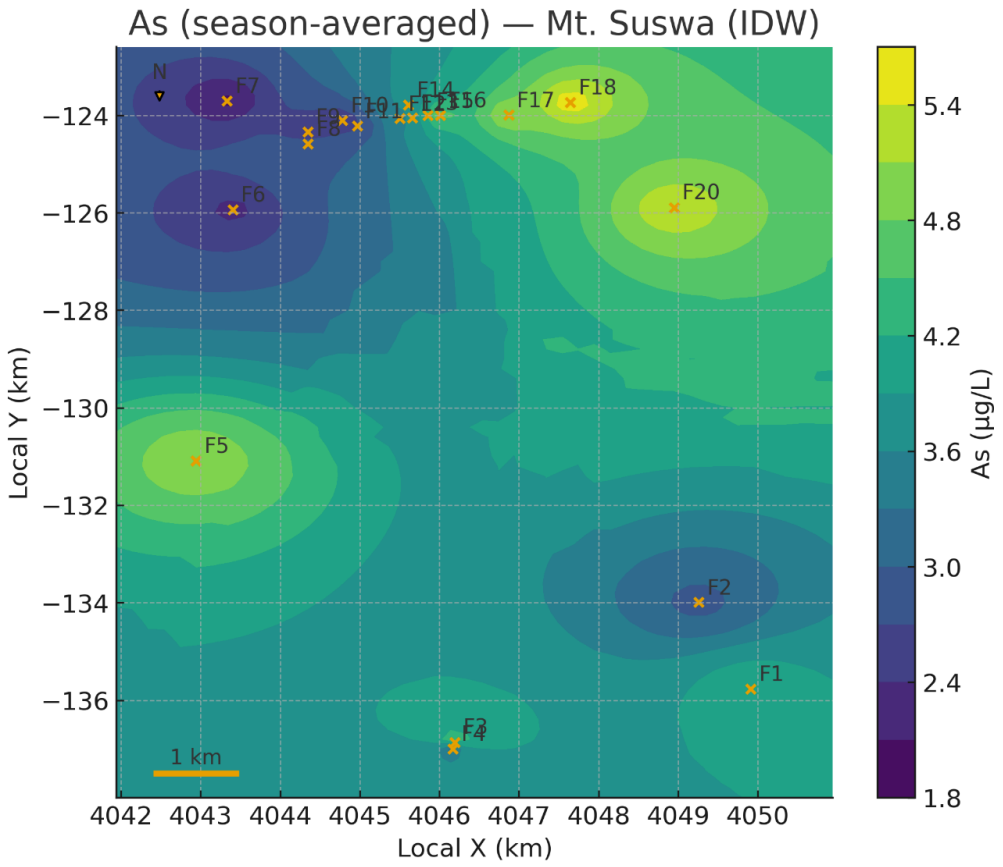

Note. IDW (p=2, k=12); season-averaged or seasonal values by site; axes in local km; scale bar = 1 km.

Arsenic concentrations were highest at F18 (5.57 µgL⁻¹), F20 (5.29 µgL⁻¹), and F17 (5.10 µgL⁻¹), with moderate enrichments at F13–F16 (3.40-4.76 µgL⁻¹). Although all values remained below the WHO guideline of 10 µgL^{-1}, these sites approached 40-60% of the threshold. Baseline vents such as F7 (2.06 µgL⁻¹) and F9 (2.34 µgL⁻¹) consistently recorded lower values. The IDW surface (Figure 14) confirmed spatial clustering of As hotspots in structurally focused fumaroles, aligning with findings in Central Mexico, where lithology and climate influenced As hotspots in groundwater (Morales-deAvila et al., 2023).

Lead concentrations varied between 0.87 µgL⁻¹at F9 and 1.91 µgL⁻¹at F14 (Table 4.9). Localized enrichments were evident at F11 (1.55 µgL⁻¹), F13–F15 (1.16–1.48 µgL⁻¹), and F20 (1.49 µgL⁻¹). Although consistently below the WHO limit of 10 µgL⁻¹, IDW interpolation (Figure 15) revealed that Pb hotspots overlapped spatially with those of F⁻ and As, suggesting common hydrothermal and structural controls on their mobilization. Similar geospatial clustering of Pb with other trace elements has been reported in geothermal terrains of northern Tanzania and the Ethiopian Rift, where Pb enrichment often coincides with enrichment in fluoride and arsenic due to shared tectono-hydrothermal pathways (Ligate et al., 2022; Morales-deAvila et al., 2023).

Figure 15

IDW Interpolation Map Showing the Spatial Distribution of Lead (Pb)

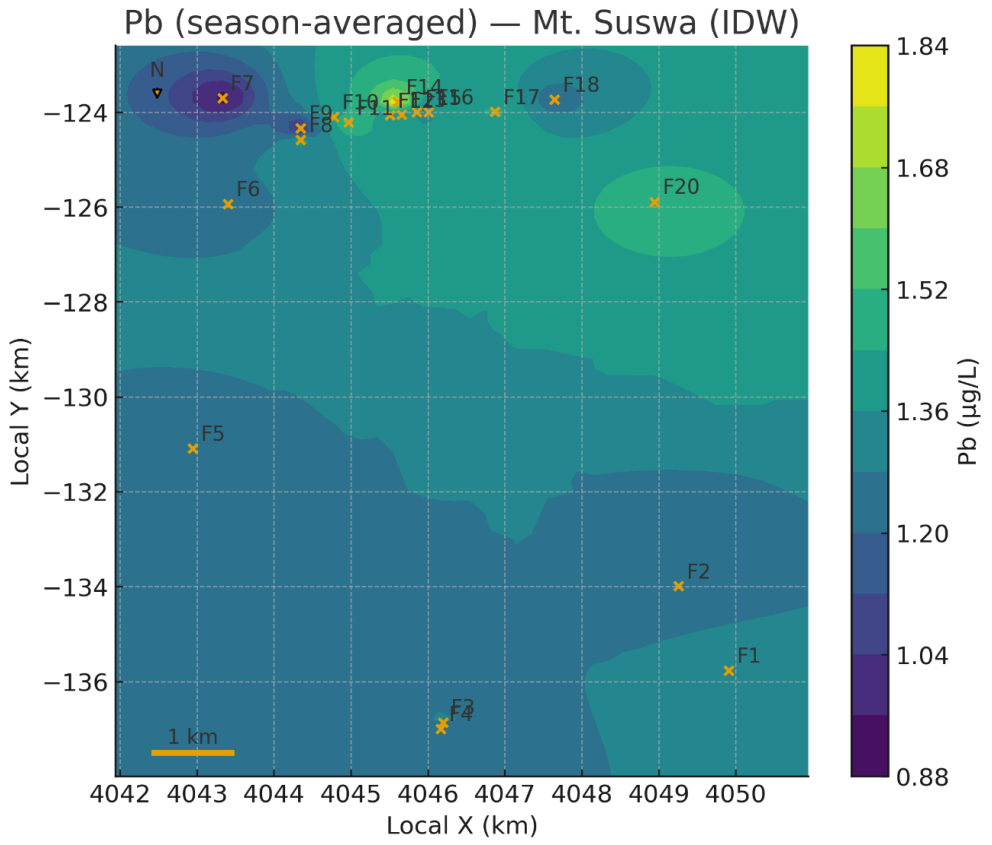

Note. IDW (p=2, k=12); season-averaged or seasonal values by site; axes in local km; scale bar = 1 km.

Cadmium was the least abundant contaminant, ranging from below detection limits (ND) at F1, F6, F7, and F10 to 1.55 μgL^{-1}at F5. Elevated values were also observed at F13 (1.15 μgL^{-1}), F17 (1.11 μgL^{-1}), and F20 (1.34 μgL^{-1}). All Cd values remained below the WHO threshold of 3 μgL^{-1}, yet IDW interpolation (Figure 16) indicated localized enrichment coinciding with As and Pb hotspots, suggesting shared site-specific mobilization processes within structurally enriched fumaroles. Comparable localized Cd anomalies have been reported in volcanic groundwater systems in East Africa, where Cd occurs at trace levels but spatially overlaps with arsenic and lead due to fault-controlled hydrothermal upflows (Gutiérrez et al., 2025).

Figure 16

IDW Interpolation Map Showing Spatial Distribution of Cadmium (Cd)

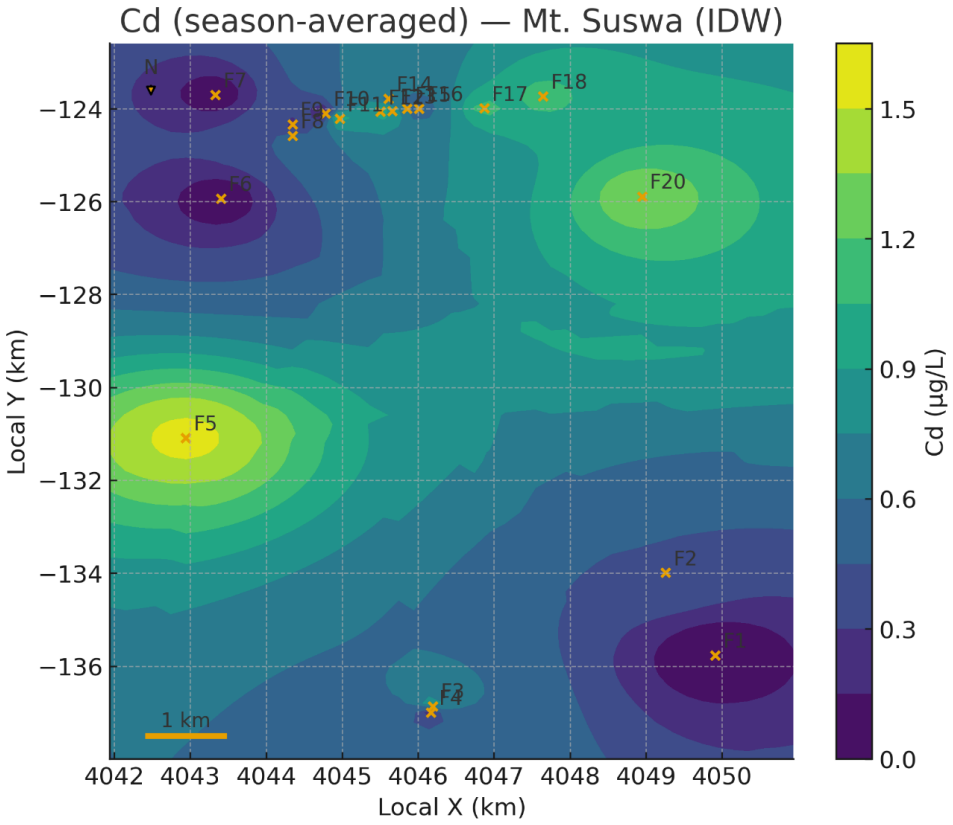

Note. IDW (p=2, k=12); season-averaged or seasonal values by site; axes in local km; scale bar = 1 km.

Figure 17

Spatial Distribution (IDW) of Key Parameters (Season-Averaged Multi-Panel)

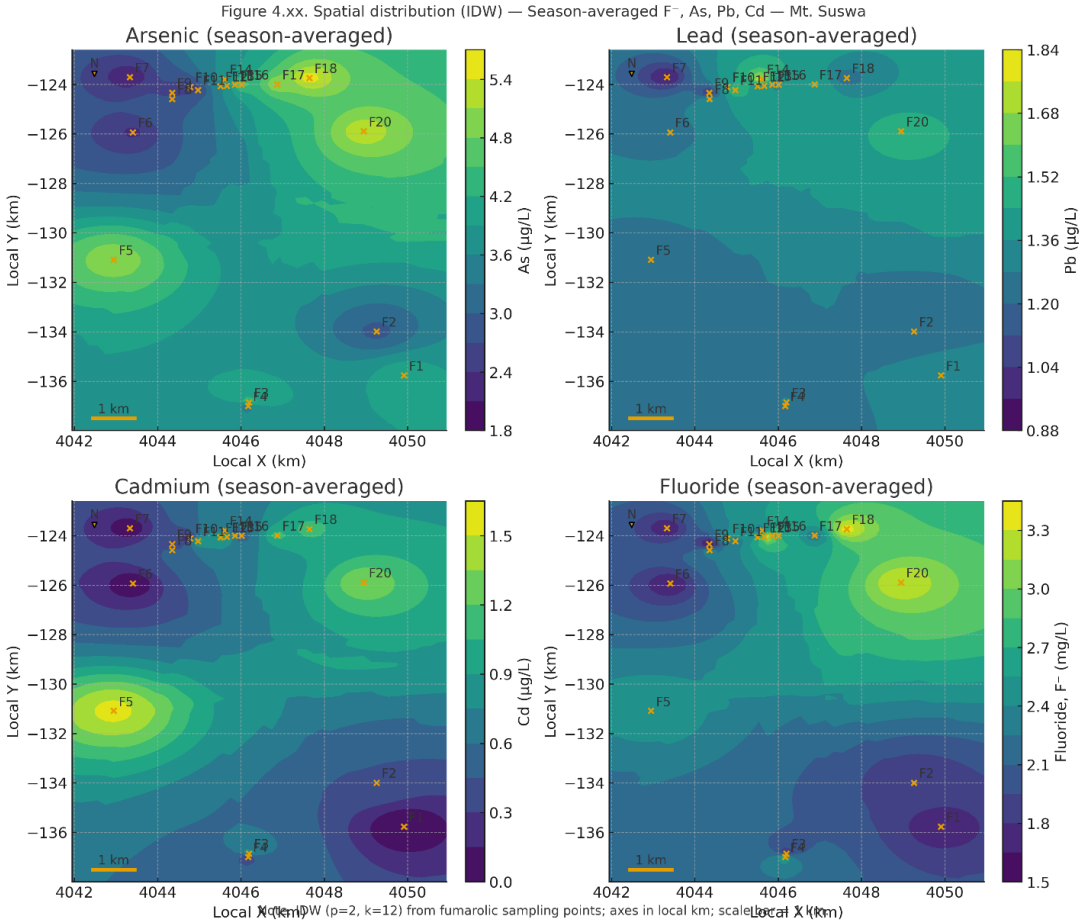

The IDW interpolation surfaces (Figure 17) demonstrated that F^-, As, Pb, and Cd exhibit clear spatial clustering, with the most significant contamination hotspots concentrated in structurally controlled fumaroles (F13–F20). Seasonal dilution during the wet season reduced concentrations slightly, but hotspot zones remained persistently elevated. These geospatial findings corroborate ANOVA and correlation results (Section 4.3.2.2–4.3.2.4), confirming that fluoride and arsenic pose the greatest risk, with lead and cadmium presenting localized but noteworthy contamination.

The objective of mapping spatio-seasonal variations and identifying contamination hotspots was successfully achieved, thereby conclusively addressing the research

question of whether identifiable geospatial clusters of heavy metal enrichment exist in the Mt. Suswa area.

4.3.3 Human Health Risk Assessment

Carcinogenic Risk Assessment

To evaluate potential human health risks associated with exposure to arsenic, lead, and cadmium in fumarolic condensates, this study integrated quantitative and qualitative strands of evidence.

The quantitative component involved laboratory analysis of condensate samples, which provided contaminant concentrations for estimating carcinogenic risk. Complementing this, the qualitative component drew on community surveys to capture water-use practices, perceived health outcomes, and awareness of contamination risks.

The triangulation of these two approaches ensured that the assessment of human health risks was grounded not only in toxicological measurements but also in the lived realities of the affected community, thereby reflecting socio-economic vulnerabilities and behavioural exposure pathways with greater accuracy and contextual relevance.

Carcinogenic risk (LCR) was evaluated to determine the probability of lifetime cancer development from exposure to toxic trace elements in fumarolic condensates. The analysis followed the United States Environmental Protection Agency (USEPA, 2011) human health risk assessment framework, where LCR is computed as the product of the chronic daily intake (CDI) and the cancer slope factor (CSF), which represents the potency of the substance to induce carcinogenic effects (U.S. EPA, 2019; Wang et al., 2023). The calculations followed the USEPA framework, where the lifetime cancer risk (LCR) is defined as:

(i) Ingestion Pathway

The Lifetime Cancer Risk via ingestion was estimated using Equation 1:

$$LCR_{ingestion} = CDI_{ingestion} + \quad SF \quad \text{Equation 1}$$

(ii) Dermal Pathway

The Lifetime Cancer Risk via dermal absorption was calculated using Equation 9:

$$LCR_{dermal} = CDI_{dermal} + \quad SF \quad \text{Equation 2}$$

Where CDI is the chronic daily intake (mg/kg-day) of a contaminant through ingestion or dermal pathways, and CSF is the cancer slope factor (mg/kg-day^{-1}). CSF, or the carcinogenic slope factor, is the risk associated with an average lifetime exposure to a chemical and is specific to a particular contaminant. In this study, the focus was on arsenic (As), Lead (Pb), and cadmium (Cd), all of which have documented slope factors in recent literature.

According to the USEPA (Kamagate et al., 2025; Mohammadpour et al., 2023), CSF values as a function of metals are CSF (As) = 1.5; CSF (Pb) = 0.0085; CSF (Cd) = 1.5. If the ILCR value is less than 10^{-6}, the carcinogenic risk is considered negligible. On the other hand, if the ILCR value is greater than 10^{-4}, there is a high risk of developing cancer in humans. The range between 10^{-6} and 10^{-4} is widely accepted as constituting an acceptable risk to humans (USEPA, 2011; Imran et al., 2021; Mohammadpour et al., 2023).

The parameters used in calculating LCR are presented in Table 17. Importantly, these values were derived from both USEPA guidelines and site-specific data collected via household surveys in the Mt. Suswa area, including daily water ingestion, bathing

frequency with fumarolic condensates, and exposure duration. This intentional integration of community-based data, rather than reliance on generic defaults, ensured that LCR estimations authentically mirrored local practices and vulnerabilities. As noted in the USEPA's Exposure Parameters compilation, exposure assessors are advised to prioritize site-specific values to reflect accurate age-dependent and behavioural patterns (U.S. EPA, 2019). Furthermore, modern risk assessment literature underscores that customizing exposure parameters substantially improves the precision and contextual relevance of human health risk estimates (Rigaud et al., 2024). The inclusion of locally derived data thus enhanced both the accuracy and defensibility of the LCR estimates in this study, grounding them firmly in the lived exposure conditions of the Mt. Suswa community.

Table 17

Exposure Parameters by Receptor Group

Parameter	Description	Units	Children	Adult Males	Adult Females	Source
IR	Ingestion rate	L/day	1	1.5	1.5	Study area (field survey), (ATSDR, 2023)
ED	Exposure duration	Year	12	40	40	Study area (field survey)
BW	Body weight	Kg	15	70	55	(USEPA, 2011; ATSDR, 2023)
AT	Average time (lifetime)	Day	25,550	25,550	25,550	(USEPA, 2011; ATSDR, 2023)
EF	Exposure frequency	Day/year	365	365	365	(ATSDR, 2023)
F	Fraction of skin surface contact	Unitless	1	1	1	(USEPA, 2011)
SA	Skin surface area	cm^2	6,597	18,085	15,475	(USEPA, 2011)
EV	Daily exposure events (skin)	Unitless	1	1	1	Study area (field survey), (USEPA, 2011)
K	Skin permeability coefficient	cm/h	0.001	0.001	0.001	(USEPA, 2011)
Time	Contact duration per day	h/day	0.13	0.1	0.17	Study area (field survey), (ATSDR, 2023)
H	Height (for SA calculation)	cm	99.4	165.3	153.4	(USEPA, 2011)
CF	Conversion factor	Unitless	0.001	0.001	0.001	(USEPA, 2011)

Results of LCR Calculations

The measured concentrations of arsenic (As), lead (Pb), and cadmium (Cd) from fumarolic vents (Table 11, Field Data F1–F20) were used to compute chronic daily intake (CDI) values for each receptor group. These CDI values were combined with cancer slope factors (CSFs) to estimate lifetime cancer risk (LCR) via ingestion and

dermal exposure. The outcomes are presented in Table 18, which summarizes carcinogenic risks for children, adult males, and adult females across both dry and wet seasons. The risks are disaggregated by pathway (oral ingestion, dermal contact) and expressed as total lifetime cancer risk (LCR_{total}).

The site-specific results in Table 18 show clear variation in carcinogenic risk (CR) across fumaroles, receptor groups, and seasons. For example, in the dry season at F1, children recorded a total CR of 4.18×10^{-5}, compared with 8.95×10^{-5} in adult males and 1.14×10^{-4} in adult females. At F3, children's CRtotal_{total}total reached 5.25×10^{-5}, while adult males and females recorded 1.13×10^{-4} and 1.43×10^{-4}, respectively. The highest risks were generally observed in fumaroles with elevated As concentrations, such as F17 and F18, where adult females recorded total CRs of 1.95×10^{-4} and 2.02×10^{-4} during the dry season. By contrast, lower risks were observed at fumaroles such as F7, where children recorded 2.12×10^{-5} and adult females recorded 4.84×10^{-5}.

Table 18

Carcinogenic Health Risks Indices for Children, Adult Males, and Adult Females

Season	Sample	Receptor	As (ppb)	Pb (ppb)	Cd (ppb)	LCR_{ing}	LCR_{dermal}	LCR_{total}
		Adult female	4.86	1.42	0	1.14E-04	2.00E-07	1.14E-04
	F1	Adult male	4.86	1.42	0	8.94E-05	1.08E-07	8.95E-05
		Children	4.86	1.42	0	4.17E-05	7.16E-08	4.18E-05
		Adult female	3.21	1.3	0.53	8.76E-05	1.54E-07	8.78E-05
	F2	Adult male	3.21	1.3	0.53	6.88E-05	8.30E-08	6.89E-05
		Children	3.21	1.3	0.53	3.21E-05	5.51E-08	3.22E-05
		Adult female	4.94	1.53	1.17	1.43E-04	2.51E-07	1.43E-04
	F3	Adult male	4.94	1.53	1.17	1.12E-04	1.35E-07	1.13E-04
		Children	4.94	1.53	1.17	5.24E-05	9.00E-08	5.25E-05
		Adult female	3.82	1.38	0.39	9.86E-05	1.73E-07	9.88E-05
	F4	Adult male	3.82	1.38	0.39	7.75E-05	9.34E-08	7.76E-05
		Children	3.82	1.38	0.39	3.62E-05	6.20E-08	3.62E-05
		Adult female	5.16	1.41	1.84	1.64E-04	2.87E-07	1.64E-04
	F5	Adult male	5.16	1.41	1.84	1.29E-04	1.55E-07	1.29E-04
		Children	5.16	1.41	1.84	6.01E-05	1.03E-07	6.02E-05
		Adult female	2.55	1.35	0	5.98E-05	1.05E-07	5.99E-05
	F6	Adult male	2.55	1.35	0	4.70E-05	5.66E-08	4.70E-05
		Children	2.55	1.35	0	2.19E-05	3.76E-08	2.20E-05
		Adult female	2.24	0.95	0	5.25E-05	9.21E-08	5.26E-05
Dry	F7	Adult male	2.24	0.95	0	4.12E-05	4.97E-08	4.13E-05
		Children	2.24	0.95	0	1.92E-05	3.30E-08	1.93E-05
		Adult female	3.08	1.43	0.61	8.64E-05	1.52E-07	8.66E-05
	F8	Adult male	3.08	1.43	0.61	6.79E-05	8.19E-08	6.80E-05
		Children	3.08	1.43	0.61	3.17E-05	5.44E-08	3.18E-05
		Adult female	2.71	1.03	0.47	7.45E-05	1.31E-07	7.46E-05
	F9	Adult male	2.71	1.03	0.47	5.85E-05	7.06E-08	5.86E-05
		Children	2.71	1.03	0.47	2.73E-05	4.68E-08	2.74E-05
		Adult female	3.45	1.62	0	8.09E-05	1.42E-07	8.10E-05
	F10	Adult male	3.45	1.62	0	6.35E-05	7.66E-08	6.36E-05
		Children	3.45	1.62	0	2.97E-05	5.09E-08	2.97E-05
		Adult female	2.83	1.84	1.36	9.82E-05	1.72E-07	9.84E-05
	F11	Adult male	2.83	1.84	1.36	7.72E-05	9.30E-08	7.72E-05
		Children	2.83	1.84	1.36	3.60E-05	6.18E-08	3.61E-05
		Adult female	3.65	1.33	1.14	1.12E-04	1.97E-07	1.12E-04
	F12	Adult male	3.65	1.33	1.14	8.81E-05	1.06E-07	8.82E-05
		Children	3.65	1.33	1.14	4.11E-05	7.05E-08	4.12E-05
		Adult female	3.88	1.71	1.26	1.20E-04	2.11E-07	1.21E-04
	F13	Adult male	3.88	1.71	1.26	9.46E-05	1.14E-07	9.47E-05
		Children	3.88	1.71	1.26	4.41E-05	7.57E-08	4.42E-05

		Adult female	3.92	1.98	0.68	1.08E-04	1.89E-07	1.08E-04
	F14	Adult male	3.92	1.98	0.68	8.47E-05	1.02E-07	8.48E-05
		Children	3.92	1.98	0.68	3.95E-05	6.78E-08	3.96E-05
		Adult female	4.63	1.5	0.49	1.20E-04	2.10E-07	1.20E-04
	F15	Adult male	4.63	1.5	0.49	9.42E-05	1.14E-07	9.43E-05
		Children	4.63	1.5	0.49	4.40E-05	7.54E-08	4.40E-05
		Adult female	5.04	1.41	0.6	1.32E-04	2.32E-07	1.32E-04
	F16	Adult male	5.04	1.41	0.6	1.04E-04	1.25E-07	1.04E-04
		Children	5.04	1.41	0.6	4.84E-05	8.30E-08	4.85E-05
		Adult female	5.13	1.48	1.17	1.47E-04	2.59E-07	1.48E-04
	F17	Adult male	5.13	1.48	1.17	1.16E-04	1.40E-07	1.16E-04
		Children	5.13	1.48	1.17	5.41E-05	9.27E-08	5.42E-05
		Adult female	5.59	1.27	1.22	1.59E-04	2.79E-07	1.60E-04
	F18	Adult male	5.59	1.27	1.22	1.25E-04	1.51E-07	1.25E-04
		Children	5.59	1.27	1.22	5.84E-05	1.00E-07	5.85E-05
		Adult female	5.35	1.52	1.41	1.58E-04	2.78E-07	1.59E-04
	F20	Adult male	5.35	1.52	1.41	1.24E-04	1.50E-07	1.24E-04
		Children	5.35	1.52	1.41	5.80E-05	9.95E-08	5.81E-05
		Adult female	3.24	1.25	0	7.59E-05	1.33E-07	7.60E-05
	F1	Adult male	3.24	1.25	0	5.96E-05	7.19E-08	5.97E-05
		Children	3.24	1.25	0	2.78E-05	4.77E-08	2.79E-05
		Adult female	2.66	1.13	0.37	7.10E-05	1.24E-07	7.11E-05
	F2	Adult male	2.66	1.13	0.37	5.58E-05	6.72E-08	5.58E-05
		Children	2.66	1.13	0.37	2.60E-05	4.46E-08	2.61E-05
		Adult female	4.34	1.09	0.72	1.18E-04	2.08E-07	1.19E-04
	F3	Adult male	4.34	1.09	0.72	9.31E-05	1.12E-07	9.32E-05
		Children	4.34	1.09	0.72	4.34E-05	7.45E-08	4.35E-05
		Adult female	2.49	1.02	0	5.83E-05	1.02E-07	5.84E-05
	F4	Adult male	2.49	1.02	0	4.58E-05	5.53E-08	4.59E-05
		Children	2.49	1.02	0	2.14E-05	3.67E-08	2.14E-05
		Adult female	4.83	1.07	1.26	1.43E-04	2.50E-07	1.43E-04
Wet	F5	Adult male	4.83	1.07	1.26	1.12E-04	1.35E-07	1.12E-04
		Children	4.83	1.07	1.26	5.23E-05	8.96E-08	5.23E-05
		Adult female	2.13	1.12	0	4.99E-05	8.76E-08	5.00E-05
	F6	Adult male	2.13	1.12	0	3.92E-05	4.73E-08	3.93E-05
		Children	2.13	1.12	0	1.83E-05	3.14E-08	1.83E-05
		Adult female	1.87	0.92	0	4.38E-05	7.69E-08	4.39E-05
	F7	Adult male	1.87	0.92	0	3.44E-05	4.15E-08	3.45E-05
		Children	1.87	0.92	0	1.61E-05	2.76E-08	1.61E-05
		Adult female	2.92	1.38	0.44	7.87E-05	1.38E-07	7.89E-05
	F8	Adult male	2.92	1.38	0.44	6.19E-05	7.46E-08	6.19E-05
		Children	2.92	1.38	0.44	2.89E-05	4.95E-08	2.89E-05
	F9	Adult female	1.97	0.87	0	4.62E-05	8.10E-08	4.62E-05
		Adult male	1.97	0.87	0	3.63E-05	4.37E-08	3.63E-05

	Children	1.97	0.87	0	1.69E-05	2.90E-08	1.70E-05
	Adult female	1.29	1.17	0	3.03E-05	5.32E-08	3.04E-05
F10	Adult male	1.29	1.17	0	2.38E-05	2.87E-08	2.38E-05
	Children	1.29	1.17	0	1.11E-05	1.91E-08	1.11E-05
	Adult female	2.43	1.27	0.85	7.68E-05	1.35E-07	7.70E-05
F11	Adult male	2.43	1.27	0.85	6.04E-05	7.28E-08	6.04E-05
	Children	2.43	1.27	0.85	2.82E-05	4.83E-08	2.82E-05
	Adult female	3.31	1.37	0.86	9.77E-05	1.71E-07	9.78E-05
F12	Adult male	3.31	1.37	0.86	7.67E-05	9.25E-08	7.68E-05
	Children	3.31	1.37	0.86	3.58E-05	6.14E-08	3.59E-05
	Adult female	2.91	1.25	1.03	9.23E-05	1.62E-07	9.24E-05
F13	Adult male	2.91	1.25	1.03	7.25E-05	8.74E-08	7.26E-05
	Children	2.91	1.25	1.03	3.38E-05	5.80E-08	3.39E-05
	Adult female	3.39	1.83	0.41	8.91E-05	1.56E-07	8.92E-05
F14	Adult male	3.39	1.83	0.41	7.00E-05	8.44E-08	7.01E-05
	Children	3.39	1.83	0.41	3.27E-05	5.60E-08	3.27E-05
	Adult female	4.56	0.81	0	1.07E-04	1.87E-07	1.07E-04
F15	Adult male	4.56	0.81	0	8.38E-05	1.01E-07	8.39E-05
	Children	4.56	0.81	0	3.91E-05	6.71E-08	3.92E-05
	Adult female	4.48	1.35	0.47	1.16E-04	2.03E-07	1.16E-04
F16	Adult male	4.48	1.35	0.47	9.11E-05	1.10E-07	9.12E-05
	Children	4.48	1.35	0.47	4.25E-05	7.29E-08	4.26E-05
	Adult female	5.07	1.42	1.05	1.43E-04	2.51E-07	1.44E-04
F17	Adult male	5.07	1.42	1.05	1.13E-04	1.36E-07	1.13E-04
	Children	5.07	1.42	1.05	5.25E-05	9.01E-08	5.26E-05
	Adult female	5.54	1.19	1.02	1.54E-04	2.69E-07	1.54E-04
F18	Adult male	5.54	1.19	1.02	1.21E-04	1.45E-07	1.21E-04
	Children	5.54	1.19	1.02	5.63E-05	9.65E-08	5.64E-05
	Adult female	5.23	1.44	1.27	1.52E-04	2.67E-07	1.52E-04
F20	Adult male	5.23	1.44	1.27	1.20E-04	1.44E-07	1.20E-04
	Children	5.23	1.44	1.27	5.58E-05	9.57E-08	5.59E-05

Table 19 provides the seasonal averages across all fumaroles. During the dry season, children exhibited average CR values of 4.09×10^{-5} (total), adult males 8.76×10^{-5}, and adult females 1.14×10^{-4}. In the wet season, mean CRs decreased to 2.81×10^{-5} for children, 5.97×10^{-5} for adult males, and 7.60×10^{-5} for adult females. Dermal contributions remained negligible in both seasons, typically between 10^{-7} and 10^{-8}, representing less than 1% of total CR values.

Table 19

Carcinogenic Risk (CR) Values for As, Cd, and Pb in Condensates Across Seasons

Season	Parameter	Value
Dry	CRoral Children	4.08E-05
	CRdermal Children	7.01E-08
	CRtotal Children	4.09E-05
	CRoral Adult male	8.75E-05
	CRdermal Adult male	1.06E-07
	CRtotal Adult male	8.76E-05
	CRoral Adult female	1.11E-04
	CRdermal Adult female	1.95E-07
	CRtotal Adult female	1.12E-04
Wet	CRoral Children	3.36E-05
	CRdermal Children	5.77E-08
	CRtotal Children	3.37E-05
	CRoral Adult male	7.21E-05
	CRdermal Adult male	8.69E-08
	CRtotal Adult male	7.21E-05
	CRoral Adult female	9.17E-05
	CRdermal Adult female	1.61E-07
	CRtotal Adult female	9.19E-05

Discussion of LCR Indices Values

The CR values demonstrate that oral ingestion is the dominant carcinogenic pathway, while dermal exposure contributes negligibly. For instance, at F3 (dry season), children recorded $CR_{oral} = 5.24 \times 10^{-5}$ and $CR_{dermal} = 9.00 \times 10^{-8}$, yielding a total of 5.25×10^{-5}. Adult males at the same site recorded a total CR of 1.13×10^{-4}, nearly double that of children, yet with dermal exposure still accounting for less than 0.1%. A similar dominance of oral exposure has been widely reported in groundwater and geothermal health-risk studies, where ingestion accounted for over 95% of total risk, while dermal contact was negligible.

The case study of the Koche River by Temesgen et al. (2024) found that oral ingestion contributed approximately 99.55% of the total carcinogenic and non-carcinogenic risk in adults and 97.85% in children, with dermal exposure accounting for only a marginal fraction of the risk. Their study confirmed that ingestion remains the critical pathway of concern in communities reliant on contaminated waters. Similarly, (2024), while assessing the health risks of trace metals in the drinking water of Isfahan, Iran, reported that ingestion exposure pathways dominated carcinogenic risk calculations, whereas dermal exposure was several orders of magnitude lower.

At F18 (dry season), adult females recorded $CR_{oral} = 2.02 \times 10^{-4}$ compared with $CR_{dermal} = 3.39 \times 10^{-7}$, showing dermal contact contributed less than 0.2%. These patterns align with findings in Italy and Iran, where dermal pathways contributed on average less than 5% of carcinogenic risk (Alidadi et al., 2019; Cocca et al., 2024). Children consistently exhibited higher risks relative to body size. For example, at F5 (dry season), children recorded $CR_{oral} = 6.87 \times 10^{-5}$, while adult males recorded 1.49×10^{-4}. Although adult risks appear higher in absolute terms, children's smaller body weight (15 kg) means their per-kilogram exposure is proportionally greater, making them the more vulnerable group.

Among adults, females exhibited the highest absolute CR values across both seasons. This outcome is largely due to parameter differences in the exposure model. Females had a lower average body weight (55 kg) than males (70 kg), but the same ingestion rate (1.5 $Lday^{-1}$). As a result, the same intake translates into a higher dose per kilogram of body mass, elevating risk estimates. For instance, in the dry season, adult females averaged $CR_{oral} = 1.14 \times 10^{-4}$ compared to 8.76×10^{-5} in males (Table 4.12). This ≈30% higher risk reflects the weight-normalization effect rather than differences in intake volume.

Comparable patterns of higher female risk have also been observed in Italy, attributed to lower body mass and a higher effective dose per unit intake (Cocca et al., 2024). While dermal exposure contributes minimally, the larger skin surface area in females relative to body mass further enhances their risk marginally.

Seasonal variation was also evident. Dry-season risks were consistently 30–40% higher than wet-season risks across receptor groups. For example, average children's CR_{oral} decreased from 4.09×10^{-5} (dry) to 2.81×10^{-5} (wet), while adult females dropped from 1.14×10^{-4} (dry) to 7.60×10^{-5} (wet). High-risk fumaroles included F17 and F18, where adult female totals exceeded 1.9×10^{-4}, whereas low-risk fumaroles such as F6 and F7 recorded children's CR values below 2.5×10^{-5}. For example,(2022), found that in a rural village in the Eastern Cape, South Africa, several metals (Arsenic, chromium, vanadium) showed elevated concentrations and health risk indices in dry-season samples relative to wet-season samples.

The findings highlight that children are the most vulnerable group relative to body size, while adult females exhibit the highest absolute risks due to lower body weight and consequent higher exposure per unit mass. Dermal contributions remained negligible across all cases, underscoring ingestion as the principal exposure route.

Table 20 below provides an integrated classification of fumarolic vents into Background, Moderate, and Hotspot clusters based on receptor-specific and season-specific total lifetime cancer risk (CR_{total}). The classification employed USEPA thresholds, where CR values $< 1.0 \times 10^{-6}$ are negligible, between 1.0×10^{-6} and 1.0×10^{-4} are considered acceptable, and $> 1.0 \times 10^{-4}$ are categorized as high risk (USEPA, 2011).

The results demonstrate that no fumarole fell into the negligible risk category, indicating that all vents pose some carcinogenic risk to exposed populations. The majority of vents

were clustered in the Moderate (acceptable) category, with CR values ranging between 10^{-6} and 10^{-4}. These vents, located mainly in the outer caldera and peripheral zones (F2, F4, F6–F9, F10, and F11), therefore represent sites where the risk, while non-negligible, is still within an internationally recognized range of tolerability. Comparable findings have been reported in groundwater and geothermal systems in Iran and Ethiopia, where most sites were classified in the moderate CR band, yet remained above negligible risk (Moradnia et al., 2024; Temesgen et al., 2024). Such vents can therefore serve as background sites, providing benchmarks for long-term monitoring and comparative analysis.

In contrast, Hotspot vents (notably F5, F17, F18, and F20) consistently exceeded the 10^{-4} threshold, especially during the dry season. These vents are concentrated in the inner caldera, an area of high geothermal intensity and active hydrothermal alteration. The elevated CR values are largely ingestion-driven, a trend consistent with studies in the Wairakei (New Zealand) geothermal field, where hydrothermal discharges led to elevated arsenic and fluoride ingestion risks that surpassed USEPA thresholds (Phillips et al., 2011). Their classification as hotspots underscores their significance as priority sites for public health interventions, since the risks exceed USEPA's upper acceptable limit (Kumar et al., 2025; Molina-Frechero et al., 2020).

The classification reinforces the need for site-specific management strategies: hotspot vents require immediate mitigation measures, such as health risk communication and alternative water provision, while background vents should be maintained as sentinel monitoring sites for long-term environmental surveillance.

Table 20

Season/Receptor-Based Clustering of Fumaroles According to Carcinogenic Risk

Season	Receptor	CRtotal	Risk Limit	Cluster	Risk Category	Samples
Dry	Adult female	1.35E-04	> 1.0e-04	Hotspot	High	F1, F12, F13, F14, F15, F16, F17, F18, F20, F3, F5
Dry	Adult female	7.99E-05	10^{-6} - 10^{-4}	Moderate	Low	F10, F11, F2, F4, F6, F7, F8, F9
Dry	Adult male	1.19E-04	> 1.0e-04	Hotspot	High	F16, F17, F18, F20, F3, F5
Dry	Adult male	7.34E-05	10^{-6} - 10^{-4}	Moderate	Low	F1, F10, F11, F12, F13, F14, F15, F2, F4, F6, F7, F8, F9
Dry	Children	4.09E-05	10^{-6} - 10^{-4}	Moderate	Low	F1, F10, F11, F12, F13, F14, F15, F16, F17, F18, F2, F20, F3, F4, F5, F6, F7, F8, F9
Wet	Adult female	1.33E-04	> 1.0e-04	Hotspot	High	F15, F16, F17, F18, F20, F3, F5
Wet	Adult female	6.76E-05	10^{-6} - 10^{-4}	Moderate	Low	F1, F10, F11, F12, F13, F14, F2, F4, F6, F7, F8, F9
Wet	Adult male	1.16E-04	> 1.0e-04	Hotspot	High	F17, F18, F20, F5
Wet	Adult male	6.04E-05	10^{-6} - 10^{-4}	Moderate	Low	F1, F10, F11, F12, F13, F14, F15, F16, F2, F3, F4, F6, F7, F8, F9
Wet	Children	3.37E-05	10^{-6} - 10^{-4}	Moderate	Low	F1, F10, F11, F12, F13, F14, F15, F16, F17, F18, F2, F20, F3, F4, F5, F6, F7, F8, F9

Figure 18 illustrates the site-specific carcinogenic risk classification of fumarolic vents at Mt. Suswa during both dry and wet seasons, based on total lifetime carcinogenic risk (CR_{total}). The classification follows the USEPA thresholds: negligible risk ($<10^{-6}$), acceptable risk (10^{-6}–10^{-4}), and high risk ($>10^{-4}$).

The analysis reveals that no fumarolic vent falls within the negligible category, underscoring that all condensates pose non-trivial carcinogenic risks. The majority of vents, particularly those situated along the outer caldera and peripheral zones (F1, F2, F4, F6–F10, F11, F12, F13, F14, and F15), fall within the acceptable risk range (10^{-6}–10^{-4}). These vents, represented by orange bars, establish the baseline or background risk against which elevated risk sites can be compared.

Conversely, fumarolic vents located within the inner caldera (F5, F17, F18, and F20) consistently exceed the 10^{-4} threshold, classifying them as high-risk hotspots. These sites, indicated in red, exhibit carcinogenic risks primarily driven by elevated concentrations of As, Pb, and Cd. The persistence of high-risk levels across both seasons, though more pronounced in the dry season due to evaporative concentration, demonstrates the stability of hotspot conditions.

From a spatial perspective, the clear separation between outer caldera (acceptable) and inner caldera (hotspot) vents reflects the strong influence of geothermal intensity and hydrothermal activity on contaminant mobilization. From a seasonal perspective, most acceptable vents show slight declines in CR_{total} during the wet season, reflecting dilution by rainfall recharge, while hotspot vents remain persistently above the high-risk threshold.

Figure 18

Site-Specific Risk Classification of Fumarolic Vents during Dry and Wet Seasons

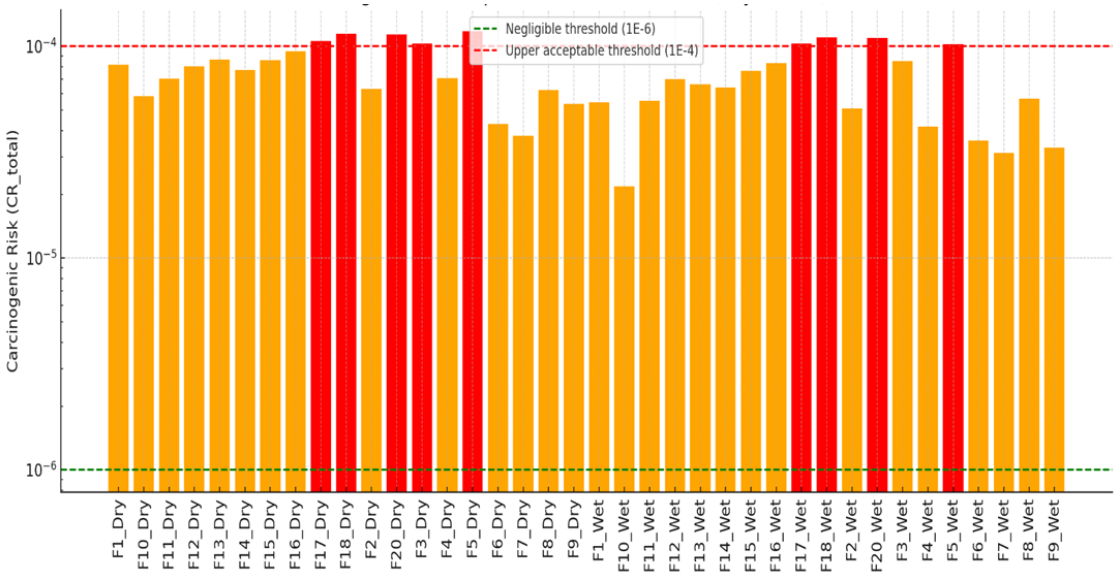

The objective of this study was to evaluate the potential human health risks posed by exposure to heavy metals (arsenic, mercury, lead, and cadmium) present in fumarolic condensates within the Mt. Suswa area. This was operationalized through carcinogenic risk assessment (Tables 17–20; Figures 19) that integrated site-specific concentrations, receptor exposure parameters, and USEPA risk thresholds.

Accordingly, the research objective has been fully achieved, the study has quantified carcinogenic risks, identified the most vulnerable receptor groups, and differentiated between background and hotspot vents. Likewise, the research question (*What are the potential human health risks associated with exposure to heavy metals in fumarolic condensates within the Mt. Suswa area?*) has been conclusively answered. The evidence indicates that fumarolic condensates in Mt. Suswa present non-negligible to high health risks, particularly ingestion-driven cancer risks at hotspot vents, thereby providing a clear scientific basis for risk management, policy interventions, and community health protection in the study area.

Triangulation of Quantitative and Qualitative Findings

The triangulation of laboratory results with community narratives provides a coherent understanding of exposure and vulnerability in Mt. Suswa. Quantitative analyses showed that arsenic (As) and cadmium (Cd) ingestion contribute most to carcinogenic risk, while fluoride dominates non-carcinogenic outcomes. These patterns are similar to findings by (2023), who report that children face elevated non-carcinogenic risks from ingesting fluoride in geothermal waters, and by Abdipour et al., who identify that rural water supplies exceed WHO fluoride guidelines and affect females and children disproportionately.

For example, hotspot vents recorded the highest exceedances: fluoride concentrations reached 3.84 mgL^{-1} at F13 (dry), 3.57 mgL^{-1} at F18, 3.32 mgL^{-1} at F20—each more than double the WHO 1.5 mgL^{-1} guideline. These findings were reinforced by household survey data on daily ingestion of condensates and by widespread reports of dental fluorosis in both children and adults. Community reports of tooth discoloration and suspected fluorosis in both children and adults echo observations of endemic fluorosis in Qinghai-Tibet geothermal areas, where fluoride levels in confined geothermal water exceed safe levels (Liu et al., 2023).

Arsenic concentrations at F18 (5.59 $\mu g\ L^{-1}$ dry) and F20 (5.35 $\mu g\ L^{-1}$ dry) approach half the WHO limit (10 $\mu g\ L^{-1}$), leading to LCR values up to 2.3×10^{-4} for adult females—above the USEPA "upper acceptable" of 1×10^{-4}. This corresponds to findings by Khosravi-Darani et al. (2022) in studies related to *Arsenic Exposure via Contaminated Water and Food Sources* (2022), , which underscore arsenic ingestion as a primary cancer risk driver in many exposed populations.

The carcinogenic risk (CR) analysis demonstrated that adult females bore the highest absolute risk values (1.12×10^{-4} in the dry season; 9.19×10^{-5} in the wet season),

followed by adult males (8.76×10^{-5} dry season) and children (4.09×10^{-5} in the dry). These differences are consistent with previous risk assessments showing that gender- and age-related physiological differences (lower body mass in females and higher intake-to-weight ratios in children) amplify exposure burdens in vulnerable groups (Pahwa et al., 2023).

Despite these elevated risks, community awareness of invisible contaminants such as arsenic and cadmium remained very low. Residents frequently described condensate as "fresh" or "salty," and reliance persisted because of the absence of alternative safe water sources. Reported coping measures, including boiling or dilution with rainwater, were ineffective in reducing heavy metal risks because dissolved contaminants are not removed by these practices.

The triangulated analysis validated the robustness of the risk assessment while anchoring the results in the realities of household water use in Mt. Suswa. This enhances the validity, policy relevance, and applicability of the findings, providing a strong basis for interventions that combine technical solutions (water treatment and alternative supply systems) with community-centered strategies (education, participation, and governance).

CHAPTER FIVE

SUMMARY, CONCLUSIONS AND RECOMMENDATIONS

5.1 Introduction

This chapter presents a synthesis of the study's key findings, conclusions, and recommendations. The discussion is structured to align with the study objectives and builds on the results and analyses presented in Chapter Four. Section 5.2 summarizes the major findings for each research objective; Section 5.3 draws conclusions based on both quantitative and qualitative evidence; and Section 5.4 outlines recommendations for policy, practice, and future research. This structured approach ensures coherence and provides a logical link between the study objectives, findings, and their broader implications.

5.2 Summary of the Findings

5.2.1 Physico-Chemical Parameters and Heavy Metal Concentrations

The study found that fumarolic condensates from vents within Mt. Suswa exhibited pH values ranging from moderately acidic to near-neutral (5.52–7.37) and temperatures from 42.3°C to 74.5°C, characteristic of geothermal systems. Electrical conductivity varied between 4.93–51.22 µS, while total dissolved solids ranged from 2.43–25.6 $mgL^{-1,}$ reflecting different levels of mineralization across vents and seasons. Major cations, such as sodium, potassium, calcium, and magnesium, were detected at appreciable levels, with sodium concentrations reaching 33.29 mg L^{-1}. Among the anions, fluoride levels were consistently elevated, peaking at 3.84 mgL^{-1} at F13 during the dry season, exceeding the WHO/NEMA permissible limit of 1.5 mgL-1 by more than twice. Heavy metal analyses further revealed the presence of arsenic (1.87–5.59 µg L^{-1}), cadmium (0.37–1.41 µg L^{-1}), and lead (0.81–1.98 µg L^{-1}) across most vents, while mercury remained below detection

limits. Although arsenic and cadmium values did not exceed WHO guidelines, several readings approached critical thresholds, highlighting the potential for chronic health risks.

5.2.2 Correlations and Hotspot Identification through Geospatial Analysis

Correlation analysis revealed significant associations among selected parameters, particularly between fluoride and other anions (chloride and sulphate), indicating common geochemical mobilization pathways within the fumarolic system. Geospatial analysis using Inverse Distance Weighting (IDW) interpolation identified distinct contamination hotspots at vents F13, F18, and F20, which consistently exhibited the highest fluoride (>3 mg L^{-1}), arsenic (>5 µg L^{-1}), and cadmium (>1 µg L^{-1}) concentrations. In contrast, background vents such as F1, F2, and F6 showed relatively lower values but still recorded fluoride levels above the WHO limit, suggesting a widespread baseline exposure risk. Seasonal variations were also observed, with higher contaminant concentrations during the dry season, likely due to reduced dilution from rainfall and greater household reliance on condensates. The spatial distribution thus confirmed that exposure risks are clustered around hotspot vents but extend across the broader fumarolic field.

5.2.3 Human Health Risk Evaluation

The human health risk assessment demonstrated that ingestion was the dominant exposure pathway, while dermal contact contributed negligibly to overall risk. Carcinogenic risk (CR) values for arsenic and cadmium ingestion indicated elevated risks across receptor groups. For children, CR values ranged between 3.36×10^{-5} (wet season) and 4.09×10^{-5} (dry season), while adult males recorded values of 7.21×10^{-5} (wet season) and 8.76×10^{-5} (dry season). Adult females exhibited the highest absolute risk, with a CR value of 1.12×10^{-4} during the dry season, exceeding the USEPA upper

acceptable threshold of 1×10^{-4}. These quantitative results were reinforced by qualitative findings: household surveys confirmed daily reliance on fumarolic condensates for drinking and cooking, widespread reports of dental discoloration and suspected fluorosis, and low awareness of invisible contaminants such as arsenic and cadmium. Coping mechanisms such as boiling or mixing condensates with rainwater were ineffective, leaving households structurally vulnerable to exposure.

5.3 Conclusions

This study set out to assess the spatio-seasonal variations in heavy metal contamination and the potential health risks associated with fumarolic condensates in Mt. Suswa. The findings lead to several important conclusions.

Based on the findings of objective one, the study concluded that the physicochemical characteristics of fumarolic condensates at Mt. Suswa vary significantly across vents and seasons. The condensates were moderately acidic to near neutral, with elevated temperatures and variable mineralization. Fluoride levels frequently exceeded WHO and NEMA limits, while arsenic, cadmium, and lead were also detected at concentrations approaching guideline thresholds. These results demonstrate that the condensates are chemically enriched and may pose health risks when relied upon as domestic water sources.

As regards to objective two, it was concluded that heavy metal contamination showed clear spatial and seasonal variability, with geospatial analysis identifying contamination hotspots at vents F13, F18, and F20. Contaminant concentrations were consistently higher during the dry season, likely due to reduced dilution from rainfall and increased dependence on condensates. Even vents considered to have lower contamination

exceeded safe fluoride limits, indicating that exposure risks are widespread and not confined to the most contaminated sites.

Based on the findings of objective three, the study concluded that communities that depend on fumarolic condensates are exposed to significant health risks, primarily through ingestion. Carcinogenic risk values, especially for adult females, exceeded USEPA's acceptable limits during the dry season, while non-carcinogenic risks linked to fluoride were notably high in hotspot vents. These risks aligned with community-reported symptoms such as dental discoloration and suspected fluorosis. Low awareness of invisible contaminants like arsenic and cadmium, coupled with ineffective coping strategies such as boiling or mixing condensates, further heightened vulnerability.

The study establishes that fumarolic condensates in Mt. Suswa are enriched with contaminants, vary across vents and seasons, and pose significant health risks to the dependent community. The integration of quantitative laboratory analyses with qualitative community evidence confirms that risk is both measurable and observable, reinforcing the urgency for interventions. Addressing these risks requires not only technical solutions, such as the provision of alternative water supplies and treatment technologies, but also community-centered strategies, including health education, awareness-raising, and participatory governance frameworks.

5.5 Recommendations

The findings and conclusions of this study highlight the urgent need for coordinated interventions to address the environmental and public health risks associated with reliance on fumarolic condensates in Mt. Suswa. To safeguard community health and promote safer water-use practices, the following actions are recommended:

i. Provide safe alternative water sources, such as boreholes, piped water systems, and rainwater harvesting facilities, to reduce reliance on contaminated condensates.

ii. Install community-level water treatment systems and promote affordable household-scale technologies capable of removing fluoride and trace metals, such as the use of bone char.

iii. Strengthen the mapping and monitoring of contamination hotspots, supported by an early-warning system and enhanced seasonal surveillance of fumarolic condensates.

iv. Implement comprehensive public health education awareness and risk communication programs related to exposure to heavy metals.

v. In future studies, conduct ecological research to evaluate the impacts of heavy metal deposition on soil, vegetation, and local wildlife, thereby expanding scientific understanding of broader environmental risks.

REFERENCES

Abd Elnabi, M. K., Elkaliny, N. E., Elyazied, M. M., Azab, S. H., Elkhalifa, S. A., Elmasry, S., Mouhamed, M. S., Shalamesh, E. M., Alhorieny, N. A., Abd Elaty, A. E., Elgendy, I. M., Etman, A. E., Saad, K. E., Tsigkou, K., Ali, S. S., Kornaros, M., & Mahmoud, Y. A. G. (2023). Toxicity of Heavy Metals and Recent Advances in Their Removal: A Review. *Toxics*, *11*(7). https://doi.org/ 10.3390 /toxics11070580

Abdipour, H., Azari, A., Kamani, H., Pirasteh, K., Mostafapour, F. K., & Rayegnnakhost, S. (2025). Human health risk assessment for fluoride and nitrate contamination in drinking water of municipal and rural areas of Zahedan, Iran. *Applied Water Science*, *15*(3), 1–12. https://doi.org/10.1007/s13201-025-02375-8

Abera, A., Aseffa, A., Mengistie, B., Malmqvist, E., & Isaxon, C. (2024). *Groundwater Fluoride Contamination and Human Health Risk Assessment in North Main Ethiopia Rift Valley*. https://doi.org/10.20944/preprints202406.1673.v2

Adu-Boahen, K., & Boateng, I. (2021). Mapping Seasonal Variation in the Distribution and Concentration of Heavy Metals Using Water Quality Index and Geographic Information System-Based Applications. *Journal of Geographical Research*, *4*(2), 31–42. https://doi.org/10.30564/jgr.v4i2.3100

Afreen, S., Kumari, P., Sulaiman, M.A. *et al.* Comparative health risk assessment of arsenic and fluoride toxicity in the rural area groundwater in the middle Gangetic plain at Muzaffarpur, India. *Bull Natl Res Cent* 49, 56 (2025). https://do i.org/ 10.1186/s42269-025-01344-0

Agusto, M., Lamberti, M. C., Tassi, F., Carbajal, F., Llano, J., Nogués, V., Núñez, N., Sánchez, H., Rizzo, A., García, S., Yiries, J., Vélez, M. L., Massenzio, A., Velasquez, G., Bucarey, C., Gómez, M., Euillades, P., & Ramos, V. (2023). Eleven-Year Survey of the Magmatic-Hydrothermal Fluids From Peteroa Volcano: Identifying Precursory Signals of the 2018–2019 Eruption. *Geochemi stry , Geophysics, Geosystems*, *24*(11), 1–19. https://doi.org/10 .1029/2 023 GC011064

Akram-Lodhi, A. H. (2025). *Gender and water (in)security in agricultural production in East Africa*. WFP; UN Women; UNICEF; CGIAR Gender Impact Platform. https://www.unicef.org/esa/media/15331/file/Gender-Water-Study-East-Africa-2025.pdf

Alacali, M. (2024). Environmental effects of geothermal energy utilization: A case study of the Seferihisar geothermal system, İzmir, Türkiye. *Gümüşhane Üniversitesi Fen Bilimleri Enstitüsü Dergisi*, *14*, 592–607. https://doi.org /10.177 14/ gumusfenbil.1394922

Alam, M. A., Mukherjee, A., Bhattacharya, P., & Bundschuh, J. (2023). An appraisal of the principal concerns and controlling factors for Arsenic contamination in Chile. *Scientific Reports*, *13*(1), 1–22. https://doi.org/10.1038/s41598-023-38437-7

Albino, B. (2021). *Magmatic Processes in the East African Rift System : Insights From a 2015 – 2020 Sentinel-1 InSAR Survey Geochemistry, Geophysics, Geosystems*. 1–24. https://doi.org/10.1029/2020GC009488

Alidadi, H., Belin, S., Sany, T., Zarif, B., Oftadeh, G., & Mohamad, T. (2019). Health risk assessments of arsenic and toxic heavy metal exposure in drinking water in northeast Iran. *Environmental Health and Preventive Medicine*, *24*(59), 1–17.

Althubaiti, A. (2023). *Sample size determination : A practical guide for health researchers*. *November 2022*, 72–78. https://doi.org/10.1002/jgf2.600

American Public Health Association. (2022). *Standard methods for the examination of water and wastewater* (24th ed.). American Public Health Association.

Argun, Y. A. (2024). Examination of heavy metal concentrations and their interaction with anthropogenic sources in Ermenek Dam Lake (Turquoise Lake). *Environmental Geochemistry and Health*, *47*(2), 1–17. https://doi.org/ 10.1007/s10653-025-02367-2

Armiento, G., Barsanti, M., Caprioli, R., Chiavarini, S., Conte, F., Crovato, C., De Cassan, M., Delbono, I., Montereali, M. R., Nardi, E., Parrella, L., Pezza, M., Proposito, M., Rimauro, J., Schirone, A., & Spaziani, F. (2022). Heavy metal background levels and pollution temporal trend assessment within the marine sediments facing a brownfield area (Gulf of Pozzuoli, Southern Italy). *Environmental Monitoring and Assessment*, *194*(11). https://doi.org /10.1007/s10661-0 22-10480-3

ATSDR. (2020). Toxicological profile for Lead. *ATSDR's Toxicological Profiles*, *August*, 1–583. https://doi.org/10.15620/cdc:95222

ATSDR. (2024). Toxicological Profile for Mercury. *ATSDR's Toxicological Profiles*, *October*. https://doi.org/10.1201/9781420061888_ch109

Awaleh, M. O., Boschetti, T., Adaneh, A. E., Daoud, M. A., Ahmed, M. M., Dabar, O. A., Soubaneh, Y. D., Kawalieh, A. D., & Kadieh, I. H. (2020). Hydrochemistry and multi-isotope study of the waters from Hanlé-Gaggadé grabens (Republic of Djibouti, East African Rift System): A low-enthalpy geothermal resource from a transboundary aquifer. *Geothermics*, *86*(September 2019). https://doi.org/10.1016/j.geot hermics.2020.101805

Ayari, J., Barbieri, M., Boschetti, T., Barhoumi, A., Sellami, A., Braham, A., Manai, F., Dhaha, F., & Charef, A. (2023). Major- and Trace-Element Geochemistry of Geothermal Water from the Nappe Zone, Northern Tunisia: Implications for Mineral Prospecting and Health Risk Assessment. *Environments - MDPI*, *10*(9). https://doi.org/10.3390/environments10090151

Aziz, K. H., Mustafa, F. S., Omer, K. M., Hama, S., Hamarawf, R. F., & Rahman, K. O. (2023). Heavy metal pollution in the aquatic environment: efficient and low-cost removal approaches to eliminate their toxicity: a review. *RSC Advances*, *13*(26), 17595–17610. https://doi.org/10.1039/d3ra00723e

Baba, A., & Uzelli, T. (2024). Source of arsenic based on geological and hydrogeochemical properties of geothermal systems: Case study of Anatolia (Turkey). In *Arsenic in the environment: Bridging science to practice for sustainable development (As2021)* (pp. 37–39). CRC Press. https://doi.org/10.1201/978100 3317395-16

Bagnato, E., Carandente, A., Alessandro, A. D., Minopoli, C., Santi, A., Bitetto, M., & Oliveri, E. (2020). First simultaneous mercury and major volatiles characterization of atmospheric hydrothermal emissions at the Pisciarelli fumarolic system (Campi Flegrei, Italy). *Journal of Volcanology and Geothermal Research*, *406*, 107074. https://doi.org/1 0.1016/j.jvolge ores.202 0.10 7074

Bai, M., Zhang, C., Bai, Y., Wang, T., Qu, S., Qi, H., Zhang, M., Tan, C., & Zhang, C. (2022). Occurrence and Health Risks of Heavy Metals in Drinking Water of Self-Supplied Wells in Northern China. *International Journal of Environmental Research and Public Health*, *19*(19). https://doi.org/10.3390/ijerph191912517

Balali-Mood, M., Naseri, K., Tahergorabi, Z., Khazdair, M. R., & Sadeghi, M. (2021). Toxic Mechanisms of Five Heavy Metals: Mercury, Lead, Chromium, Cadmium, and Arsenic. *Frontiers in Pharmacology*, *12*(April), 1–19. https: //doi. org/10. 3389/fp har.2021.643972

Barkat, A., Bouaicha, F., Ziad, S., Mester, T., Sajtos, Z., Balla, D., Makhloufi, I., & Szabó, G. (2023). The Integrated Use of Heavy-Metal Pollution Indices and the Assessment of Metallic Health Risks in the Phreatic Groundwater Aquifer—The Case of the Oued Souf Valley in Algeria. *Hydrology*, *10*(10). https://doi.or g/10.3390/ hydrology10100201

Bay, P., Voudouris, P., Schwarz-Schampera, U., Strauss, H., Kati, M., & Magganas, A. (2021). Trace element signatures in pyrite and marcasite from shallow marine island arc-related hydrothermal vents: Calypso Vents, New Zealand. *Frontiers in Earth Science*, *9*, 641654. https://doi.org/10.3389/feart.2021.641654

Bennett, G., Van Reybrouck, J., Shemsanga, C., Kisaka, M., Tomašek, I., Fontijn, K., Kervyn, M., & Walraevens, K. (2021). Hydrochemical characterisation of high-fluoride groundwater and development of a conceptual groundwater flow model using a combined hydrogeological and hydrochemical approach on an active volcano: Mount Meru, Northern Tanzania. *Water (Switzerland)*, *13*(16). https://doi.org/10.3390/w13162159

Bhalla, S., & Kanapathy, K. (2023). Pre-testing Semi-structured Interview Questions Using Expert Review and Cognitive Interview Methods. *International Journal of Business and Management*, *7*(5), 11–19. https://doi.org /10.26666 /rmp.ij bm. 2023.5.2

Bianchini, G., Brombin, V., Marchina, C., Natali, C., Godebo, T. R., Rasini, A., & Salani, G. M. (2020). Origin of fluoride and arsenic in the main ethiopian rift waters. *Minerals*, *10*(5). https://doi.org/10.3390/min10050453

Birkle, P., Arabia, S., & Bundschuh, J. (2008). *The abundance of natural arsenic in deep thermal fluids of geothermal and petroleum reservoirs in Mexico*. *January 2009*, 145–153. https://doi.org/10.1201/b11334-18

Bonetto, S. M. R., Caselle, C., de Luca, D. A., & Lasagna, M. (2021). Groundwater Resources in the Main Ethiopian Rift Valley: An Overview for Sustainable Development. *Sustainability (Switzerland)*, *13*(3), 1–15. https://doi.org/1 0.3390/su1 3031347

Bowman, S., Agrawal, V., & Sharma, S. (2023). Role of pH and Eh in geothermal systems: Thermodynamic examples and impacts on scaling and corrosion. *Geothermics*, *111*. https://doi.org/10.1016/j.geothermics.2023.102710

Boyden, H., Gillan, M., Molina, J., Gadgil, A., & Tseng, W. (2023). Community perceptions of arsenic contaminated drinking water and preferences for risk communication in California's San Joaquin Valley. *International Journal of Environmental Research and Public Health*, *20*(1), 813. https://doi.org /10.339 0/ijerph20010813

Braun, V., & Clarke, V. (2023). Toward good practice in thematic analysis : Avoiding common problems and becoming a knowing researcher. *International Journal of Transgender Health*, *24*(1), 1–6. https://doi.org/10.1080/26895269.2022.2129597

Burnside, N., Montcoudiol, N., Becker, K., & Lewi, E. (2021). Geothermal energy resources in Ethiopia: Status review and insights from hydrochemistry of surface and groundwaters. *Wiley Interdisciplinary Reviews: Water*, *8*(6), 1–27. https://doi.org/10.1002/wat2.1554

Bushra, B., Bazneh, L., Deka, L., Wood, P. J., McGowan, S., & Das, D. B. (2023). Temporal modelling of long-term heavy metal concentrations in aquatic ecosystems. *Journal of Hydroinformatics*, *25*(4), 1188–1209. https://doi.org/1 0.2166/h ydro.2023.151

Campeny, M., Menéndez, I., Ibáñez-Insa, J., Rivera-Martínez, J., Yepes, J., Álvarez-Pousa, S., Méndez-Ramos, J., & Mangas, J. (2023). The ephemeral fumarolic mineralization of the 2021 Tajogaite volcanic eruption (La Palma, Canary Islands, Spain). *Scientific Reports*, *13*(1), 1–14. https://doi.org/10.1038/s41598-023-33387-6

Caputo, A., Tomai, M., Lai, C., Desideri, A., Pomoni, E., Méndez, H. C., Castellanos, B. A., La Longa, F., Crescimbene, M., & Langher, V. (2022). The Perception of Water Contamination and Risky Consumption in El Salvador from a Community Clinical Psychology Perspective. *International Journal of Environmental Research and Public Health*, *19*(3), 1–13. https://doi.org/10.3390/ijerph19031109

Chihobve, E., Zhou, M., Zhao, B., & Song, Z. (2022). *Sampling size determination: Application in geochemical sampling for environmental impact assessment* (Version 1). Research Square. https://doi.org/10.21203/rs.3.rs-1234842/v1

Chiodini, G., Bini, G., Massaro, S., Caliro, S., Kanellopoulos, C., Tassi, F., Vaselli, O., Vougioukalakis, G., & Bachmann, O. (2023). Ascent and decompressional boiling of geothermal liquids tracked by solute mass balances: a key to understanding the hydrothermal explosions of Milos (Greece). *Frontiers in Earth Science*, *11*(October), 1–14. https://doi.org/10.3389/feart.2023.1254547

Chowdhury, T. N., Hasan, M. M., Munna, G. M., Alam, M. J. Bin, Nury, A. H., Islam, S., & Naher, T. (2024). Hazard-mapping and health risk analysis of iron and arsenic contamination in the groundwater of Sylhet district. *Journal of Water and Health*, *22*(4), 757–772. https://doi.org/10.2166/wh.2024.018

Cocca, D., Lasagna, M., Destefanis, E., Bottasso, C., & De Luca, D. A. (2024). Human Health Risk Assessment of Heavy Metals and Nitrates Associated with Oral and Dermal Groundwater Exposure: The Poirino Plateau Case Study (NW Italy). *Sustainability (Switzerland)*, *16*(1). https://doi.org/10.3390/su16010222

Cochran, W. G. (1977). *Sampling Techniques* (3rd Ed.). John Wiley & Sons. https://www.academia.edu/29684662/Cochran_1977_Sampling_Techniques_Third_Edition

Demarchi, P., Garbarino, F., Mascolo, A., Silvestrini Biavati, F., & Ugolini, A. (2023). Fluorosis and Oral Health Status in Adolescents Living in a High-Fluoride Groundwater Area: A Case Study of Nairobi Suburbs (Kenya). *Applied Sciences (Switzerland)*, *13*(1). https://doi.org/10.3390/app13010368

Demelash, H., Beyene, A., Abebe, Z., & Melese, A. (2019). Fluoride concentration in ground water and prevalence of dental fluorosis in Ethiopian Rift Valley: Systematic review and meta-analysis. *BMC Public Health*, *19*(1), 1–9. https://doi.org/10.1186/s12889-019-7646-8

Demissie, S., Mekonen, S., Awoke, T., Teshome, B., & Mengistie, B. (2024). Examining carcinogenic and noncarcinogenic health risks related to arsenic exposure in Ethiopia: A longitudinal study. *Toxicology Reports*, *12*(January), 100–110. https://doi.org/10.1016/j.toxrep.2024.01.001

Di Sano, C., Di Vincenzo, S., Lo Piparo, D., D'Anna, C., Taverna, S., Lazzara, V., Pinto, P., Sortino, F., & Pace, E. (2023). Effects of condensates from volcanic fumaroles and cigarette smoke extracts on airway epithelial cells. *Human Cell*, *36*(5), 1689–1702. https://doi.org/10.1007/s13577-023-00927-1

Douvris, C., Vaughan, T., Bussan, D., Bartzas, G., & Thomas, R. (2023). How ICP-OES changed the face of trace element analysis: Review of the global application landscape. *Science of the Total Environment*, *905*(September), 167242. https://doi.org/10.1016/j.scitotenv.2023.167242

Duku, E. O., Ongarora, B. G., & Tanui, P. (2022). Effect of Boiling and Cooling of Geothermal Fluids on Precipitation of Secondary Minerals: A Case Study of Olkaria Fields, Kenya. *Journal of Geoscience and Environment Protection*, *10*(09), 251–270. https://doi.org/10.4236/gep.2022.109015

Durowoju, O. S., Ekosse, G. I. E., & Odiyo, J. O. (2020). Occurrence and health-risk assessment of trace metals in geothermal springs within Soutpansberg, Limpopo Province, South Africa. *International Journal of Environmental Research and Public Health*, *17*(12), 1–20. https://doi.org/10.3390/ijerph17124438

Durowoju, O. S., Odiyo, J. O., & Ekosse, G. I. E. (2016). Variations of heavy metals from geothermal spring to surrounding soil and Mangifera indica-Siloam village, Limpopo Province. *Sustainability (Switzerland)*, *8*(1). https://doi.org/ 10.3390/ su80 10060

Edmonds, M., Mason, E., & Hogg, O. (2022). Volcanic outgassing of volatile trace metals. *Annual Review of Earth and Planetary Sciences*, *50*, 79–98. https://doi.o rg/10 .1146/annurev-earth-070921-062047

Edwards, B. A., Outridge, P. M., & Wang, F. (2024). Mercury from Icelandic geothermal activity: High enrichments in soils, low emissions to the atmosphere. *Geochimica et Cosmochimica Acta*, *378*, 286–299. https://doi.org/10 .1016/ j.gca .2024.06.026

Elbarbary, S., Abdel Zaher, M., Saibi, H., Fowler, A. R., & Saibi, K. (2022). Geothermal renewable energy prospects of the African continent using GIS. *Geothermal Energy*, *10*(1), 1–19. https://doi.org/10.1186/s40517-022-00219-1

Elhami, A., & Khoshnevisan, B. (2022). *Conducting an interview in qualitative research: The modus operandi*. MEXTESOL Journal, 46(1), 1–7. https://www .mex tesol.net/journal/index.php?id_article=45957&page=journal

Energy and Petroleum Regulatory Authority. (2025). *Energy & petroleum statistics report for the financial year ended 30 June 2025*.

Favorito, J. E., Harris, R. N., Sohn, R. A., Hurwitz, S., & Luttrell, K. M. (2021). Heat Flux From a Vapor-Dominated Hydrothermal Field Beneath Yellowstone Lake. *Journal of Geophysical Research: Solid Earth*, *126*(5), 1–20. https://doi.org /10.1029 /2020JB021098

Feng, Y., Liu, C., Huang, L., Qian, J., Li, N., Tan, H., & Liu, X. (2025). Associations between heavy metal exposure and vascular age: a large cross-sectional study. *Journal of Translational Medicine*, *23*(1). https://doi.org/10.1186/s12967-024-06021-w

Ferreira, L., Cruz, J. V., Viveiros, F., Durães, N., Coutinho, R., Andrade, C., & Santos, J. F. (2024). Chemical and 87Sr/86Sr signatures of rainwaters at two active central volcanoes in São Miguel (Azores) – first survey. *Journal of Volcanology and Geothermal Research*, *447*(February). https://doi.org/10.1 016/j.jvolg eores. 2024.108033

Friðleifsson, G. Ó., Elders, W. A., Zierenberg, R. A., Fowler, A. P. G., Weisenberger, T. B., Mes, G., Sigurðsson, Ó., Níelsson, S., Einarsson, G., Óskarsson, F., Guðnason, E. Á., Tulinius, H., Hokstad, K., Benoit, G., Nono, F., Loggia, D., Parat, F., Cichy, S. B., Escobedo, D., & Mainprice, D. (2020). The Iceland deep drilling project at Reykjanes: Drilling into the root zone of a black smoker analog. *Journal of Volcanology and Geothermal Research*, *391*, 106269. https://doi.org/10.1016/j.jvolgeores.2018.08.013

Ganie, S. Y., Javaid, D., Hajam, Y. A., & Reshi, M. S. (2023). Arsenic toxicity: sources, pathophysiology and mechanism. *Toxicology research*, *13*(1), tfad111. https://doi.org/10.1093/toxres/tfad111

Garg, D. M., Dhull, D. H., Kalluri, D. N., & Agrawal, S. (2024). Understanding Sample Size Determination In Research: A Practical Guide. *Educational Administration: Theory and Practice*, *30*(5), 13800–13810. https://doi.org/10.53555 /kuey.v30i5.6 040

Gayapersad, A., O'Brien, M. A., Meaney, C., Aditya, I., Baxter, J., & Selby, P. (2024). Key informants' perspectives on creating a high-impact research department in family and community medicine: a qualitative project. *BMC Primary Care*, *25*(1), 1–13. https://doi.org/10.1186/s12875-024-02288-6

Gill, J. C., & Malamud, B. D. (2017). Anthropogenic processes, natural hazards, and interactions in a multi-hazard framework. *Earth-Science Reviews*, *166*, 246–269. https://doi.org/10.1016/j.earscirev.2017.01.002

Gong, C., Lu, H., Zhang, Z., Wang, L., Xia, X., Wang, L., Xiang, Z., Shuai, L., Ding, Y., Chen, Y., & Wang, S. (2022). Spatial distribution characteristics of heavy metal(loid)s health risk in soil at the town level. *Scientific Reports*, *12*(1), 1–12. https://doi.org/10.1038/s41598-022-20867-4

Gray, K. M., Triana, V., Lindsey, M., Richmond, B., Hoover, A. G., & Wiesen, C. (2021). Knowledge and beliefs associated with environmental health literacy: A case study focused on toxic metals contamination of well water. *International Journal of Environmental Research and Public Health*, *18*(17). https://doi.or g/10.3 390/ijerph18179298

Gutiérrez, M., Alarcón-Herrera, M. T., Espino-Valdés, M. S., & Valenzuela-García, L. I. (2025). Current State of Arsenic, Fluoride, and Nitrate Groundwater Contamination in Northern Mexico: Distribution, Health Impacts, and Emerging Research. *Water (Switzerland)*, *17*(13), 1–19. https://doi.org/10.3390/w17131990

Howell, C. R., Su, W., Nassel, A. F., Agne, A. A., & Cherrington, A. L. (2020). Area based stratified random sampling using geospatial technology in a community-based survey. *BMC Public Health*, *20*(1), 1–9. https://doi.org/10.1186/s12889-020-09793-0

Hsu, F. H., Su, C. C., Lin, Y. S., Lee, H. F., Chu, M. F., Lan, T., Wu, S. F., & Chen, S. C. (2024). Geochemical indications of hydrothermal fluid through sediments within the Geolin Mounds and Mienhua Volcano hydrothermal fields, southernmost Okinawa Trough. *Deep-Sea Research Part I: Oceanographic Research Papers*, *207*(March), 104293. https://doi.org/10.1016/j.dsr.2024.104293

Imran, U., Mahar, R. B., Ullah, A., & Shaikh, K. (2021). Seasonal variability of heavy metals in Manchar Lake of arid southern Pakistan and its consequential human health risk. *Polish Journal of Environmental Studies*, *30*(1), 163–175. https://doi.org/10.15244/pjoes/120363

Inostroza, M., Aguilera, F., Menzies, A., Layana, S., González, C., Ureta, G., Sepúlveda, J., Scheller, S., Böehm, S., Barraza, M., Tagle, R., & Patzschke, M. (2020). Deposition of metals and metalloids in the fumarolic fields of Guallatiri and Lastarria volcanoes, northern Chile. *Journal of Volcanology and Geothermal Research*, *393*, 106803. https://doi.org/10.1016/j.jvolgeores.2020.106803

Inostroza, M., Moune, S., Moretti, R., Bonifacie, M., Robert, V., Burtin, A., & Chilin-Eusebe, E. (2022). Decoding water-rock interaction and volatile input at La Soufriere volcano (Guadeloupe) using time-series major and trace element analyses in gas condensates. *Journal of Volcanology and Geothermal Research*, *425*. https://doi.org/10.1016/j.jvolgeores.2022.107517

Inostroza, M., Moune, S., Moretti, R., Burckel, P., Chilin-Eusebe, E., Dessert, C., Robert, V., & Gorge, C. (2023). Major and trace element emission rates in hydrothermal plumes in a tropical environment. The case of La Soufrière de Guadeloupe volcano. *Chemical Geology*, *632*. https://doi.org/10.1 016/j.ch emg eo.2023.121552

Inostroza, M., Moune, S., Moretti, R., Robert, V., Bonifacie, M., Chilin-Eusebe, E., Burtin, A., & Burckel, P. (2022). Monitoring Hydrothermal Activity Using Major and Trace Elements in Low-Temperature Fumarolic Condensates: The Case of La Soufriere de Guadeloupe Volcano. *Geosciences (Switzerland)*, *12*(7). https://doi.org/10.3390/geosciences12070267

Iqbal, M. M., Li, L., Hussain, S., Lee, J. L., Mumtaz, F., Elbeltagi, A., Waqas, M. S., & Dilawar, A. (2022). Analysis of Seasonal Variations in Surface Water Quality over Wet and Dry Regions. *Water (Switzerland)*, *14*(7). https://doi.org/10. 3390/w1 4071058

International Renewable Energy Agency. (2020). *Geothermal development in Eastern Africa: Recommendations for power and direct use*. https://www. irena.org/p ublications

Ishida, M., Fujinaga, K., Tanimizu, M., Ishikawa, T., Nagaishi, K., & Kato, Y. (2024). New Pb isotopic data from Japanese hydrothermal deposits for tracing heavy metal sources. *Geochemistry*, *84*(1), 126045. https://doi.org/ 10.1016/j. chemer. 2023.126045

Izah, S. C., Sylva, L., & Hait, M. (2024). Cronbach's Alpha: A Cornerstone in Ensuring Reliability and Validity in Environmental Health Assessment. *ES Energy and Environment*, *23*, 1–14. https://doi.org/10.30919/esee1057

James, K., Daniel, O., George, O., Gilbert, O., & Joshua, O. (2021). Cultural heritage as a pathway for sustaining natural resources in the Maasais Pastoral Social-Ecological System in Kajiado County, Kenya. *African Journal of Agricultural Research*, *17*(6), 844–852. https://doi.org/10.5897/ajar2021.15545

Jia, L., Liang, H., Fan, M., Guo, S., Yue, T., Wang, M., Su, M., Chen, S., Wang, Z., & Fu, K. (2024). Spatial distribution and source apportionment of soil heavy metals in the areas affected by non-ferrous metal slag field in southwest China. *Frontiers in Environmental Science*, *12*(July), 1–11. https://doi.org/ 10.3389/ fenvs. 2024.1407319

Jin, S., Kemp, D. B., Shen, J., Yin, R., Jolley, D. W., Vieira, M., & Huang, C. (2024). Spatiotemporal distribution of global mercury enrichments through the Paleocene-Eocene Thermal Maximum and links to volcanism. *Earth-Science Reviews*, *248*(November 2023), 104647. https://doi.org/ 10.1016/j.e arscirev. 2023. 104647

Johnson, M. A., Abuya, T., Wickramanayake, A., Miller, H., Sambu, D., Mwanga, D., Odwe, G., Ndwiga, C., Piedrahita, R., Rossanese, M., Gatari, M. J., Giordano, M. R., Westervelt, D. M., Wotton, L., & Rajasekharan, S. (2024). Patterns and drivers of maternal personal exposure to PM2.5 in informal settlements in Nairobi, Kenya. *Environmental Science: Atmospheres*, *4*(5), 578–591. https://doi.o rg/10.1039/d3ea00074e

Kabanda, R., Ocaatre, R. M., Atwine, D., Kim, B., Waiswa, S. E., Kavuma, P. D., Lee, Y., Mutoni, L., Kim, S., Park, Y., Okuga, M., & Tweheyo, R. (2025). Community health system capacities and capabilities within an evolving community health policy framework: mixed methods study of stakeholders in central Uganda. *BMJ Open*, *15*(1), 1–10. https://doi.org/10.1136/bmjopen-2023-082085

Kamagate, M., Lanciné, T., Berthe, K. A. N., Droh Lanciné, G., Kriaa, K., Assadi, A. A., Zhang, J., & Tahraoui, H. (2025). Assessment of the Human Health Risks Associated with Heavy Metals in Surface Water Near Gold Mining Sites in Côte d'Ivoire. *Water (Switzerland)*, *17*(13), 1–13. https://doi.org/10.3390/w17131891

Khalili, F., Mahvi, A. H., Nasseri, S., Yunesian, M., Yaseri, M., & Djahed, B. (2019). Health risk assessment of dermal exposure to the heavy metals content of chemical hair dyes. *Iranian Journal of Public Health*, *48*(5), 902–911. https://doi.org/10.18502/ijph.v48i5.1807

Khosravi-Darani, K., Rehman, Y., Katsoyiannis, I. A., Kokkinos, E., & Zouboulis, A. I. (2022). Arsenic Exposure via Contaminated Water and Food Sources. *Water (Switzerland)*, *14*(12). https://doi.org/10.3390/w14121884

Khouni, I., Louhichi, G., & Ghrabi, A. (2021). Use of GIS-based Inverse Distance Weighted interpolation to assess surface water quality: Case of Wadi El Bey, Tunisia. *Environmental Technology and Innovation*, *24*, 101892. https://doi.org/10.1016/j.eti.2021.101892

King, A. L., Meyers, J. S., & Brown, J. M. (2019). Hydraulic conductivity of quaternary surficial units within the Eklutna Valley, southcentral Alaska. *Journal of Hydrology*, *575*(May), 166–174. https://doi.org/10.1016/j.jhydrol.2019.05.024

Kipngok, J., Magnússon, R., Melosh, G., Haizlip, J., Cumming, W., Hinz, N., Harvey, M., Alexander, K., Lopeyok, T., Mwakirani, R., Wamalwa, A. M., Malimo, S. J., & Auko, L. O. (2017). *Geothermal conceptual model of Suswa Volcano, Kenya*. GRC Transactions, 41, 1–19.

Klockmann, I., Jaß, L., Härter, M., von dem Knesebeck, O., Lüdecke, D., & Heeg, J. (2023). Multi-staged development and pilot testing of a self-assessment tool for organizational health literacy. *BMC Health Services Research*, *23*(1), 1–9. https://doi.org/10.1186/s12913-023-10448-0

KNBS. (2019). *2019 Kenya population and housing census: Volume II – Distribution of population by administrative units.* http://www.knbs.or.ke

Kenya National Bureau of Statistics, Ministry of Health, & ICF. (2023). *Kenya Demographic and Health Survey 2022: Volume 2*. KNBS & ICF. https://www.knbs.or.ke/wp-content/uploads/2023/07/Kenya-DHS-2022-Main-Report-Volume-2.pdf

Kost, O., González-Lemos, S., Rodríguez-Rodríguez, L., Sliwinski, J., Endres, L., Haghipour, N., & Stoll, H. (2023). Relationship of seasonal variations in drip water δ13CDIC, δ18O, and trace elements with surface and physical cave conditions of la Vallina cave, NW Spain. *Hydrology and Earth System Sciences*, *27*(11), 2227–2255. https://doi.org/10.5194/hess-27-2227-2023

Kumar, P., Khan, P. K., & Kumar, A. (2025). Health risk assessment upon exposure to groundwater arsenic among individuals of different sexes and age groups of Vaishali district, Bihar (India). *Toxicology Reports*, *14*(March), 102024. https://doi.org/10.1016/j.toxrep.2025.102024

Kush, K., Ramprasad, V., Harikripa, N. U., Vishnu, S., Nishu, S., & Prajna, N. (2022). Seasonal variations in groundwater fluoride of Swarna River Basin in Southern India: A GIS-based study. *Journal of International Society of Preventive & Community Dentistry*, *8*(4), 34–37. https://doi.org/10.4103/jispcd.JISPCD

Lakens, D. (2022). Sample Size Justification. *Collabra: Psychology*, *8*(1), 1–28. https://doi.org/10.1525/collabra.33267

Lambebo, I. H., Eba, K., & Tucho, G. T. (2025). Community's perceptions on health and ecological impacts of climate change and adaptation strategies in rural areas of the central Ethiopian region. *BMC public health*, *25*(1), 3310. https://doi.org/10.1186/s12889-025-24719-4

Lawer, J., Babadimas, J., Bretherton, J., van Deijl, B., Harfoushian, J., Gerard, D., Toole, B., & Anderson, M. (2023). Mercury in natural gas: delivering accurate reservoir sampling and analysis. *The APPEA Journal*, *63*(1), 56–67. https://doi.or g/10.1071/aj22270

Lemeshow, S., & Ferketich, A. (2020). Simple Random Sampling. *Polling America: An Encyclopedia of Public Opinion, Second Edition: Volumes 1-2, December*, 661–664. https://doi.org/10.4324/9780203128640-6

Lewis, N. A., Bravo, M., Naiman, S., Pearson, A. R., Romero-Canyas, R., Schuldt, J. P., & Song, H. (2020). Using qualitative approaches to improve quantitative inferences in environmental psychology. *MethodsX*, *7*. https://doi.org/1 0.1016/j. mex.2020.100943

Li, Li, G., Yi, M., Zhou, J., Deng, Y., Huang, Y., He, S., Meng, X., & Liu, L. (2024). Sex-specific associations of urinary mixed-metal concentrations with femoral bone mineral density among older people: an NHANES (2017–2020) analysis. *Frontiers in Public Health*, *12*(May), 1–10. https://doi.org/ 10.3389/fp ubh. 2024.1363362

Lichti, K. A., Ghaziof, S., Julian, R., & Mountain, B. W. (2024). Geochemical modelling of heavy metal deposition in a geothermal heat exchanger. *Geothermics*, *118*, 102884. https://doi.org/10.1016/J.GEOTHERMICS.2023.102884

Ligate, F., Ijumulana, J., Ahmad, A., Kimambo, V., Irunde, R., Mtamba, J. O., Mtalo, F., & Bhattacharya, P. (2021). Groundwater resources in the East African Rift Valley: Understanding the geogenic contamination and water quality challenges in Tanzania. *Scientific African*, *13*(July), e00831. https://doi.o rg/10. 1016/ j.sciaf .2021.e00831

Ligate, F., Lucca, E., Ijumulana, J., Irunde, R., Kimambo, V., Mtamba, J., Ahmad, A., Hamisi, R., Maity, J. P., Mtalo, F., & Bhattacharya, P. (2022). Geogenic contaminants and groundwater quality around Lake Victoria goldfields in northwestern Tanzania. *Chemosphere*, *307*(July), 135732. https://doi.org/10. 1016/j.chem osphere.2022.135732

Ligate, F. J. (2023). Hydrogeochemistry and spatial variability of arsenic and fluoride co-occurrence in groundwater from Geita district in Lake Victoria Basin, northwest Tanzania. Retrieved from https://urn.kb.se/re solve?urn=urn :nbn:se: kth:diva-324682

Linhares, D., Gaspar, D., Bernardo, F., Beney, I., Garcia, P., & Rodrigues, A. (2025). Fluoride levels in water sources inside the crater of Furnas volcano: Potential health implications for local communities and tourists. *Science of the Total Environment*, *982*(January), 179635. https://doi.org/10 .1016/j.scito tenv.2 025.179635

Liu, C., Hu, C., Wu, X., Li, C., Wu, X., Li, C., Sun, B., Qi, H., & Xu, Q. (2024). Integrated study of hydrochemistry, quality and risk to human health of groundwater in the upper reaches of the Wulong River Basin. *PLoS ONE*, *19*(10), 1–20. https://doi.org/10.1371/journal.pone.0312000

Liu, L., Zhang, S., He, J., & Wang, L. (2025). The Genetic Mechanism of Fluoride-Enriched Geothermal Groundwater in Southeast Coastal Areas in China: Hydrochemistry, Isotope, and Machine Learning Analysis. *Water (Switzerland)*, *17*(10), 1–18. https://doi.org/10.3390/w17101498

Liu, Liu, F., Xu, Y., Zhu, H., Jiao, J., & El-Wardany, R. M. (2023). Hydrogeochemical Characteristics and Human Health Risk Assessment of Fluoride Enrichment in Water in Faulted Basins of Qinghai-Tibet Plateau—A Case Study of Sanhe Plain in Guide Basin. *Water (Switzerland)*, *15*(10). https://doi.org/10.3390/w15101968

Lo Medico, F., Rizzo, P., Rotigliano, E., & Celico, F. (2025). Groundwater Contamination: Study on the Distribution and Mobility of Metals and Metalloids in Soil and Rocks. *International Journal of Environmental Research and Public Health*, *22*(2), 11–17. https://doi.org/10.3390/ijerph22020182

Lumumba, E. A., Riederer, A. M., Onyatta, J. O., Benki-Nugent, S., Karr, C. J., & Were, F. H. (2024). Maternal and Umbilical Cord Blood Lead Levels in Selected Informal Settlements in Nairobi, Kenya: A Cross-Sectional Study. *Environmental Health Perspectives*, *132*(3), 3–5. https://doi.org/10.1289/EHP13567

Luo, L., Wang, B., Jiang, J., Fitzgerald, M., Huang, Q., Yu, Z., Li, H., Zhang, J., Wei, J., Yang, C., Zhang, H., Dong, L., & Chen, S. (2021). Heavy Metal Contaminations in Herbal Medicines: Determination, Comprehensive Risk Assessments, and Solutions. *Frontiers in Pharmacology*, *11*(January), 1–14. https://doi.org/10.3 389/fphar.20 20.595335

Lv, G., Zhang, X., Wei, D., Yu, Z., Yuan, X., Sun, M., Kong, X., & Zhang, Y. (2023). Water–Rock Interactions, Genesis Mechanism, and Mineral Scaling of Geothermal Waters in Northwestern Sichuan, SW China. *Water*, *15*(21), 3730. https://doi.org /10.3390/w15213730

Majewski, G., Klik, B., Rogula-Kozłowska, W., Rogula-Kopiec, P., Rybak, J., Radziemska, M., & Liniauskienė, E. (2023). Assessment of Heavy Metal Inhalation Risks in Urban Environments in Poland: A Case Study. *Journal of Ecological Engineering*, *24*(11), 330–340. https://doi.org/ 10.12911/ 229989 93/171591

Mandindi, W. Z., Nyaba, L., Mketo, N., & Nomngongo, P. N. (2022). Seasonal Variation of Drinking Water Quality and Human Health Risk Assessment: A Case Study in Rural Village of the Eastern Cape, South Africa. *Water (Switzerland)*, *14*(13). https://doi.org/10.3390/w14132013

Manousi, N., Isaakidou, E., & Zachariadis, G. A. (2022). An Inductively Coupled Plasma Optical Emission Spectrometric Method for the Determination of Toxic and Nutrient Metals in Spices after Pressure-Assisted Digestion. *Applied Sciences (Switzerland)*, *12*(2). https://doi.org/10.3390/app12020534

Martínez-Acuña, M. I., Reyes-Hernández, H., Covarrubias, S. A., Martínez-Esquivel, R. A., & Estudillo-Wong, L. A. (2024). Mapping the Environmental Risk of Fluoride Exposure of Drinking Water in a Community of Zacatecas, Mexico. *Water (Switzerland)*, *16*(17), 1–14. https://doi.org/10.3390/w16172428

Martínez-Guijarro, R. M.-, Paches, M., Romero, I., & Aguado, D. (2021). Sources, Mobility, Reactivity, and Remediation of Heavy Metal(loid) Pollution: A Review. *Advances in Environmental and Engineering Research*, *2*(4), 1–1. https://doi.org/10.21926/aeer.2104033

Masikonte, L. N. (2020). *Potential Environmental and Socio-economic Effects of Geothermal Exploitation on the Local Community: a Case of Suswa Geothermal Plant*.

Merusomayajula, K. V., Tirukkovalluri, S. R., Kommula, R. S., Chakkirala, S. V., Vundavilli, J. K., & Kottapalli, P. K. S. R. (2021). Development and validation of a simple and rapid ICP-OES method for quantification of elemental impurities in voriconazole drug substance. *Future Journal of Pharmaceutical Sciences*, *7*(1). https://doi.org/10.1186/s43094-020-00159-2

Michalicová, R., Hegrová, J., Svoboda, J., & Ličbinský, R. (2024). Seasonal and spatial variations of arsenic and its species in particulate matter in an urban environment of Brno, Czech Republic. *Environmental Science and Pollution Research*, *31*(43), 55251–55262. https://doi.org/10.1007/s11356-024-34645-4

Minami, Y., Matsumoto, K., Geshi, N., & Shinohara, H. (2022). Influence of hydrothermal recharge on the evolution of eruption styles and hazards during the 2018–2019 activity at Kuchinoerabujima Volcano, Japan. *Earth, Planets and Space*, *74*(1). https://doi.org/10.1186/s40623-022-01580-y

Missana, T., Alonso, U., Mayordomo, N., & García-Gutiérrez, M. (2023). Analysis of Cadmium Retention Mechanisms by a Smectite Clay in the Presence of Carbonates. *Toxics*, *11*(2), 1–14. https://doi.org/10.3390/toxics11020130

Mohajan, H. (2017). Two Criteria for Good Measurements in Research: Validity and Reliability. *Administrative Science Quarterly*, *36*(3), 421–458. http://www.j stor.org/stable/2393203

Mohammadpour, A., Rajabi, S., Bell, M., Baghapour, M. A., Aliyeva, A., & Mousavi Khaneghah, A. (2023). Seasonal variations of potentially toxic elements (PTEs) in drinking water and health risk assessment via Monte Carlo simulation and Sobol sensitivity analysis in southern Iran's largest city. *Applied Water Science*, *13*(12), 1–17. https://doi.org/10.1007/s13201-023-02041-x

Molina-Frechero, N., Nevarez-Rascón, M., Tremillo-Maldonado, O., Vergara-Onofre, M., Gutiérrez-Tolentino, R., Gaona, E., Castañeda, E., Jarquin-Yañez, L., & Bologna-Molina, R. (2020). Environmental exposure to arsenic in groundwater associated with carcinogenic risk in underweight children exposed to fluorides. *International Journal of Environmental Research and Public Health*, *17*(3), 1–10. https://doi.org/10.3390/ijerph17030724

Montcoudiol, N., Burnside, N. M., Göre, D., Mariita, N., Mutia, T., & Boyce, A. (2019). Surface and groundwater hydrochemistry of the Menengai caldera geothermal field and surrounding Nakuru County, Kenya. *Energies*, *12*(16). https://doi.org/10.3390/en12163131

Moradnia, M., Attar, H. M., Hajizadeh, Y., Lundh, T., Salari, M., & Darvishmotevalli, M. (2024). Assessing the carcinogenic and non-carcinogenic health risks of metals in the drinking water of Isfahan, Iran. *Scientific Reports*, *14*(1), 1–9. https://doi.org/10.1038/s41598-024-55615-3

Morales-deAvila, H., Gutiérrez, M., Colmenero-Chacón, C. P., Júnez-Ferreira, H. E., & Esteller-Alberich, M. V. (2023). Upward Trends and Lithological and Climatic Controls of Groundwater Arsenic, Fluoride, and Nitrate in Central Mexico. *Minerals*, *13*(9). https://doi.org/10.3390/min13091145

Moretti, R. (2022). Redox behavior of degassing magmas: critical review and comparison of glass-based oxybarometers with application to Etna volcano. *Comptes Rendus - Geoscience*, *354*(August), 249–280. https://doi.o rg/10. 5802/crgeos.135

Mukromin, A., & Wibowo, Y. M. (2023). Penentuan kadar ion klorida (Cl-) pada sampel air sumur gali di Kecamatan Kaliwungu, Kendal menggunakan metode argentometri Mohr. *Jurnal Kimia Dan Rekayasa*, *4*(1), 17–22.

Mukwevho, N., Mabowa, M. H., Ntsasa, N., Mkhohlakali, A., Chimuka, L., Tshilongo, J., & Letsoalo, M. R. (2025). Seasonal Pollution Levels and Heavy Metal Contamination in the Jukskei River, South Africa. *Applied Sciences (Switzerland)*, *15*(6), 1–20. https://doi.org/10.3390/app15063117

Müller, D., Walter, T. R., Troll, V. R., Stammeier, J., Karlsson, A., Paolo, E. de, Pisciotta, A. F., Zimmer, M., & De Jarnatt, B. (2024). Anatomy of a fumarole field: drone remote-sensing and petrological approaches reveal the degassing and alteration structure at La Fossa cone, Vulcano, Italy. *Solid Earth*, *15*(9), 1155–1184. https://doi.org/10.5194/se-15-1155-2024

Mulonga, J., & Olago, D. (2023). Perceptions of climate variability and change in coastal: The case of mangrove-dependent communities in the Lower Tana Delta. *Environmental Challenges*, *13*(July), 100799. https://doi.org/10.10 16/j.envc .2023 .100799

Mumbi, A. W., & Watanabe, T. (2020). Differences in risk perception of water quality and its influencing factors between lay people and factory workers for water management in River Sosiani, Eldoret Municipality Kenya. *Water (Switzerland)*, *12*(8), 1–25. https://doi.org/10.3390/w12082248

Musoke, D., Ndejjo, R., Atusingwize, E., Mukama, T., Ssemugabo, C., & Gibson, L. (2019). Performance of community health workers and associated factors in a rural community in Wakiso district, Uganda. *African Health Sciences*, *19*(3), 2784–2797. https://doi.org/10.4314/ahs.v19i3.55

Musonye, X. S. (2022). *The role of geothermal in energy mix: Kenya's case study* (Paper presented at Short Course VI on Exploration for Geothermal Resources). GRÓ GTP, GDC, and KenGen, Lake Bogoria and Lake Naivasha, Kenya.

Mwiathi, N. F., Gao, X., Li, C., & Rashid, A. (2022). The occurrence of geogenic fluoride in shallow aquifers of the Kenya Rift Valley and its implications in groundwater management. *Ecotoxicology and Environmental Safety*, *229*, 113046. https://doi.org/10.1016/j.ecoenv.2021.113046

Nakazawa, K., Nagafuchi, O., Otede, U., Chen, J. Q., Kanefuji, K., & Shinozuka, K. (2020). Risk assessment of fluoride and arsenic in groundwater and a scenario analysis for reducing exposure in Inner Mongolia. *RSC Advances*, *10*(31), 18296–18304. https://doi.org/10.1039/d0ra00435a

Nanjundeswaraswamy, T. S., & Divakar, S. (2021). Determination of Sample Size and Sampling Methods in Applied Research. *Proceedings on Engineering Sciences*, *3*(1), 25–32. https://doi.org/10.24874/pes03.01.003

Narayanan, M. S. S., Pitchaimani, V. S., Sivakumar, M., Dinesh Kumar, T., Abishek, S. R., & Karuppannan, S. (2025). Spatial assessment of heavy metal contamination in groundwater in the Kadaladi region, Tamil Nadu, India. *Scientific Reports*, *15*(1), 1–21. https://doi.org/10.1038/s41598-025-12120-5

Nations, U. (2022). World Population Prospects 2022. In the *United Nations* (Issue 9). www.un.org/development/ desa/pd/.

National Environment Management Authority (NEMA). (2024). *Environmental Management and Co-ordination (Water Quality) Regulations* (Kenya Gazette Supplement No. 68, 177, 1–25.). Kenya Gazette.

Ngwenya, S., Mashau, N. S., Mudau, A. G., Mhlongo, S. E., & Traoré, A. N. (2024). Community Perceptions on Health Risks Associated With Toxic Chemical Pollutants in Kwekwe City, Zimbabwe: A Qualitative Study. *Environmental Health Insights*, *18*. https://doi.org/10.1177/11786302241260487

Niknejad, H., Ala, A., Ahmadi, F., Mahmoodi, H., Saeedi, R., Gholami-Borujeni, F., & Abtahi, M. (2023). Carcinogenic and non-carcinogenic risk assessment of exposure to trace elements in groundwater resources of Sari city, Iran. *Journal of Water and Health*, *21*(4), 501–513. https://doi.org/10.2166/WH.2023.308

Nowicki, S., Birhanu, B., Tanui, F., Sule, M. N., Charles, K., Olago, D., & Kebede, S. (2023). Water chemistry poses health risks as reliance on groundwater increases: A systematic review of hydrogeochemistry research from Ethiopia and Kenya. *Science of the Total Environment*, *904*(November), 166929. https://doi.org/10.1016/j.scitotenv.2023.166929

Odongo, R. A., De Moel, H., Wens, M., Coumou, D., Limones, N., Otieno, V., & Van Loon, A. F. (2025). From indices to impacts using environmental and socio-economic clustering in Kenya. *Journal of Hydrology: Regional Studies*, *58*(February), 102269. https://doi.org/10.1016/j.ejrh.2025.102269

Ofman, E., Skorbiłowicz, P., Skorbiłowicz, M., Sidoruk, M., & Tarasiuk, U. (2024). Geochemical Assessment of Heavy Metal Distribution in Bug River Sediments, Poland: The Impacts of Urbanization and Agricultural Practices. *Water*, *16*(11), 1573. https://doi.org/10.3390/w16111573

Ohba, T., Yaguchi, M., Nishino, K., Numanami, N., Daita, Y., Sukigara, C., Ito, M., & Tsunogai, U. (2019). Time variations in the chemical and isotopic composition of fumarolic gases at Hakone volcano, Honshu Island, Japan, over the earthquake swarm and eruption in 2015, interpreted by the magma sealing model. *Earth, Planets and Space*, *71*(1). https://doi.org/10.1186/s40623-019-1027-5

Ohba, T., Yaguchi, M., Tsunogai, U., Ito, M., & Shingubara, R. (2021). Behavior of magmatic components in fumarolic gases related to the 2018 phreatic eruption at Ebinokogen Ioyama volcano, Kirishima Volcanic Group, Kyushu, Japan. *Earth, Planets and Space*, *73*(1). https://doi.org/10.1186/s40623-021-01405-4

Ondiek, R. A., Vuolo, F., Kipkemboi, J., Kitaka, N., Lautsch, E., Hein, T., & Schmid, E. (2020). Socio-Economic Determinants of Land Use/Cover Change in Wetlands in East Africa: A Case Study Analysis of the Anyiko Wetland, Kenya. *Frontiers in Environmental Science*, *7*(January). https://doi.org/10.3389/fenvs.2019.00207

Onipe, T., Edokpayi, J. N., & Odiyo, J. O. (2021). Geochemical characterization and assessment of fluoride sources in groundwater of Siloam area, Limpopo Province, South Africa. *Scientific Reports*, *11*(1), 1–19. https://doi.org/10.1038/s41598-021-93385-4

Pahwa, M., Cavanagh, A., & Vanstone, M. (2023). Key Informants in Applied Qualitative Health Research. *Qualitative Health Research*, *33*(14), 1251–1261. https://doi.org/10.1177/10497323231198796

Pan, F., Huang, J. H., & Feng, X. (2024). Sources, Fates, and Geochemical Cycling of Mercury in Geothermal Fields: Insights From Mercury Isotopes. *Geophysical Research Letters*, *51*(9), 1–10. https://doi.org/10.1029/2023GL107384

Pardis, W., Grabb, K. C., DeGrandpre, M. D., Spaulding, R., Beck, J., Pfeifer, J. A., & Long, D. M. (2022). Measuring Protons with Photons: A Hand-Held, Spectrophotometric pH Analyzer for Ocean Acidification Research, Community Science and Education. *Sensors (Basel, Switzerland)*, *22*(20). https://doi.org/10.3390/s22207924

Parrone, D., Ghergo, S., Frollini, E., Rossi, D., & Preziosi, E. (2020). Arsenic-fluoride co-contamination in groundwater: Background and anomalies in a volcanic-sedimentary aquifer in central Italy. *Journal of Geochemical Exploration*, *217*(March), 106590. https://doi.org/10.1016/j.gexplo.2020.106590

Phillips, N., Stewart, M., Olsen, G., & Hickey, C. (2011). *Contaminants in kai – Te Arawa rohe Part 1: Data Report Contaminants in Kai – Te Arawa rohe Part 1: Data Report Te Arawa Lakes Trust Health Research Council of New Zealand. March*.

Pichler, T. (2024). Environmental inventory of mercury (Hg) for the marine shallow water hydrothermal system at Panarea, Italy. *Science of the Total Environment*, *911*(November), 168575. https://doi.org/10.1016/j.scitotenv.2023.168575

Pieter, J. (2023). A critical review of arsenic occurrence, fate and transport in natural and modified groundwater systems in the Netherlands. *Applied Geochemistry*, *150*, 105596. https://doi.org/10.1016/j.apgeochem.2023.105596

Pitiya, R., Jacob, L., & Emilinot, R. J. (2022). A Pilot Study on the Concentration of Heavy Metals in Sediments from the Lower Orange River, //Karas Region, Namibia. *Journal of Materials Science and Chemical Engineering*, *10*(03), 1–14. https://doi.org/10.4236/msce.2022.103001

Podgorski, J., & Berg, M. (2022). Global analysis and prediction of fluoride in groundwater. *Nature Communications*, *13*(1), 1–9. https://doi.org/10.1038/s41467-0 22-31940-x

Pohl, P., Welna, M., Szymczycha-Madeja, A., Cyganowski, P., Jamroz, P., & Dzimitrowicz, A. (2022). Rapid and easy ICP OES determination of selected major, minor and trace elements in Pu-erh tea infusions using the response surface methodology along with the joint desirability function approach. *Talanta*, *249*(June), 123650. https://doi.org/10.1016/j.talanta.2022.123650

Prajapati, A., Tanwar, D., Yadav, S., & Bajar, S. (2025). Assessment of Heavy Metal Contamination and Seasonal Variability in Groundwater of Indian NCR: Geospatial and Statistical Approach. *Cleaner Water*, *4*(April), 100107. https://doi.org/10.1016/j.clwat.2025.100107

Provete, C. S., Dalfior, B. M., Mantovaneli, R., Carneiro, M. T. W. D., & Brandão, G. P. (2024). Comparison of the Performance of ICP-MS, CV-ICP-OES, and TDA AAS in Determining Mercury in Marine Sediment Samples. *ACS Omega*, *9*(50), 49229–49238. https://doi.org/10.1021/acsomega.4c06144

Pulungan, L., Ashari, Y., & Wicaksana, I. K. (2019). Preliminary study of the potential of heavy metals in geothermal sludge. *Journal of Physics: Conference Series*, *1375*(1). https://doi.org/10.1088/1742-6596/1375/1/012063

Quingda, F., Zhang, H., Zhao, W., Shi, S., Zhou, J., Zhu, G., Niu, Z., & Zhang, S. (2024). *Forms and sources of arsenic in the groundwater of the northeastern tectonic active zone of the Qinghai-Tibet Plateau.* Research Square. https://doi.org/1 0.21203/rs.3.rs-3862111/v1

R. Herdianita, N., & Priadi, B. (2008). Arsenic and Mercury Concentrations at Several Geothermal Systems in West Java, Indonesia. *ITB Journal of Sciences*, *40*(1), 1–14. https://doi.org/10.5614/itbj.sci.2008.40.1.1

Raad, H. F., Pardakhti, A., & Kalarestaghi, H. (2021). Carcinogenic and Non-Carcinogenic Health Risk Assessment of Heavy Metals in Ground Drinking Water Wells of Bandar Abbas. *Pollution*, *7*(2), 395–404. https://doi.org/10.22059/ poll.2021.317359.995

Raja, S. (2023). *Arsenic in groundwater and its carcinogenicity. International Journal of High School Research*, *5*(6), 130–135. https://doi.org/10.36838/v5i6.21

Rezaei, H., Zarei, A., Kamarehie, B., Jafari, A., Fakhri, Y., Bidarpoor, F., Karami, M. A., Farhang, M., Ghaderpoori, M., Sadeghi, H., & Shalyari, N. (2019). Levels, Distributions and Health Risk Assessment of Lead, Cadmium and Arsenic Found in Drinking Groundwater of Dehgolan's Villages, Iran. *Toxicology and Environmental Health Sciences*, *11*(1), 54–62. https://doi.org/10.1007/s13530-019-0388-2

Riebesell, U., Basso, D., Geilert, S., Dale, A. W., & Kreuzburg, M. (2023). Mesocosm experiments in ocean alkalinity enhancement research. *State of the Planet, 2-oae2023*, 6. https://sp.copernicus.org/articles/2-oae2023/6/2023/

Rigaud, M., Buekers, J., Bessems, J., Basagaña, X., Mathy, S., Nieuwenhuijsen, M., & Slama, R. (2024). The methodology of quantitative risk assessment studies. In *Environmental Health: A Global Access Science Source* (Vol. 23, Issue 1). BioMed Central. https://doi.org/10.1186/s12940-023-01039-x

Rotich, I., Hilda, C., Musyimi, P., & Kipruto, G. (2024). Geothermal energy in Kenya: Evaluating health impacts and environmental challenges. In *Energy Policy* (Vol. 10, Issue 1, pp. 63–64). https://doi.org/10.1016/0301-4215(82)90079-9

Rouwet, D., Mora-Amador, R., Ramírez, C., González, G., Baldoni, E., Pecoraino, G., Inguaggiato, S., Capaccioni, B., Lucchi, F., & Tranne, C. A. (2021). Response of a hydrothermal system to escalating phreatic unrest: the case of Turrialba and Irazú in Costa Rica (2007–2012). *Earth, Planets and Space*, *73*(1). https://doi.org/10.1186/s40623-021-01471-8

Rusiniak, P., Wątor, K., Kmiecik, E., & Vakanjac, V. R. (2024). Method validation and geochemical modelling of chromium speciation in natural waters. *Scientific Reports*, *14*(1), 1–13. https://doi.org/10.1038/s41598-024-77425-3

Sabzkoohi, H. A., Dodier, V., & Kolliopoulos, G. (2023). A validated analytical method to measure metals dissolved in deep eutectic solvents. *RSC Advances*, *13*(22), 14887–14898. https://doi.org/10.1039/d3ra02372a

Josephat, S., Stefánsson, A., & Óskarsson, F. (2024). *Major and trace elements geochemistry of natural waters at Mt. Meru volcano, Tanzania.* In Proceedings of the 49th Workshop on Geothermal Reservoir Engineering (pp. 1–23). Stanford University.

Schlesinger, W. H., Klein, E. M., & Vengosh, A. (2022). The global biogeochemical cycle of arsenic. *Global Biogeochemical Cycles, 36*(x), 1–26. https://doi.or g/1 0.1029/2022GB007515

Senila, M. (2024). Recent Advances in the Determination of Major and Trace Elements in Plants Using Inductively Coupled Plasma Optical Emission Spectrometry. *Molecules*, *29*(13). https://doi.org/10.3390/molecules29133169

Sharifnia, A. M., Kpormegbey, D. E., Thapa, D. K., & Cleary, M. (2025). A Primer of Data Cleaning in Quantitative Research: Handling Missing Values and Outliers. *Journal of advanced nursing*, 10.1111/jan.16908. Advance online publication. https://doi.org/10.1111/jan.16908

Shevko, E. P., Bortnikova, S. B., Abrosimova, N. A., Kamenetsky, V. S., Bortnikova, S. P., Panin, G. L., & Zelenski, M. (2018). Trace elements and minerals in fumarolic sulfur: The case of Ebeko Volcano, Kuriles. *Geofluids*, *2018*. https://doi.org/10.1155/2018/4586363

Shi, S., Feng, Q., Zhang, H., Zhao, W., Zhou, J., Zhu, G., Niu, Z., & Zhang, S. (2024a). Arsenic in the Tibetan Plateau's geothermal systems: a detailed analysis of forms, sources, and geochemical behaviors. *Discover Applied Sciences*, *6*(4). https://doi.org/10.1007/s42452-024-05798-1

Shi, S., Feng, Q., Zhang, H., Zhao, W., Zhou, J., Zhu, G., Niu, Z., & Zhang, S. (2024b). Arsenic in the Tibetan Plateau's geothermal systems: a detailed analysis of forms, sources, and geochemical behaviors. *Discover Applied Sciences*, *6*(4). https://doi.org/10.1007/s42452-024-05798-1

Spitzmüller, L., Goldberg, V., Held, S., Grimmer, J. C., & Winter, D. (2021). *Selective Silica Removal in Geothermal Brines : Implications for Applications for Geothermal Power Plant Operation and Brine Mining*. 1–21. https://doi.org/10.1016/ j.geothermics.2021.102141

Stefánsson, A., Keller, N. S., Robin, J. G., Kaasalainen, H., Björnsdóttir, S., Pétursdóttir, S., Jóhannesson, H., & Hreggvidsson, G. Ó. (2016). Quantifying mixing, boiling, degassing, oxidation and reactivity of thermal waters at Vonarskard, Iceland. *Journal of Volcanology and Geothermal Research*, *309*, 53–62. https://doi.org /10.1016/j.jvolgeores.2015.10.014

Stetson, S. J., Lawrence, C., Whitcomb, S., & Kanagy, C. (2021). Determination of four arsenic species in environmental water samples by liquid chromatography-inductively coupled plasma - tandem mass spectrometry. *MethodsX*, *8*, 101183. https://doi.org/10.1016/j.mex.2020.101183

Sumbl, K., & Deeba, K. (2023). The research design. *Journal of Nursing Administration*, *12*(2), 35–41. https://doi.org/10.1097/00005110-198202000-00007

Sun, M., Zhang, X., Yuan, X., Yu, Z., Xiao, Y., Wang, Y., & Zhang, Y. (2022). Hydrochemical Characteristics and Genetic Mechanism of Geothermal Springs in the Aba Area, Western Sichuan Province, China. *Sustainability (Switzerland)*, *14*(19). https://doi.org/10.3390/su141912824

Sunguti, A. E., Kibet, J. K., Kinyanjui, T. K., Oyugi, A. M., & Muhizi, T. (2024). The analysis of potentially toxic heavy metal contamination in the Lake Bogoria geothermal springs. *Discover Toxicology*, *1*(1). https://doi.org/10.1007/s44339-024-00003-9

Sunkari, E. D., & Ambushe, A. A. (2024). Groundwater fluoride contamination, sources, hotspots, health hazards, and sustainable containment measures: A systematic review of the Ghanaian context. *Groundwater for Sustainable Development*, *27*(October), 101352. https://doi.org/10.1016/j.gsd.2024.101352

Szymczycha-Madeja, A., Welna, M., Zabłocka-Malicka, M., Pohl, P., & Szczepaniak, W. (2021). Development and validation of an analytical method for determination of al, ca, cd, fe, mg and p in calcium-rich materials by icp oes. *Molecules*, *26*(20). https://doi.org/10.3390/molecules26206269

Taherdoost, H., & Madanchian, M. (2024). The impact of survey response rates on research validity and reliability. In *Design and Validation of Research Tools and Methodologies*. https://doi.org/10.4018/979-8-3693-1135-6.ch009

Taran, Y., & Kalacheva, E. (2020). Acid sulfate-chloride volcanic waters; Formation and potential for monitoring of volcanic activity. *Journal of Volcanology and Geothermal Research*, *405*, 107036. https://doi.org/1 0.1016 /j.jvolgeores .2020.107036

Temesgen, M., Alemu, T., & Shasho, E. (2024). Heavy Metals Pollution and Potential Health Risks: The Case of the Koche River, Tatek Industrial Zone, Burayu, Ethiopia. *Journal of Toxicology*, *2024*(1). https://doi.org/10.1155/jt/9425206

Terada, A., Yaguchi, M., & Ohba, T. (2022). Quantitative Assessment of Temporal Changes in Subaqueous Hydrothermal Activity in Active Crater Lakes During Unrest Based on a Time-Series of Lake Water Chemistry. *Frontiers in Earth Science*, *9*(January), 1–14. https://doi.org/10.3389/feart.2021.740671

Torres-Rodriguez, N., Yuan, J., Petersen, S., Dufour, A., González-Santana, D., Chavagnac, V., Planquette, H., Horvat, M., Amouroux, D., Cathalot, C., Pelleter, E., Sun, R., Sonke, J. E., Luther, G. W., & Heimbürger-Boavida, L. E. (2024). Mercury fluxes from hydrothermal venting at mid-ocean ridges constrained by measurements. *Nature Geoscience*, *17*(1), 51–57. https://doi.org/10.1038/s41561-023-01341-w

UNICEF & WHO. (2023). *Progress on household drinking water, sanitation and hygiene 2000–2022: special focus on gender*. https://washdata .org/sites/d efault/files /2022-01/jmp-2021-wash-households_3.pdf

U.S. Environmental Protection Agency. (2011). *Exposure factors handbook: 2011 edition* (EPA/600/R-09/052F). https://www.epa.gov/expobox/exposure-factors-handbook-2011-edition

Usman, U. S., Salh, Y. H. M., Yan, B., Namahoro, J. P., Zeng, Q., & Sallah, I. (2024). Fluoride contamination in African groundwater: Predictive modeling using stacking ensemble techniques. *Science of the Total Environment*, *957*(November). https://doi.org/10.1016/j.scitotenv.2024.177693

Wamalwa, H. (2017). Characterization of borehole water quality from a volcanic area for drinking. Case of the Menengai geothermal project boreholes, Kenya. *Transactions - Geothermal Resources Council*, *41*, 2706–2713.

Wan, Y., Liu, J., Zhuang, Z., Wang, Q., & Li, H. (2024). Heavy Metals in Agricultural Soils: Sources, Influencing Factors, and Remediation Strategies. *Toxics*, *12*(1). https://doi.org/10.3390/toxics12010063

Wang, W., Zhao, Y., Ma, Y., Guo, C., & Jia, J. (2023). An Assessment Framework for Human Health Risk from Heavy Metals in Coal Chemical Industry Soils in Northwest China. *Sustainability*, *15*(20), 14768. https://doi.org/ 10.3390 /su 152014768

Wang, Y., Cao, D., Qin, J., Zhao, S., Lin, J., Zhang, X., Wang, J., & Zhu, M. (2023). Deterministic and Probabilistic Health Risk Assessment of Toxic Metals in the Daily Diets of Residents in Industrial Regions of Northern Ningxia, China. *Biological Trace Element Research*, *201*(9), 4334–4348. https://doi.org/1 0.1007/s 12011-022-03538-3

Wang, Y., & Cheng, H. (2023). Influence of Mineral Deposition on the Retention of Potentially Hazardous Elements in Geothermal Spring Sediments. *Sustainability (Switzerland)*, *15*(10). https://doi.org/10.3390/su15108040

Waseem, K., Akhtar, A. S., & Nawaz, A. (2025). Assessment of lead contamination in drinking water in zone I and zone III of Islamabad, Pakistan. *Discover Water*. https://doi.org/10.1007/s43832-025-00231-z

Watson, M., Nikić, J., Pešić Bajić, J., Vujić, M., Apostolović, T., Atanasijević, J., & Agbaba, J. (2025). Public Perception of Drinking Water Quality in an Arsenic-Affected Region: Implications for Sustainable Water Management. *Water (Switzerland)*, *17*(11). https://doi.org/10.3390/w17111613

Welna, M., Szymczycha-Madeja, A., & Pohl, P. (2023). Novel ICP-OES-Based Method for the Reliable Determination of the Total Content of 15 Elements in Yerba Mate Drinks along with the Determination of Caffeine and the In Vitro Bioaccessibility of the Compounds. *Molecules*, *28*(8), 1–22. https://doi.org/10. 3390/molec ules28083374

Weydt, L. M., Lucci, F., Lacinska, A., Scheuvens, D., Núñez, G. C., Giordano, G., Rochelle, C. A., Schmidt, S., Bär, K., & Sass, I. (2023). The impact of hydrothermal alteration on the physiochemical characteristics of reservoir rocks : the case of the Los Humeros geothermal field (Mexico). In *Geothermal Energy* (Issue 2022). Springer Berlin Heidelberg. https://doi.org/10.1186/s40517-022-00231-5

World Health Organization (WHO). (2011a). *Guidelines for drinking-water quality* (4th ed.). Encyclopedia of Earth Sciences Series, 876–883. https://doi.o rg/10.100 7/978-1-4020-4410-6_184

World Health Organization (WHO). (2011b). *Guidelines for drinking-water quality* (Vol. 55). Proceedings of the Royal Society of Medicine. https://doi .org/10.500 5/jp/books/11431_8

World Health Organization (WHO). (2022). *Guidelines for drinking-water quality: Fourth edition incorporating the first and second addenda*. *ReVision*, *21*(6).

Wróblewski, M., Miłek, J., Godlewski, A., & Wróblewska, J. (2025). The Impact of Arsenic, Cadmium, Lead, Mercury, and Thallium Exposure on the Cardiovascular System and Oxidative Mechanisms in Children. *Current Issues in Molecular Biology*, *47*(7), 1–20. https://doi.org/10.3390/cimb47070483

Xing, R., Yang, Z., Zhou, Y., & Wang, S. (2020). Rapid determination of total sulfur content in green liquors by turbidimetric method. *BioResources*, *15*(1), 721–728. https://doi.org/10.15376/biores.15.1.721-728

Yaguchi, M., Ohba, T., & Kanno, S. (2025). Geochemical evaluation for the fumarolic gases collected at Ojigokudani, Iwate volcano, Japan in September 2024. *Earth, Planets and Space*, *77*(1). https://doi.org/10.1186/s40623-025-02260-3

Yao, B., Zhou, X., Qiu, D., Du, J., He, M., Tian, J., Zeng, Z., Wang, Y., Yan, Y., Xing, G., Cui, S., Li, J., Dong, J., Li, Y., & Zhang, F. (2024). Geochemical Characteristics of Trace Elements of Hot Springs in the Xianshuihe–Xiaojiang Fault Zone. *Water (Switzerland)*, *16*(5). https://doi.org/10.3390/w16050680

Yu, X., Wei, Z., Wang, G., Ma, X., Zhang, T., Yang, H., Li, L., Zhou, S., & Wang, X. (2022). Hot Spring Gas Geochemical Characteristics and Geological Implications of the Northern Yadong-Gulu Rift in the Tibetan Plateau. *Frontiers in Earth Science*, *10*(May), 1–10. https://doi.org/10.3389/feart.2022.863559

Yujie, H., Zhang, Q., Li, H., Wang, W., & Hua, J. (2024). Heavy metal pollution characteristics and systemic risk assessment of the environment around the tailings site. *Journal of Soils and Sediments*, *24*(1), 217–229. https://doi.org/10.1007/s11368-023-03588-7

Zelenski, M. E., Fischer, T. P., de Moor, J. M., Marty, B., Zimmermann, L., Ayalew, D., Nekrasov, A. N., & Karandashev, V. K. (2013). Trace elements in the gas emissions from the Erta Ale volcano, Afar, Ethiopia. *Chemical Geology*, *357*, 95–116. https://doi.org/10.1016/j.chemgeo.2013.08.022

Zhang, R., Wang, Z., Li, X., She, Z., & Wang, B. (2023). Water Quality Sampling and Multi-Parameter Monitoring System Based on Multi-Rotor UAV Implementation. *Water (Switzerland)*, *15*(11). https://doi.org/10.3390/w15112129

Zhao, S., Zhao, Y., Cui, Z., Zhang, H., & Zhang, J. (2024). Effect of pH, Temperature, and Salinity Levels on Heavy Metal Fraction in Lake Sediments. *Toxics*, *12*(7). https://doi.org/10.3390/toxics12070494

Zhao, X., & Dou, M. (2024). A measurement method for a zero-degree thermostat. *Journal of Measurements in Engineering*, 1–12. https://doi.org/10. 21595/jme .2024.23862

Zhu, W., Zhang, Z., Zhao, S., Guo, X., Das, P., Feng, S., & Liu, B. (2022). Vegetation Greenness Trend in Dry Seasons and Its Responses to Temperature and Precipitation in Mara River Basin, Africa. *ISPRS International Journal of Geo-Information*, *11*(8). https://doi.org/10.3390/ijgi11080426

APPENDICES

Appendix I: Introductory Letter

Dear Participant,

My name is **Gideon Yator**, a Master of Science in Environmental Science student at **Kabarak University**. I am conducting a research study titled: **"Assessment of Spatio-Seasonal Variations in Heavy Metal Contamination and Health Risks of Fumarolic Condensates in Mt. Suswa, Kajiado County, Kenya."**

This study aims to gather information on the community's interaction with fumarolic condensate water sources, patterns of use, and potential health risks associated with long-term exposure to heavy metals. The information collected through this questionnaire will be used strictly for academic and scientific purposes to help understand environmental and public health risks and support sustainable water resource management.

Your participation in this research is entirely voluntary, and your responses will remain strictly confidential. No names or identifying personal information will be used in the reporting of findings.

Thank you for taking the time to contribute to this important research.

Yours sincerely,

Gideon Yator

Appendix II: Household Head Survey Questionnaire for Kisharu Residents

Introduction

Dear Respondent,

Thank you for participating in this survey. We are studying the potential health effects of consuming water from fumarolic condensates in your area. Your responses will help us understand community experiences and improve local health and environmental knowledge. Participation is entirely voluntary. You may skip any question or stop the survey at any point without any consequences. All answers are confidential and will be used only for research purposes. This will take about 10-15 minutes.

Date:

Household Head ID:

Location:

SECTION A. Demographic and Water Usage Patterns

Please tick (√) the appropriate response.

1. **What is your age, sex, and primary occupation?**

   Age: □ □ years

   Sex: □ Male □ Female □ Other

   Level of Education: □ No formal education □ Primary □ Secondary □ Tertiary

   Occupation: □ Farmer □ Herder □ Student □ Trader □ Homemaker

   □ Other (specify): _____

2. **How far is your home from the nearest fumarole vent?**
   □ Less than 1 km □ 1–2 km □ 2–5 km □ More than 5 km

3. **What is your household's primary drinking water source?**

   □ Fumarole condensate (specify vent: □ Vent 1 □ Vent 2 □ Vent 3 □ Other: ___)

   □ Tap water □ Borehole □ Bottled water □ Other (specify): _____

4. **How often and how much does your household use fumarolic condensate?**

   Frequency of drinking: □ Daily □ Weekly □ Rarely □ Never

   Amount daily: □ Less than one Liter □ 1-2 Liters □ 2-3 Liters □ More than 3 Liters

   Other uses: □ Bathing □ Washing □ Cooking □ Other (specify): _____

5. **How long have you been using this condensate as a water source?**

   □ Less than 1 year □ 1-5 years □ 5-10 years □ More than 10 years

B. Exposure Pathways and Risk Perception

6. **Do you treat fumarolic condensate before drinking it?**

   □ Yes, I boil it □ Yes, I filter it □ Yes, Other (specify): _____ □ No

7. **How often do you bathe or wash with fumarolic condensate?**

   □ Once a day □ Twice a day □ More than twice a day □ Rarely □ Never

   Average duration per session:
   □ Less than 5 min □ 5-10 min □ More than 10 min

8. **What do you think about the safety of fumarolic condensate?**

   Do you believe fumarolic condensate is safe to drink??

   □ Very safe □ Somewhat safe □ Unsafe □ Don't know

Are you aware of any health risks (For example., heavy metals) linked to fumarolic condensate?

□ Yes (source: □ Family □ Health workers □ Media □ Other: _____)
□ No □ Unsure

9. **Are there cultural or spiritual beliefs about fumarolic water in your community?**

   □ Yes, (For example., healing powers, Explain: _____) □ No □ Unsure

C. Health and Environmental Concerns

10. **Have you or your household experienced these symptoms since using fumarolic condensate? (Check all that apply)**

    □ Headaches □ Nausea □ Skin rashes □ Kidney pain □ None

□ Stomach pain □ Breathing difficulties □ Other (specify): _____

If yes, when did the symptoms begin? (Month/Year): _____

11. **Do symptoms vary by season??**

□ Yes, worse in the dry season (January–February)

□ Yes, worse in the wet season (March–April)

□ No change □ Unsure

If yes, describe the differences: _____

12. Have you sought medical help for these symptoms?

□ Yes □ No

If yes, what diagnosis or treatment was prescribed? _____

13. **Has anyone in your household been diagnosed with a chronic condition?**

□ Yes (Age: ____; Condition: _____; Year: _____) □ No

□ Prefer not to say

14. How concerned are you about health risks from water use?

□ Not concerned □ Slightly □ Moderately □ Very □ Extremely

D: Socio-Economic Factors and Solutions

15. Does your household have access to alternative water sources?

□ Yes, always □ Yes, sometimes □ No

16. How much does your household spend on water each month?

□ Nothing (free sources) □ Less than KSH 500 □ KSH 500–1000 □ More than KSH 1000

17. **How difficult is it for your household to afford safe drinking water?**

(For example., *filtered, boiled, bottled, or piped water*).

□Not difficult □Slightly □Moderately □Very □Extremely

18. **What would you do to ensure safer water? (Check all that apply)**

□ Switch water source □ Treat water □ Seek medical advice □ Other: _____

Is there anything else you'd like to share about your water use, health concerns, observations, or suggestions?

_____

_____

_____

_____

Appendix III: Interview Guide for Village Elder in Kisharu Sub-Location

Introduction (to be read to the informant)

Thank you for agreeing to participate in this interview. I am researching the potential health effects of heavy metal exposure from fumarolic condensates used as a water source in Kisharu sub-location, which has a population of 720 people across three villages. As a respected elder and community leader, your knowledge of household practices and experiences is invaluable in helping us understand how the use of condensate water from the five local vents may affect health. This interview will take approximately 20–30 minutes. Your responses will be kept confidential and will be used solely for research purposes. Please feel free to share your insights openly.

Date:

Interviewer:

Informant Name & Role:

Village Represented:

Section A: Background and Context

1. Can you describe your role in the village and how long you have served as a leader or elder?

   _____

   _____

2. What is the history/ cultural beliefs of households using water from the ten fumarolic vents in Kisharu?

   _____

   _____

Section B: Community Practices and Condensate Use

3. How common is it for households in your village to rely on condensates from the vents as a water source?

   _____

   _____

4. Are there any traditional or cultural beliefs in your community about the use of condensate water from these vents?

   _____

   _____

5. Have you observed any changes in how households use condensate water from the vents over the past 5–10 years?

   _____

   _____

Section C: Health Perceptions and Community Awareness

6. Have people in your village ever mentioned health problems they think might be related to drinking or using condensate water from the vents?

   _____

   _____

7. Do you observe differences in health complaints between the dry and wet seasons that may be related to condensate use?

   _____

   _____

8. Have there been any serious illnesses or deaths in your village that people attribute to water from the vents, even informally?

   _____

   _____

Section D: Community Awareness and Responses

9. How aware do you think your village is of potential risks from using fumarolic condensate water, such as heavy metal contamination?

   _____

   _____

10. When people suspect illness from the water, what actions do they usually take? (home remedies, health facility visits, cultural practices)

_____

_____

Section E: Coping Strategies and Recommendations

11. What traditional or practical methods do households use to make condensate water safer (for example, boiling, mixing with other water sources, limiting children's use)?

_____

_____

12. What do you think could be done to improve water safety in your village?

_____

_____

13. What role do elders and cultural leaders play in guiding the community on safe water practices?

_____

_____

Section F: Closing

13. Is there anything else you would like to share about water use, health concerns, or community experiences in Kisharu that has not been covered?

_____

_____

Closing Statement:

Thank you for your time and wisdom. Your insights will greatly enhance our understanding of how condensate use might affect health in Kisharu and help guide potential solutions.

If follow-up questions arise, may I contact you again? [Record response: ☐ Yes ☐ No]

Appendix IV: Interview Guide for the Chief in Kisharu Sub-Location

Introduction (to be read to the informant)

Thank you for taking the time to participate in this interview. I am conducting research on the potential health effects of heavy metal exposure from fumarolic condensates used as a water source in Kisharu sub-location, which has a population of approximately 720 people across three villages.

As a senior local administrator, your insights are essential in understanding community governance, water use practices, health concerns, and any interventions in place to address potential risks. This interview will take approximately 20–30 minutes, and your responses will remain confidential, used solely for research purposes. Please feel free to share your perspectives openly.

Date:

Interviewer:

Informant Name & Role:

Village Represented:

Section A: Background and Administrative Responsibilities

1. Can you describe your role as chief in relation to water access and how long you have served in this position?

   _____

   _____

2. From your perspective, what is the history of households using water from the ten fumarolic vents in this area?

   _____

   _____

3. How widespread is household reliance on fumarolic condensates today?

   _____

   _____

Section B: Community Practices and Challenges

4. What challenges have you observed in water access for households in Kisharu (for example., shortages, seasonal dependence, cost)?

   _____

   _____

5. Are there any cultural or community practices that shape how households use condensate water from the vents?

   _____

   _____

6. Have you noticed any changes in water use patterns over the years?

   _____

   _____

Section C: Health Concerns and Reports

8. Have you received any reports or complaints from residents about health issues they associate with using condensate water?

   _____

   _____

9. Are there any observed differences in health concerns between the dry season and the wet season?

   _____

_____

10. From an administrative perspective, have there been cases of illness or deaths that residents informally attribute to condensate water?

    _____

    _____

Section D: Community Awareness and Governance

11. How aware do you think community members are of potential risks, such as contamination of fumarolic condensates?

    _____

    _____

12. What steps, if any, has the local administration taken to educate the community on water safety and potential health risks?

    _____

    _____

13. Have government agencies or NGOs ever raised concerns or conducted interventions regarding water from fumarolic vents in this area?

_____

_____

Section E: Policy and Recommendations

15. From your perspective, do you think condensate water from the vents affects people's health in Kisharu? Why or why not?

    _____

    _____

16. What interventions or policies would you recommend to improve safe water access in your community?

_____

_____

17. In your view, what roles should local leadership, public health officers, and government agencies play in addressing these challenges?

    _____

    _____

Section F: Closing

19. Is there anything else you would like to add regarding water use, community health, or governance challenges in Kisharu?

    _____

    _____

Closing Statement

Thank you for your time and valuable insights. Your perspectives will greatly contribute to understanding the impact of fumarolic condensate use on community health and help guide future interventions.

Appendix V: Interview Guide for Health Professionals- Kisharu Dispensary

Introduction (To be Read to the Informant)

Thank you for taking the time to participate in this interview. I am conducting research on the potential health effects of heavy metal exposure from fumarolic condensates used as a water source in Kisharu sub-location. Given your role in healthcare service delivery, your insights are essential in understanding the health conditions affecting residents and any potential links to water quality.

This interview will take approximately 20–30 minutes. Your responses will remain confidential and will be used solely for research purposes. Please feel free to share your perspectives openly.

Date:

Interviewer:

Informant Name & Role:

Facility Name:

Years of Experience in Kisharu:

Section A: General Health Trends in the Community

1. Have you observed common health conditions among patients that may be linked to water use, particularly fumarolic condensates (for example., dental discoloration)?

   _____

   _____

2. Do patients ever mention water from fumarolic vents as a possible cause of illness?

   _____

   _____

3. Are there differences in the types or frequency of health complaints between the dry season and the wet season?

   _____

   _____

Section B: Awareness and Community Health Education

4. In your opinion, how aware are community members of the potential health risks associated with using fumarolic condensate water?

   _____

   _____

5. Has the dispensary or any health authority provided health education or awareness programs regarding safe water use in Kisharu?

   _____

   _____

Section C: Responses and Interventions

8. When patients present with symptoms potentially linked to water use, how does the dispensary respond in terms of diagnosis, treatment, or referral?

   _____

_____

9. Have there been notable cases of chronic illness that you suspect may be related to long-term use of fumarolic condensates?

_____

   _____

10. What challenges do you face in managing health conditions that could be linked to environmental exposures such as contaminated water?

    _____

    _____

Section D: Insights and Recommendations

11. From your perspective, do you think fumarolic condensates are contributing to health problems in this community? Why or why not?

    _____

    _____

12. What measures would you recommend to improve health outcomes and ensure safer water use for residents of Kisharu?

    _____

    _____

13. What role should healthcare providers, local leaders, and government agencies play in addressing these issues?

_____

_____

Section F: Closing

17. Is there anything else you would like to add regarding community health, water quality, or disease trends in Kisharu?

_____

_____

Closing Statement

Thank you for your time and valuable insights. Your perspectives will greatly contribute to understanding the health impacts of fumarolic condensate use in Kisharu and guide future interventions.

Appendix VI: Calibration Curves

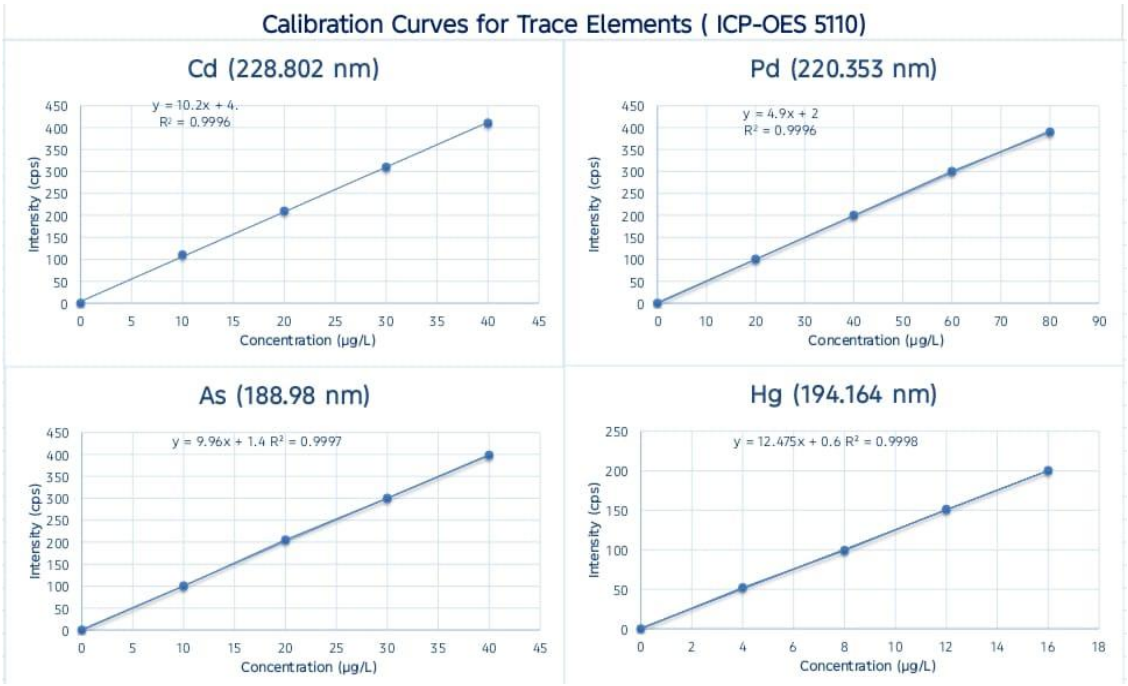

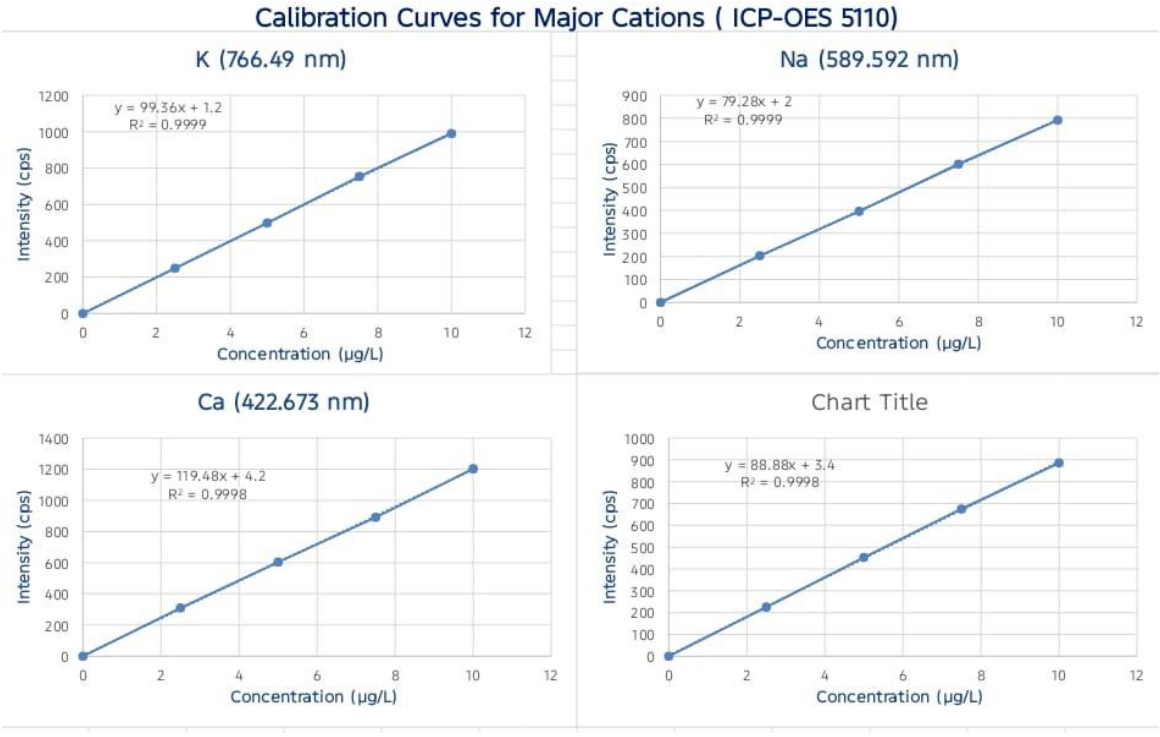

Appendix VII :KUREC Clearance Letter

KABARAK UNIVERSITY RESEARCH ETHICS COMMITTEE

Private Bag - 20157
KABARAK, KENYA
Email: kurec@kabarak.ac.ke

Tel: 254-51-343234/5
Fax: 254-051-343529
www.kabarak.ac.ke

OUR REF: KABU01/KUREC/001/09/06/25

Date: 24th June, 2025

Gideon Yator.
Reg. No: GMEN/NE/0571/05/23
Kabarak University,

Dear Gideon,

RE: ASSESSMENT OF SPATIO-SEASONAL VARIATIONS IN HEAVY METAL CONTAMINATION AND HEALTH RISKS OF FUMAROLIC CONDENSATES IN MT. SUSWA, KAJIADO COUNTY, KENYA

This is to inform you that ***KUREC*** has reviewed and approved your above research proposal. Your application approval number is ***KUREC-090625.*** The approval period is 24***/06/2025*** – ***24/06/ 2026.***

This approval is subject to compliance with the following requirements:

i. All researchers shall obtain an introduction letter to NACOSTI from the relevant head of institutions (Institute of postgraduate, School dean or Directorate of research)
ii. The researcher shall further obtain a RESEARCH PERMIT from NACOSTI before commencement of data collection & submit a copy of the permit to **KUREC.**
iii. Only approved documents including (informed consents, study instruments, MTA Material Transfer Agreement) will be used
iv. All changes including (amendments, deviations, and violations) are submitted for review and approval by ***KUREC***:
v. Death and life-threatening problems and serious adverse events or unexpected adverse events whether related or unrelated to the study must be reported to ***KUREC*** within 72 hours of notification;
vi. Any changes, anticipated or otherwise that may increase the risk(s) or affected safety or welfare of study participants and others or affect the integrity of the research must be reported to ***KUREC*** within 72 hours;
vii. Clearance for export of biological specimens must be obtained from relevant institutions and submit a copy of the permit to KUREC;
viii. Submission of a request for renewal of approval at least 60 days prior to expiry of the approval period. Attach a comprehensive progress report to support the renewal and;
ix. Submission of an executive summary report within 90 days upon completion of the study to ***KUREC***

Sincerely,

KABARAK UNIVERSITY
INSTITUTIONAL RESEARCH ETHICS COMMITTEE
APPROVED
P. O. PRIVATE BAG - 20157, KABARAK

Prof. Jackson Kitetu PhD.
KUREC-Chairman

Cc Vice Chancellor
DVC-Academic & Research
Registrar-Academic & Research
Director-Research Innovation & Outreach
Institute of Post Graduate Studies

Appendix VIII: NACOSTI Research Permit

REPUBLIC OF KENYA

NATIONAL COMMISSION FOR SCIENCE,TECHNOLOGY & INNOVATION

Ref No: **144542**

Date of Issue: **12/July/2025**

RESEARCH LICENSE

This is to Certify that Mr.. Gideon Yator of Kabarak University, has been licensed to conduct research as per the provision of the Science, Technology and Innovation Act, 2013 (Rev.2014) in Kajiado on the topic: ASSESSMENT OF SPATIO-SEASONAL VARIATIONS IN HEAVY METAL CONTAMINATION AND HEALTH RISKS OF FUMAROLIC CONDENSATES IN MT. SUSWA, KAJIADO COUNTY, KENYA for the period ending : 12/July/2026.

License No: **NACOSTI/P/25/4176440**

144542

Applicant Identification Number

Ag. Director General
NATIONAL COMMISSION FOR SCIENCE,TECHNOLOGY & INNOVATION

Verification QR Code

NOTE: This is a computer generated License. To verify the authenticity of this document, Scan the QR Code using QR scanner application.

See overleaf for conditions

Appendix IX: Evidence of Conference Participation

KABARAK UNIVERSITY

Certificate of Participation

Awarded to

GIDEON YATOR

For successfully participating in the 15th Annual Kabarak University International Research Conference held from 10th-11th July 2025 and presented a paper entitled ***"Health Risks Assessment of Selected Trace Elements in Mt. Suswa's Fumarolic Condensates: Informing Participatory Natural Resource Management."***

Conference Theme

Enhancing Environmental Resilience for Food Production and Energy Sustainability.

Prof. Peter Rugiri
Dean, School of Science, Engineering & Technology

Dr. Phillip Nyawere
Director - Research, Innovation and Outreach

Kabarak University Moral Code

As members of Kabarak University family, we purpose at all times and in all places, to set apart in one's heart, Jesus as Lord.

(1 Peter 3:15)

Kabarak University is ISO 9001:2015 Certified

Appendix X: List of Publication

INTERNATIONAL JOURNAL OF RESEARCH AND SCIENTIFIC INNOVATION (IJRSI)
ISSN No. 2321-2705 | DOI: 10.51244/IJRSI |Volume XII Issue X October 2025

Evaluation of Human Health Risks Associated with Selected Heavy Metal Exposure from Fumarolic Condensates in Mt. Suswa, Kenya

Gideon Yator*, Jackson John Kitetu, Caroline Chepkirui

Department of Physical and Biological Sciences, Kabarak University, P.O. Private Bag 20157, Nakuru - Kenya.

*** Corresponding author**

DOI: https://dx.doi.org/10.51244/IJRSI.2025.1210000078

Received: 02 October 2025; Accepted: 08 October 2025; Published: 04 November 2025

ABSTRACT

Fumarolic condensates in volcanic terrains often serve as critical water sources for nearby communities but may contain toxic heavy metals mobilized through magmatic degassing and hydrothermal leaching. This study evaluated the potential human health risks associated with exposure to selected heavy metals (arsenic (As), cadmium (Cd), lead (Pb), and mercury (Hg)) in fumarolic condensates from Mt. Suswa, Kenya. Condensate samples were collected from ten modified fumarolic vents actively used by local residents and analyzed using an Agilent 5110 ICP-OES for trace-metal quantification. The mean concentrations of As (3.86 ppb), Pb (1.43 ppb), and Cd (0.85 ppb) were all below World Health Organization (2022) and NEMA (2024) limits, while Hg remained undetected in all samples. The Heavy Metal Pollution Index (HPI) and Heavy Metal Evaluation Index (HEI) indicated moderate contamination (mean HPI = 20.46 ± 12.75; HEI = 0.70 ± 0.28), with higher enrichment observed in inner-caldera fumaroles, reflecting stronger magmatic influence. Health-risk assessment following USEPA (2011) methodology showed that non-carcinogenic hazard quotients (HQ) for As and Cd were below unity for both adults and children, though relatively higher in children, indicating greater susceptibility to chronic exposure. The carcinogenic risk (CR) for As ranged from 9.98×10^{-5} (F2) to 1.00×10^{-4} (F4) for adults and 9.78×10^{-5} (F10) to 1.92×10^{-5} (F6) for children, with the former slightly exceeding the upper USEPA threshold (10^{-6}–10^{-4}), suggesting a low but notable lifetime cancer probability from prolonged exposure. Although overall contamination levels were low, localized enrichment and cumulative exposure may pose health risks to vulnerable populations. These findings underscore the importance of continuous monitoring, community education, and sustainable mitigation strategies such as alternative safe-water supplies and affordable point-of-use treatment technologies in geothermal-affected regions.

Keywords: Mt. Suswa, fumarolic condensates, heavy metals, human health risk

INTRODUCTION

Geothermal and volcanic regions are characterized by extensive hydrothermal activity that releases gases and condensates enriched with various trace elements and heavy metals. These condensates often provide vital freshwater sources for surrounding communities, especially in arid or semi-arid volcanic terrains where alternative supplies are limited. However, geothermal fluids commonly carry toxic metals such as arsenic (As), cadmium (Cd), lead (Pb), and mercury (Hg), which originate from magmatic degassing, mineral dissolution, and rock–water interactions (Ayari et al., 2023; Yao et al., 2024). When these metals enter fumarolic waters, they can accumulate in biota or drinking-water systems, posing long-term health threats even at trace concentrations (Durowoju et al., 2020; Sunguti et al., 2024)

Globally, geothermal fields such as Rotorua (New Zealand), Aluto–Langano (Ethiopia), and Larderello (Italy) have been shown to contain elevated levels of As, Cd, and Pb in geothermal discharges that exceed international drinking-water limits(Morales-deAvila et al., 2023; Sanjuan, 2024). Chronic ingestion or inhalation of these metals has been linked to systemic and carcinogenic health effects, including skin lesions and keratosis, renal tubular dysfunction, neurological impairment, and various cancers (Charkiewicz et al., 2023; kaur et al., 2024).